

Diversity and Adaptive Modulation & Coding Aware Routing in WLAN Multihop Networks with Centrally Scheduled Multiple Access

By

ShoaeV Hares

A thesis submitted to
the Faculty of Graduate Studies and Research
in partial fulfillment of
the requirements of the degree of

Master of Engineering

Ottawa-Carleton Institute for Electrical and Computer Engineering

Department of Systems and Computer Engineering

Carleton University

Ottawa, Ontario

Copyright 2004, ShoaeV Hares

The undersigned hereby recommended to the Faculty of Graduate Studies and Research acceptance of the thesis

Diversity and Adaptive Modulation & Coding Aware Routing in WLAN Multihop Networks with Centrally Scheduled Multiple Access

Submitted by Shoaev Hares
In partial fulfillment of the requirements for the
Degree of Master of Engineering

Thesis Supervisor
Prof. Halim Yanikomeroglu

Thesis Co-Supervisor
Dr. Bassam Hashem

Chair, Department of Systems and Computer Engineering
Prof. Rafik A. Goubran

Carleton University
2004

Abstract

This thesis presents novel multihop relaying schemes capable of incorporating multihop diversity in routing calculations for centrally scheduled systems using adaptive modulation and coding. The routing algorithms can factor multihop selection combining and multihop maximal ratio combining (MRC) in digital or hybrid digital and analog relaying systems (HDAR). These diversity schemes do not require additional bandwidth or transmit power beyond that already required for multihop relaying. Furthermore the frame segmentation scheme incorporates modulation and coding used on route hops and can adjust to maximize diversity gains and enhance performance. The energy consumed when using multihop relaying is equal to that when using singlehop relaying due to frame segmentation, yet we can achieve considerable performance gains. These novel routing algorithms and diversity techniques are the main contribution of this thesis.

The performance of these schemes is investigated for both 2-hop and multihop networks in the downlink scenario using a HiperLAN/2 wireless LAN test-bed. 2-hop relaying with proposed multihop diversity techniques was observed to offer considerable throughput increases particularly when the relaying terminal is situated nearer to the destination and using adaptive modulation and coding. Our results also show that 2-hop relaying can extend the coverage area to three times that of a singlehop network while offering significant throughput increases. Multihop quadruples the extension of the coverage area and offers further increase in throughput with respect to singlehop. Advanced routing incorporating modulation and coding can also significantly increase network performance in HDAR systems.

Acknowledgements

First and foremost, I would like to thank my thesis supervisors Prof. Halim Yanikomeroglu and Dr. Bassam Hashem for their time, guidance, and support. Their passion for research and their knowledgeable advice have made this endeavour an enjoyable and successful experience.

I am also grateful to Mr. Narendra Mehta for his efforts in installing the software necessary for this research and for making his software-guru knowledge available to me. Additionally I would like to thank the administrative staff in the Systems and Computer Engineering Department for making the copying, presentation etc. resources available and informing me of deadlines and protocols.

Finally I would like to express my gratitude to my parents and my sister for their constant encouragement and support.

TABLE OF CONTENTS

Abstract	iii
Acknowledgement	iv
Table of Contents	v
List of Figures & Tables	vii
List of Acronyms	x
List of Symbols	xi
Chapter 1 INTRODUCTION	1
1.1 Thesis Motivation	1
1.2 Thesis Objectives	2
1.3 Thesis Organization	3
Chapter 2 SYSTEM MODEL	5
2.1 Radio Propagation Model	5
2.2 Adaptive Modulation and Coding	8
2.3 Frame Segmentation	9
2.4 Packet Error Rate and Diversity	11
2.4.1 Multihop	13
2.4.2 Multihop Selection Combining Diversity	13
2.4.3 Multihop Maximal Ratio Combining Diversity	16
2.4.4 Hybrid Digital and Analog Relaying	22
Chapter 3 ROUTING STRATEGIES	27
3.1 Routing Metric	27
3.2 Multihop Routing Algorithms	29
3.3 Adaptive Modulation and Coding Maximization	36
3.4 Examples of Algorithms	39
Chapter 4 SIMULATION MODEL	47
4.1 Environment Parameters and Assumptions	47
4.2 Network Parameters and Assumptions	48
4.3 Simulation Algorithm	51
Chapter 5 SIMULATION RESULTS	52
5.1 The Effect of Diversity in 2-hop Relaying	52
5.2 2-hop Relaying Networks	58
5.3 Multihop Relaying Networks	65

Chapter 6	CONCLUSIONS -----	83
	6.1 Summary	83
	6.2 Further Discussions	84
	6.3 Thesis Contributions	87
	6.4 Future Work	88
	REFERENCES -----	90

List of Figures & Tables

Fig. 2.1	PER vs. C/I.	7
Fig. 2.2	An example network.	9
Fig. 2.3	n-hop relaying without multihop diversity.	10
Fig. 2.4	Frame segmentation of an n-hop connection.	11
Fig. 2.5	Interleaving of hops.	12
Fig. 2.6	Multihop diversity.	14
Fig. 2.7	Receiver architecture for MHSC.	15
Fig. 2.8	Example of MHSC and receiver operation.	16
Fig. 2.9	Receiver architecture for MHMRC	17
Fig. 2.10	Example of MHMRC and receiver operation	20
Fig. 2.11	Amplification in analog relaying	24
Fig. 3.1	MH routing flowchart.	32
Fig. 3.2	MHAM routing flowchart.	35
Fig. 3.3	AMCM flowchart.	38
Fig. 3.4	Routing example: Iteration 1.	40
Fig. 3.5	Routing example: Iteration 2.	41
Fig. 3.6	Routing example: Iteration 3.	42
Fig. 3.7	MH Algorithm 3.1 mode selection.	43
Fig. 3.8	MHAM Algorithm 3.2 mode selection.	43
Fig. 3.9	AMCM example.	45
Fig. 4.1	Throughput vs. SNR for various modes	49
Table 4.1	Adaptive modulation and coding settings	50

Fig. 4.2	Simulation flowchart	51
Fig. 5.1	2-hop relaying scenario	53
Fig. 5.2	2-hop simulation, $m_{0,2} = r:1/2$ QPSK, $SNR_{0,2} = 0.46$ dB	53
Fig. 5.3	2-hop simulation, $m_{0,2} = r:3/4$ 16QAM, $SNR_{0,2} = 15.8$ dB	54
Fig. 5.4	2-hop simulation, $m_{0,2} = r:3/4$ 64QAM, $SNR_{0,2} = 20.41$ dB	54
Fig. 5.5	Generic 2-hop relaying using AMC and MHSC diversity.	57
Fig. 5.6	2-hop avg. aggregate throughput as a function of cell radius	59
Fig. 5.7	2-hop avg. aggregate throughput as a function of cell radius	60
Table 5.1	2-hop throughput performance	60
Fig. 5.8	2-hop min. aggregate throughput as a function of cell radius	61
Fig. 5.9	2-hop min. aggregate throughput as a function of cell radius	62
Fig. 5.10	2-hop outage probability as a function of cell radius	63
Fig. 5.11	2-hop maximum load as a function of cell radius	64
Fig. 5.12	2-hop maximum load as a function of cell radius	64
Fig. 5.13	The effect of $k^{(\max)}$ on avg. min. throughput for MH	66
Fig. 5.14	The effect of $k^{(\max)}$ on avg. min. throughput for MH	66
Fig. 5.15	Multihop avg. aggregate throughput as a function of cell radius	67
Fig. 5.16	Multihop avg. aggregate throughput as a function of cell radius	68
Table 5.2	Multihop throughput performance	68
Fig. 5.17	Multihop min. aggregate throughput as a function of cell radius	69
Fig. 5.18	Multihop min. aggregate throughput as a function of cell radius	70
Fig. 5.19	CDF of throughput for 100 m cells	71
Fig. 5.20	CDF of throughput for 200 m cells	71

Fig. 5.21	Multihop maximum load as a function of cell radius	72
Fig. 5.22	Multihop maximum load as a function of cell radius	72
Fig. 5.23	PDF of number of hops for 100 m cells	73
Fig. 5.24	PDF of number of hops for 200 m cells	74
Table 5.3	Performance categorized by mode between AP and destination	75
Fig. 5.25	Example topology of a MH network	77
Fig. 5.26	Example topology of a MH SC network	77
Fig. 5.27	Example topology of a MH MRC network	78
Fig. 5.28	Example topology of a MH HDAR network	78
Fig. 5.29	Example topology of a MHAM HDAR network	79
Fig. 5.30	Example of a cycle in the topology of a MH SC network	79

List of Abbreviations & Acronyms

AMC	Adaptive Modulation and Coding
AMCM	Adaptive Modulation and Coding Maximization
AP	Access Point
ARQ	Automatic Repeat Request
CC	Central Controller
ETSI	European Telecommunications Standards Institute
GHz	Giga Hertz
HDAR	Hybrid Digital and Analog Relaying
HIPERLAN	High Performance Radio LAN
LOS	Line-of-sight
MH	Multihop
MHAM	Multihop Adaptive Modulation
MHMRC	Multihop Maximal Ratio Combiner
MHSC	Multihop Selection Combiner
MRC	Maximal Ratio Combiner
NLOS	Non-Line-of-Sight
PER	Packet Error Rate
QAM	Quadrature Amplitude Modulation
QPSK	Quaternary Phase Shift Keying
SC	Selection Combiner
SH	Singlehop
SINR	Signal-to-interference-plus-noise ratio
SNR	Signal-to-noise ratio
TDMA	Time Division Multiple Access
WLAN	Wireless Local Area Network

List of Symbols

α	Propagation exponent
β	Ratio of distance between source and relaying node to distance between source and destination, $\beta = d_{0,1}/d_{0,2}$
γ	Signal to noise (plus interference) ratio
η_i	Noise (plus interference) at node r_i
a_i	Amplification factor at node r_i
$C(R_d, M_d)$	Metric to node d using relaying node set R_d and mode set M_d
D_i	Modulation efficiency in bits/symbol of i 'th hop. $D_i = D_{i,i+1}$
$D_{i,j}$	Modulation efficiency in bits/symbol between nodes r_i and r_j
d	Distance
d_0	Reference distance
$d_{i,j}$	Distance between nodes r_i and r_j
F	Frames per second
f	Carrier frequency
G	Link/hop gain
$G_{i,j}$	Link/hop gain between nodes r_i and r_j
g_t	Transmit antenna gain
g_r	Receive antenna gain
$k^{(max)}$	Maximum number of routing algorithm iterations
M_d	Mode set to destination node d
m_i	i 'th mode in the mode set M_d
$m_{i,j}$	Mode between nodes r_i and r_j
$m_{i-1,i}^{(max)}$	Mode between nodes r_{i-1} and r_i maximizing link/hop throughput
$N_i^{(m)}$	Set of nodes in route transmitting with mode m
N_m	Set of wireless nodes
n	Number of hops in a connection
PL	Mean path-loss
$P_e(SNR, m)$	Packet error rate of link/hop as a function of SNR and mode m
$P_{i,j}$	Packet error rate between nodes r_i and r_j . $P_{i,j} = P_e(SNR_{i,j}, m_{i,j})$
PER_i	Packet error rate at node r_i
$PER_i^{(m)}$	Packet error rate at node r_i of signals received using mode m
P_r	Receive power
P_t	Transmit power
R_d	Relaying node set to destination d
r_i	i 'th node in the relaying node set R_d
S_l	Symbols allocated for a link
S_c	Symbols allocated for a connection
$SNR_{i,j}$	Signal to noise (plus interference) ratio between nodes r_i and r_j
$s_{i,j}$	Number of symbols of hop between nodes r_i and r_j
T_l	Throughput for a link
T_n	Throughput for a n -hop connection
X_σ	Normally distributed random variable for lognormal shadowing

Chapter 1

Introduction

Multihop relaying has recently garnered significant interest from academia and industry in order to augment conventional infrastructure-based networks with multihop capability [6, 29, 30]. In particular the concept of relaying in centrally scheduled Wireless Local Area Networks (WLANs) is gaining in popularity and studies have shown that relaying can extend coverage and increase throughput [7, 20].

This thesis will focus on relaying in centrally scheduled WLANs but unlike other studies we will not limit our relaying to a fixed number of hops and we benefit from use of coding & modulation and diversity in route selection. Although two main variants of WLANs exist, emphasis is given to relaying in HiperLAN/2 systems in our thesis. The alternative IEEE 802.11 may not be suitable for multihop relaying networks due to the negative impacts of unfairness of contention-based multiple access and hidden/exposed node situations [28]. HiperLAN/2 being a centrally scheduled network, where the access point schedules access to the medium in a time-division-multiple-access (TDMA) fashion, is more suitable for multihop relaying. In fact, recent studies have proposed relaying extensions to HiperLAN/2 [33] and modifications to the IEEE 802.11 MAC protocol to support relaying [12].

1.1 Thesis Motivation

With the increasing popularity of wireless networks and increasing enterprise and consumer demand for high data-rate services, WLANs using 802.11 and HiperLAN/2 technology are expected to be deployed extensively in the foreseeable future [7, 20]. However, the high carrier frequency of these systems (in the 5GHz band) implies severe

signal attenuation as compared to the lower carrier frequency WLANs of the previous generation [31, 32]. As a result, next generation WLANs are confronted with overcoming the obstacle of limited communication range and reduced data-rates. In particular, providing high data-rates in the downlink will prove to be a major challenge in data-centric networks such as WLANs.

Multihop relaying with wireless terminals offers an economical solution to overcoming limited communication range and extending high data-rate coverage without deployment delays and associated relaying infrastructure costs. However with the mobile nature of the network, the selection of the relaying nodes, or routing, becomes a critical factor in the performance of multihop relaying. While there is a large body of research devoted to routing in ad-hoc and cellular networks [13, 26], they may be limited by the number of hops or are primarily focused on establishing connectivity and decreasing outage. Furthermore, traditional wireless routing algorithms do not factor concepts such as multihop diversity or adaptive modulation and coding in calculations. The most similar work to this thesis is [2], where it discusses theoretical aspects of multihop diversity and indicates routing with multihop diversity as a possible extension. In this thesis we present novel multihop routing algorithms which can increase data-rate performance significantly as well as extend coverage. More notably, routing incorporates the benefits of multihop diversity and adaptive modulation & coding in routing.

1.2 Thesis Objectives

Our thesis focuses on multihop relaying in the context of downlink communications using a HiperLAN/2 test-bed, however our work may be extended to

other systems such as cellular networks that use centrally scheduled TDMA access. Bearing this in mind, the objectives of this thesis are as follows:

- To introduce multihop diversity schemes for TDMA systems using adaptive modulation and coding and develop the corresponding packet error rate expressions.
- To investigate the effects of various diversity techniques in multihop systems when using adaptive modulation & coding.
- To introduce novel multihop relaying algorithms using TDMA scheduling capable of factoring the effects of multihop diversity and adaptive modulation and coding in route selection.
- To introduce novel adaptive modulation & coding maximization algorithms designed to increase the benefits of multihop maximal ratio combining when relaying.
- To determine the impact of these relaying algorithms on network performance, particularly throughput and coverage.

1.3 Thesis Organization

The remainder of this thesis is divided into five chapters. In chapter 2 we begin by introducing our system model including topics such as adaptive modulation and coding, frame segmentation, and packet error rate models when using multihop diversity. Chapter 3 utilizes the models described in chapter 2 to form a routing metric and subsequently introduces routing and modulation and coding maximization algorithms. Chapter 4 describes the simulation model used to simulate relaying networks and adaptive modulation and coding. Chapter 5 provides simulation results and discussion relating to

our thesis objectives outlined in the previous section. The thesis concludes with Chapter 6 devoted to summarizing the key results of our research and provides suggestions on future research.

Chapter 2

System Model

Relaying modulation and coding efficiency, frame segmentation, and relaying packet error rates are key factors in selecting a route that maximizes throughput in systems using a TDMA MAC. A disadvantage of using relaying in TDMA systems is the additional time slots or symbols required to relay data on multiple hops; we term this effect frame segmentation. However, it may be possible to increase throughput by relaying if the route provides lower error rates and increased modulation efficiency reducing frame segmentation. Multiple copies of data inherently generated while relaying can also prove beneficial using multihop diversity techniques to further reduce error rates.

In this chapter we introduce our radio propagation model and discuss frame segmentation, packet error rates and relaying diversity as they affect multihop TDMA systems.

2.1 Radio Propagation Model

Both path loss and fading characteristics of the radio channel can vary significantly depending on the specifics of the indoor environment including many factors such as building structure and material type. We have elected to use a simple propagation model that incorporates path loss as well as large-scale and small-scale signal variation consistent with indoor propagation characteristics.

The average power of a received signal is an inverse function of the distance d between transmitter and receiver. The average received power, \bar{P}_r , decays exponentially according to [23, 24],

$$\bar{P}_r = P_t \frac{g_t g_r}{PL}, \quad (2.1)$$

where the mean path-loss PL at distance d is given by

$$PL = \left(\frac{4\pi d_0 f}{c} \right)^2 \left(\frac{d}{d_0} \right)^\alpha, \quad (2.2)$$

and P_t is the transmit power, g_t and g_r are transmit and receive antenna gains, d_0 is the reference distance, f is the carrier frequency, $c = 3.0 * 10^8$ m/s is the constant of light, and α is the propagation exponent.

Possible obstructions such as walls or other large objects can also cause shadowing effects. This large-scale path loss variation known as lognormal shadowing causes the received signal power to fluctuate from the average received power in (2.1).

To account for shadow fading, (2.1) is rewritten as,

$$P_r = P_t G = P_t \frac{g_t g_r}{PL} 10^{\frac{X_\sigma}{10}}. \quad (2.3)$$

Here G represents the link gain. X_σ is a Normally distributed random variable with mean $\mu = 0$ and standard deviation σ : $X_\sigma \sim N(0, \sigma)$. Combining (2.2) and (2.3), and expressing in the log domain we obtain,

$$P_r[dBm] = P_t[dBm] - 10 \log \left(\frac{1}{g_t g_r} \cdot \left(\frac{4\pi d_0 f}{c} \right)^2 \right) - 10 \log \left(\frac{d}{d_0} \right)^\alpha + X_\sigma. \quad (2.4)$$

Due to reflection, scattering, and refraction off various structures in indoor environments, the transmitted signal often reaches the receiver through multiple indirect

and delayed paths when there is no line-of-sight path between transmitter and receiver. The signals from the indirect paths combine to produce a distorted representation of the transmitted signal resulting in small-scale path-loss variation known as multipath fading. Depending on whether the signal components constructively or destructively combine, we observe rapid fluctuations of signal strength over a period of time. To account for multipath fading we use the ETSI-A channel [22]. This model incorporates multipath fading with rms delay spread of 50 ns – a typical channel profile for office environments [16] and can be classified as a slow-fading Rayleigh channel. Fig. 2.1 [9] provides measured data of HiperLAN/2 packet error rate versus signal to noise using an ETSI-A channel model. HiperLAN/2 uses convolutional coding, puncturing, interleaving and transmits using OFDM [34] to reduce the negative effects of multipath fading. Fig. 2.1 is obtained by transmitting 54 byte packets over an ETSI-A channel.

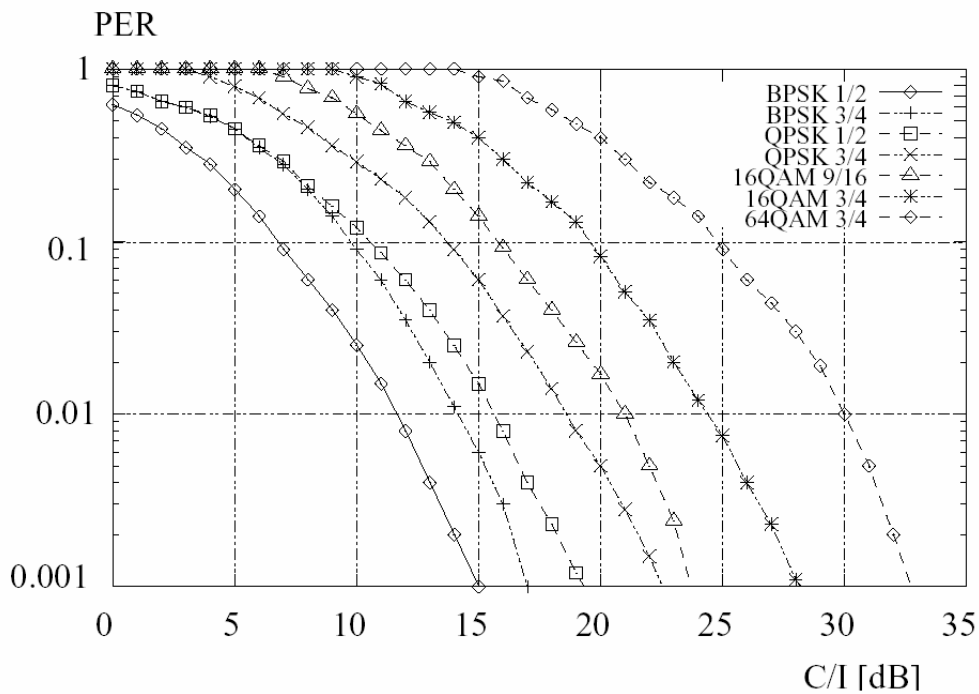


Fig. 2.1 – PER vs. C/I.

Using this data in look-up tables and SNR values factoring path-loss and shadow fading, we can determine the packet error rate for ETSI-A radio channels. This PER estimation will be necessary for routing schemes introduced in later chapters. We emphasize that the schemes and algorithms described in this thesis can be extended to systems other than HiperLAN/2 provided we can estimate packet error rates for the particular system.

2.2 Adaptive Modulation and Coding (AMC)

Networks using AMC can increase or decrease modulation efficiency by selecting an appropriate modulation and coding level or mode (denoted by m). Adaptive modulation and coding allow a link to be adapted such that the throughput is maximized for channel conditions. We define link throughput, T_l , seen between two consecutive nodes r_{i-1} , and r_i as

$$T_l = F \cdot S_l \cdot D_{i-1,i}(m_{i-1,i}) \cdot (1 - P_e(SNR_{i-1,i}, m_{i-1,i})). \quad (2.5)$$

Selecting a particular mode for the link, $m_{i-1,i}$, in turn selects a particular modulation efficiency, $D_{i-1,i}$, in information bits/sym. F is frames per second and S_l is the number of symbols allocated per frame. The packet error rate of the link, $P_e(SNR, m)$, is a function of $m_{i-1,i}$ and link signal to noise ratio, $SNR_{i-1,i}$. $P_e(SNR, m)$ can be evaluated using Fig. 2.1.

Using expression (2.5), the selected AMC mode can be expressed as,

$$m_{i-1,i}^{(\max)} = \arg \max_{m \in M} (D_{i-1,i}(m_{i-1,i}) \cdot (1 - P_e(SNR_{i-1,i}, m_{i-1,i}))). \quad (2.6)$$

Here $m_{i-1,i}^{(\max)}$ is the mode selected from the set of all modes, M , which maximizes the throughput for the link. Relaying networks can benefit from AMC by selecting the modulation efficiency per link/hop to maximize the end-to-end or connection throughput.

2.3 Frame Segmentation [10]

The access point or central controller (CC) divides the MAC frame into connections to nodes for downlink and uplink communication. Depending on the state of traffic buffers and quality-of-service provisioning, the CC reserves the appropriate number of time slots for connections. Since our system does not use multiple frequency channels for multihop transmission, a connection requires further segmentation of its allocated resources (time slots) for the purpose of relaying. Each segment of a connection corresponds to a hop in a relaying route. All connections and all hop segments are scheduled by the CC and are orthogonal in the time domain. Fig. 2.2 illustrates the concept of connections and segmentation.

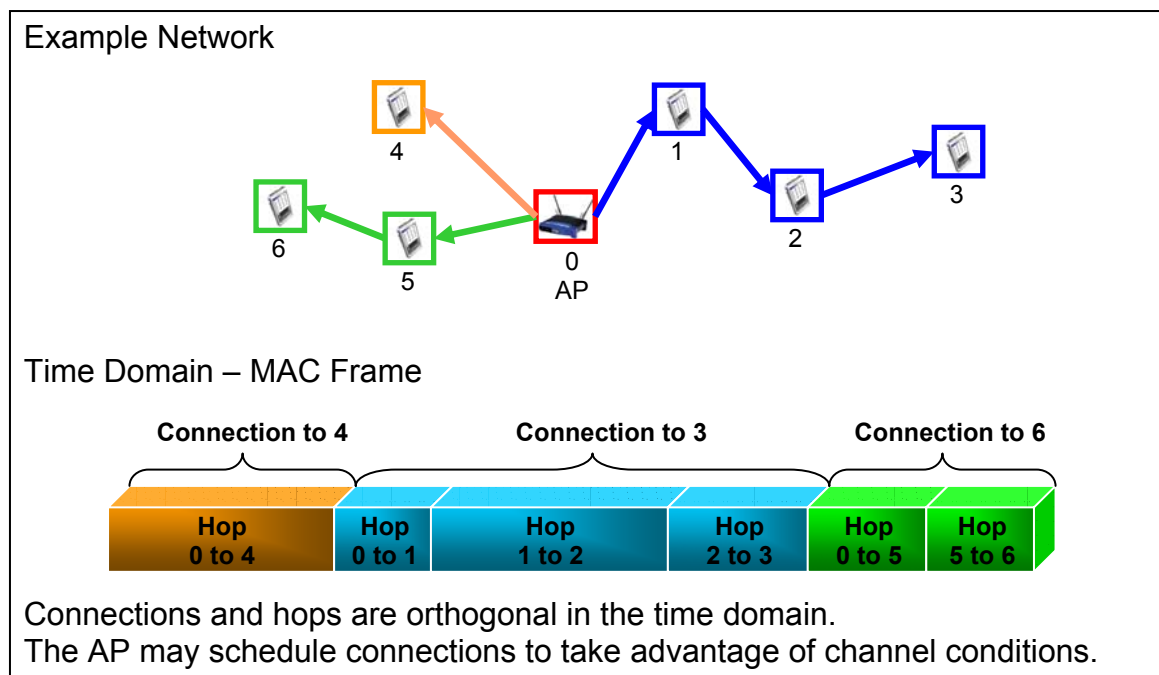


Fig. 2.2 – An example network illustrating the orthogonality of connections and hops.

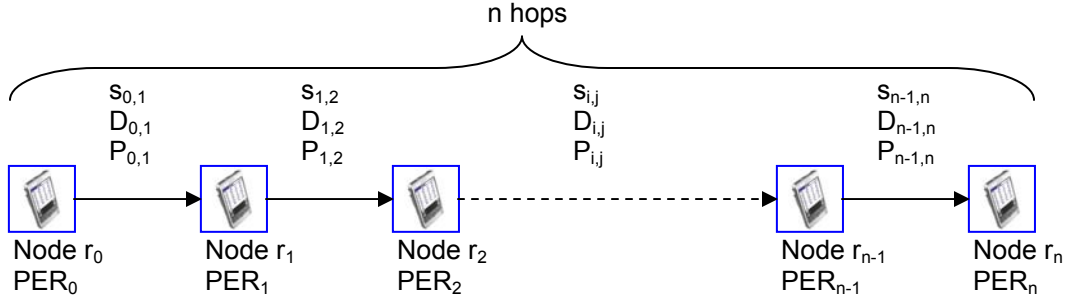


Fig. 2.3 – n -hop relaying without multihop diversity.

Let us consider the generic relaying scenario, depicted in Fig. 2.3, involving n hops, the θ 'th node in the route, r_θ , represents the source (the central controller in the downlink scenario), node r_n represents the destination, and nodes r_1 through r_{n-1} represent relaying nodes according to the order of the route. The following constraint states that the amount of data entering any given relaying node, r_i , must be equal to the amount of data exiting the node:

$$s_{i-1,i} \cdot D_{i-1,i} = s_{i,i+1} \cdot D_{i,i+1} \quad i \in \{1, 2, \dots, n-1\}. \quad (2.7)$$

Here $s_{i-1,i}$ represents the number of symbols allocated for the hop between nodes r_{i-1} and r_i , and $D_{i-1,i}$ represents the information bits per symbol of the hop between nodes r_{i-1} and r_i . Note that expression (2.7) applies to the generic case where AMC is used in the system and the hop data rates in the route, $D_{i-1,i}$, are dissimilar.

Furthermore, if a total of S_c symbols/frame have been allocated for a connection from source (node r_0) to destination (node r_n) then,

$$S_c = \sum_{i=1}^n s_{i-1,i}. \quad (2.8)$$

Solving for the equations from (2.7) and (2.8) yields

$$s_{i-1,i} = \frac{S_c}{\sum_{j=1}^n \frac{D_{i-1,i}}{D_{j-1,j}}} \quad i \in \{1,2,\dots,n\}. \quad (2.9)$$

Expression (2.9) implies that for any hop between nodes r_{i-1} and r_i , with link modulation efficiency $D_{i-1,i}$, $s_{i-1,i}$ symbols should be allocated per frame for the $i-1$ 'th hop. Frame segmentation is illustrated in Fig. 2.4. When $n = 1$, $s_{0,1} = S_c$ indicates the complete frame or time resource can be used to transmit data. When relaying, $n > 1$, expression (2.9) evaluates to $s_{i-1,i} < S_c$ indicating frame segmentation, or fewer time resources for original data transmission since resources are used to relay the data. Note that frame segmentation implies that the total energy per connection (end-to-end) remains the same. Multihop relaying will use the same amount of energy as singlehop relaying.

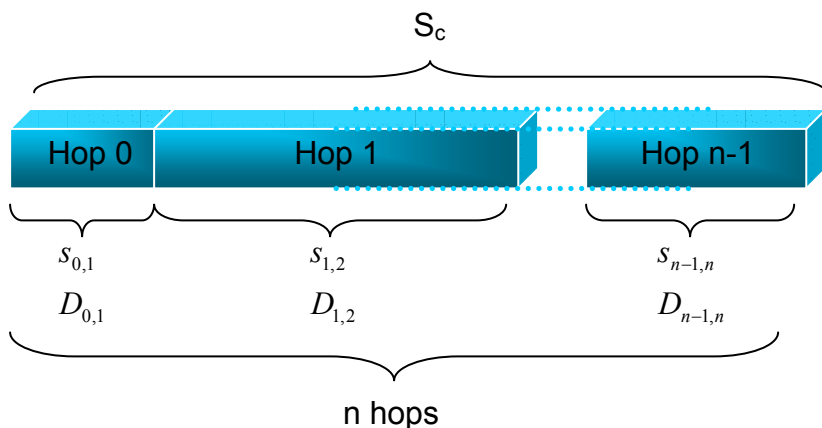


Fig. 2.4 – Frame segmentation of an n-hop connection.

2.4 Packet Error Rate and Diversity [10, 11]¹

In addition to higher spectral efficiency, the reduction in packet error rate when using multiple hops for a connection may also offset the loss of resources due to frame

¹ Certain equations for MHMRC and HDAR appear in a mathematically more rigorous form in this thesis, however the equations and results as published in [10, 11] are still correct.

segmentation. Depending on diversity, relaying via multiple hops may have greater effect on maximizing connection throughput.

The packet error rate models discussed here assume all relaying nodes employ digital forwarding with the added condition that incorrectly detected packets are not relayed to subsequent nodes in the route, thereby eliminating detection error propagation. Nodes perform relaying using a “best-effort” scheme where ARQ is not applied to hops. ARQ may be performed on an end-to-end basis (source to destination). We also assume the processing delay for “best-effort” relaying is negligible. In practice it may be possible to mitigate delays due to relaying with proper scheduling of transmissions. The CC may interleave hops for various connections thereby reducing the processing delay incurred at relaying nodes. Fig. 2.5 depicts the scenario from Fig. 2.2, however, the hops are interleaved in the frame thereby reducing potential delays at relaying nodes.

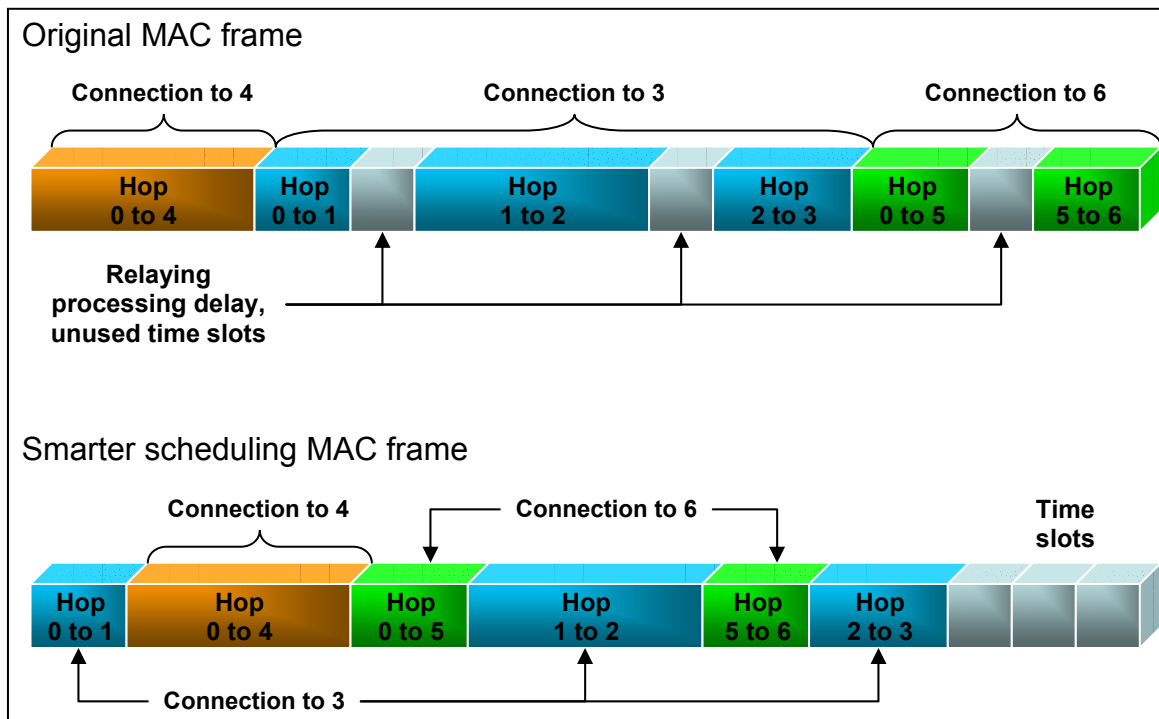


Fig. 2.5 – Interleaving of hops reduces relaying delay and increase capacity (see Fig 2.2).

Under the assumptions of “best-effort” digital relaying, simple packet error rate models can be created for multihop, multihop selection diversity, and multihop MRC diversity forms of relaying. Multihop MRC diversity is further extended to hybrid digital and analog relaying.

2.4.1 Multihop

Generalizing the multihop scenario involving n hops, illustrated in Fig. 2.3, the packet error rate seen at the i 'th node in a route, r_i , can be expressed as

$$PER_i = PER_{i-1} + (1 - PER_{i-1})P_{i-1,i} \quad i \in \{1, 2, \dots, n\}, \quad (2.10)$$

where $P_{i,j} = P_e(SNR_{i,j}, m_{i,j})$.

The packet error rate at the source node, r_0 , is $PER_0=0$ and the packet error rate for the link between any nodes r_i and r_j is denoted by $P_{i,j}$. The packet error rate observed at the destination node for a n -hop connection can simply be calculated by evaluating the case for $i = n$.

Expanding (2.10) to avoid recursion, we obtain,

$$PER_i = 1 - \prod_{j=0}^{i-1} (1 - P_{j,j+1}) \quad \forall i, i \in \{1 \dots n\} \quad (2.11)$$

2.4.2 Multihop Selection Combining Diversity (MHSC)

Nodes involved in relaying can receive signals transmitted during previous hops and utilize them for diversity. Fig. 2.6 illustrates the multihop diversity concept.

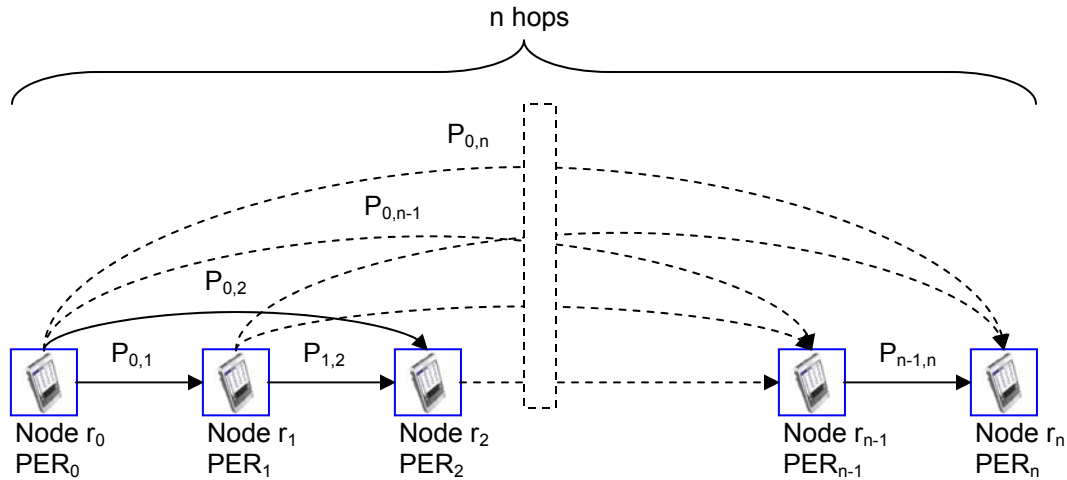


Fig. 2.6 – Multihop diversity.

As illustrated in the figure, it is assumed that all nodes involved in the route use diversity, not just the destination. Using multihop selection diversity, nodes receive signals from all previous nodes in the route and attempt to decode the multiple signals individually until the packet is decoded correctly. An advantage of using multihop forms of diversity is that their use is essentially “free” since they do not require resources such as transmit power or bandwidth (time slots) in addition to the resources already used in multihop relaying. However, there is added complexity at receivers. Fig. 2.7 illustrates simple receiver architecture for multihop selection diversity and Fig. 2.8 depicts a relaying example where nodes use MHSC diversity. As described by the figures, a receiver attempts to decode each signal received separately until the CRC indicates the packet was decoded correctly. Using our “best-effort” relaying approach, the i 'th node in a route, r_i , will receive a maximum of i independent signals from the previous i nodes in the route. If a node preceding the i 'th node fails to decode a packet they do not perform relaying and there will be less than i received signals.

The packet error rate observed at node r_i can be expressed as,

$$PER_i = \prod_{j=0}^{i-1} (PER_j + (1 - PER_j)P_{j,i}) \quad i \in \{1, 2, \dots, n\}. \quad (2.12)$$

This expression can be simplified as a function of the hop packet error rates similar to (2.11), $PER_i = f(P_{0,1}, P_{0,2}, P_{0,3}, \dots, P_{1,2}, P_{1,3}, \dots)$, however we choose to express it in its recursive form for simplicity. We also note that (2.12) incorporates the elimination of propagated error assumption. If there is a packet error earlier in the route at node $r_j, j < i$, then $PER_j = 1$ and $PER_j + (1 - PER_j)P_{j,i} = 1$.

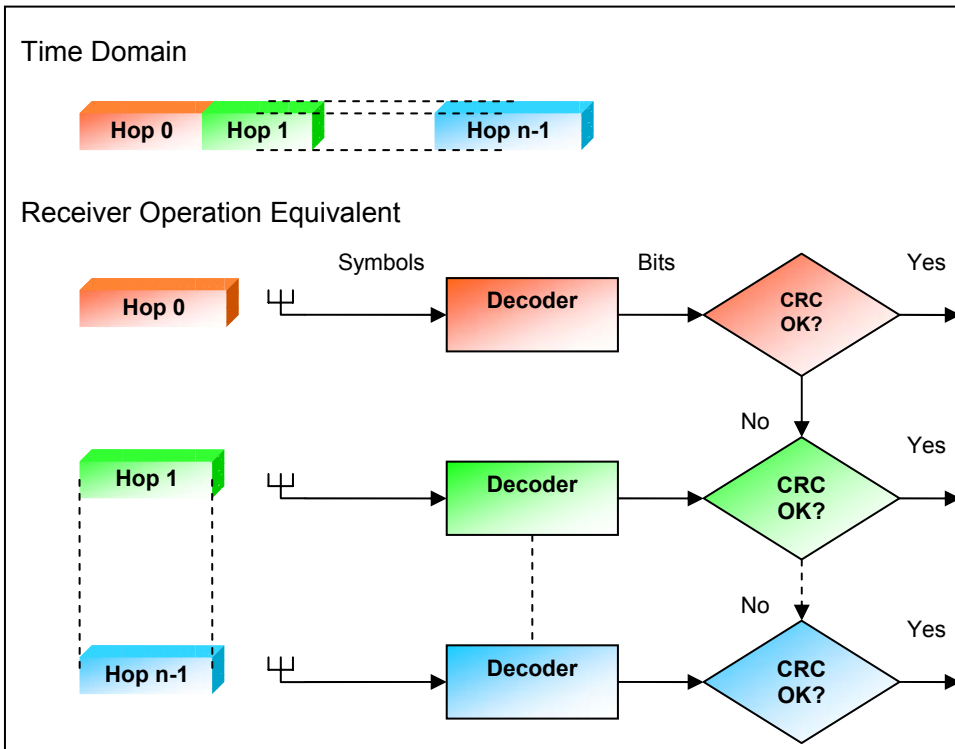


Fig. 2.7 – Receiver architecture for MHSC.

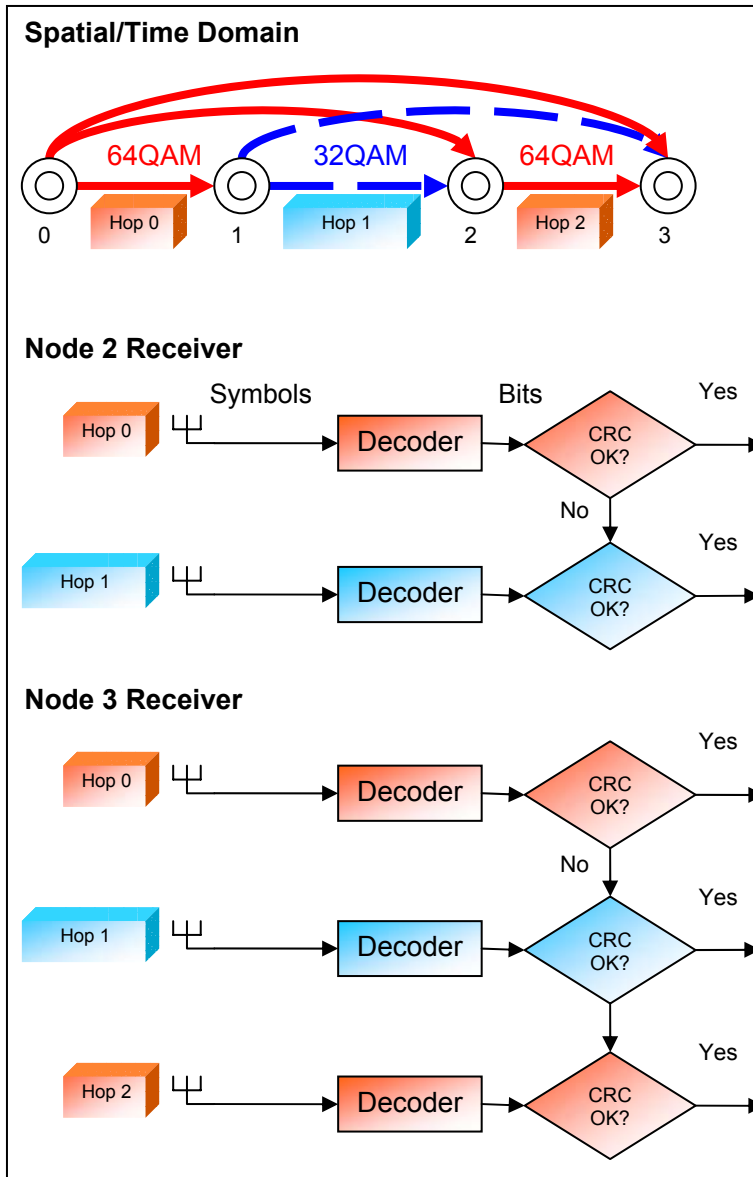


Fig. 2.8 – Example of MHSC and receiver operation.

2.4.3 Multihop Maximal Ratio Combining Diversity (MHMRC)

Multihop maximal ratio combining diversity incorporates the benefit of maximal ratio combining signals received on previous hops. Multiple signals transmitted during previous hops with similar modes can be MRC combined resulting in higher SNR and reduced PER of the resultant signal. Receivers perform multihop selection diversity for signals using dissimilar modes in a secondary stage. Fig. 2.9 illustrates a generalized

receiver architecture used in MRC combining nodes. The first stage of the receiver MRC combines received signals of similar mode, and the second stage selects a signal from the multiple branches (selection combining). The receiver is in effect a hybrid MRC/SC combiner. We also note that since packet transmissions occur during different times, the receiver is required to phase align signals to perform MRC using a post-detection receiver [25]. Buffering of the sampled analog waveform as soft symbols is performed as we receive packets before we MRC combine them. We ignore quantization errors introduced by sampling of the analog waveform.

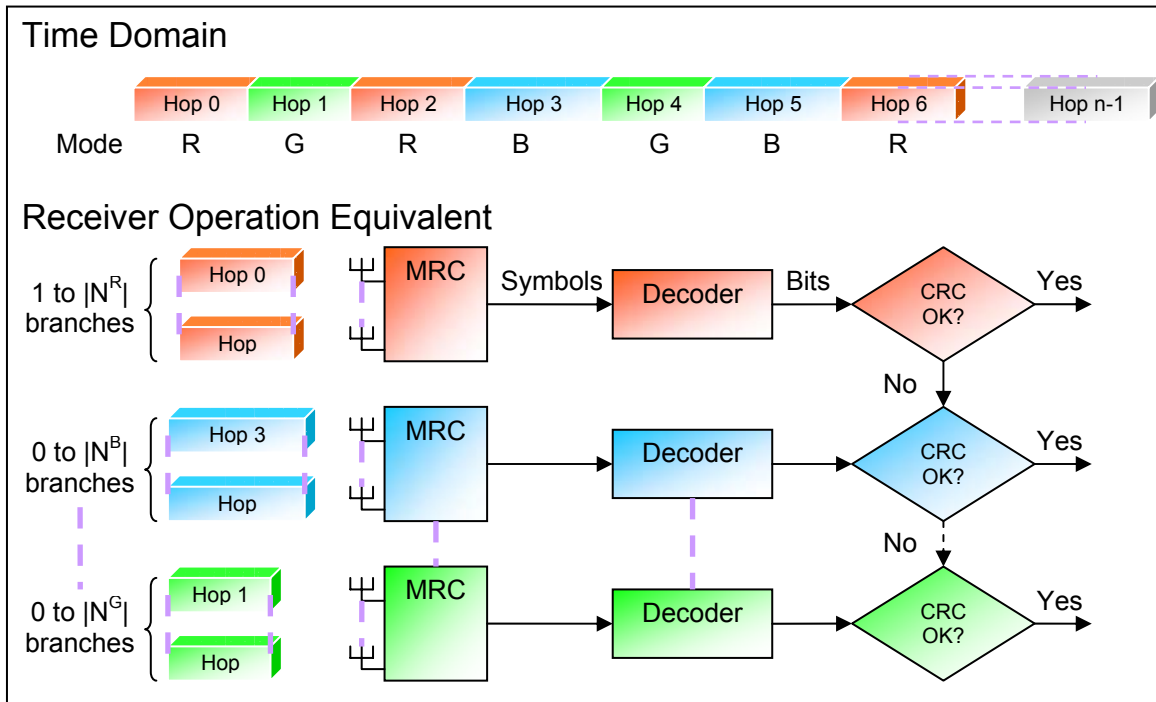


Fig. 2.9 – Receiver architecture for MHMRC.

For connections where nodes utilize diversity through MRC (which is indeed a hybrid selection combining and MRC scheme as illustrated in Fig. 2.9), the packet error rate seen at any node, r_i , is expressed as

$$PER_i = \prod_{m \in M} PER_i^{(m)}(N_i^{(m)}) \quad i \in \{1, 2, \dots, n\}, \quad (2.13)$$

where M denotes the set of possible AMC modes, m denotes the mode of the signals we are attempting to combine, and $N_i^{(m)}$ denotes the set of nodes transmitting with mode m :

$$N_i^{(m)} = \{j \mid m_{j,j+1} = m, j = \{0, 1, \dots, i-1\}\}.$$

$PER_i^{(m)}(N_i^{(m)})$ is the collective contribution of all the links using mode m (prior to node r_i) towards the reduction of the PER at node r_i , PER_i . This contribution will first depend on whether that particular m is used at all ($|N_i^{(m)}| > 0$) and if so whether selection combining ($|N_i^{(m)}| = 1$) or MRC ($|N_i^{(m)}| > 1$) is used:

$$PER_i^{(m)}(N_i^{(m)}) = \begin{cases} 1 & \text{if } |N_i^{(m)}| = 0 \\ PER_j + (1 - PER_j)P_{j,i} & \text{if } |N_i^{(m)}| = 1 \text{ with } N_i^{(m)} = \{j\} \\ E(P_i^{(m)}) & \text{if } |N_i^{(m)}| > 1 \end{cases} \quad (2.14)$$

$E(P_i^{(m)})$ is the mean PER, when MRC is used, of the signal received at node r_i from the previous nodes transmitting with mode m :

$$E(P_i^{(m)}) = \sum_{N \in 2^{N_i^{(m)}} - \phi} \left[\left(\prod_{k \in N_i^{(m)}} PER_k^{1-I_k(N)} \cdot (1 - PER_k)^{I_k(N)} \right) \cdot P_i \left(\sum_{j \in N} SNR_{j,i}, m \right) \right] + \prod_{k \in N_i^{(m)}} PER_k \quad (2.15)$$

where $I_k(N) = \begin{cases} 1 & \text{if } k \in N \\ 0 & \text{otherwise} \end{cases}$ is the indicator function.

In the above, $SNR_{j,i}$ represents the SNR of the signal received at node r_i from node r_j : $SNR_{j,i} = P_t G_{j,i} / \eta_i$. Here P_t is the transmit power, $G_{j,i}$ is the link gain between nodes r_j

and r_i , and η_i is the noise (and interference, if any). It is well known that when MRC is used the overall SNR after combining is equal to the sum of the branch SNRs [27].

$P_i\left(\sum_{j \in N} SNR_{j,i}, m\right)$ is the corresponding PER for mode m (read from the lookup table produced from Fig. 2.1).

The $E(P_i^{(m)})$ expression is complicated by the fact that nodes only relay a packet if it was received correctly. Therefore the $P_i\left(\sum_{j \in N} SNR_{j,i}, m\right)$ expression has to be weighted by the probability that a number of nodes using mode m are indeed transmitting and some others are not; the $\prod_{k \in N_i^{(m)}} PER_k^{1-I_k(N)} \cdot (1 - PER_k)^{I_k(N)}$ expression is this weighting coefficient. This process has to be repeated for all possible transmit/non-transmit combinations; the outer summation stands for this purpose. Here $2^{N_i^{(m)}}$ denotes the power set of $N_i^{(m)}$ which contains all combinations of node transmission. The PER for the case of no node transmitting, $N = \phi$, is given by the stand alone expression $\prod_{k \in N_i^{(m)}} PER_k$.

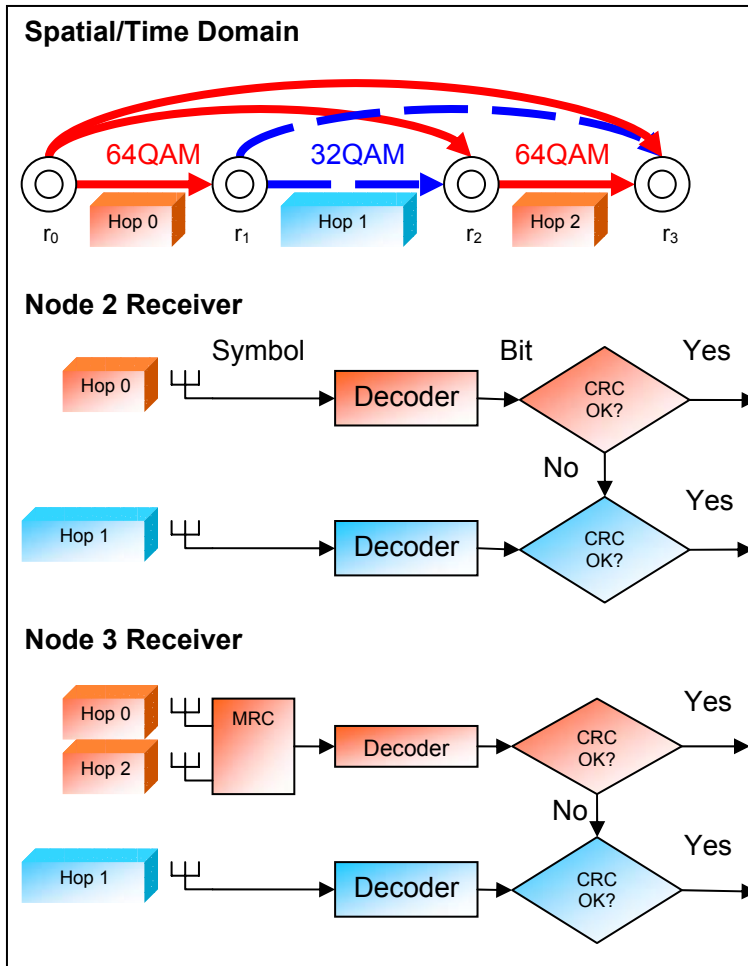


Fig. 2.10 – Example of MHRMRC and receiver operation.

Example (MHRMRC):

An example scenario (similar to Fig. 2.9) describing MHRMRC receiver operation is depicted in Fig. 2.10. From the diagram, node r_1 simply receives a single $64QAM$ signal from the source, node r_0 . Node r_2 receives the same $64QAM$ signal transmitted from node r_0 to node r_1 as well as a relayed $32QAM$ signal from node r_1 . Node r_2 can only utilize the two dissimilar mode signals using multihop selection diversity, as shown by the receiver operation in Fig. 2.8. The destination node, node r_3 , receives $64QAM$ signals from both node r_0 and node r_2 as well as the $32QAM$ signal from node r_1 . The destination node MRC combines the two $64QAM$ signals and uses multihop selection

diversity by decoding both the $64QAM$ and $32QAM$ branch. At node r_3 , $N_3^{(32QAM)} = \{1\}$ and $N_3^{(64QAM)} = \{0, 2\}$. To calculate the packet error rate at node r_3 , we have,

$$PER_3 = PER_3^{32QAM}(N_3^{(32QAM)}) \cdot PER_3^{64QAM}(N_3^{(64QAM)}) \quad (2.16)$$

Here $N_3^{(32QAM)} = \{1\}$, $|N_3^{(32QAM)}| = 1$, and

$$PER_3^{(32QAM)}(N_3^{(32QAM)}) = PER_1 + (1 - PER_1)P_{1,3}. \quad (2.17)$$

$N_3^{(64QAM)} = \{0, 2\}$, $|N_3^{(64QAM)}| = 2$, and

$$PER_3^{(64QAM)}(N_3^{(64QAM)}) = E(P_3^{(64QAM)}). \quad (2.18)$$

The power set of $N_3^{(64QAM)}$, written as $2^{N_3^{(64QAM)}} = \{ \phi, \{0\}, \{2\}, \{0, 2\} \}$, is used to determine whether no nodes, only node r_0 , only node r_2 , or both nodes relayed a packet.

Each event is weighted when calculating mean packet error rate, $E(P_3^{(64QAM)})$, given by,

$$\begin{aligned} E(P_3^{(64QAM)}) &= PER_0 PER_2 + (1 - PER_0) PER_2 \cdot P_3(SNR_{0,3}, 64QAM) \\ &\quad + PER_0 (1 - PER_2) \cdot P_3(SNR_{2,3}, 64QAM) \\ &\quad + (1 - PER_0)(1 - PER_2) \cdot P_3(SNR_{0,3} + SNR_{2,3}, 64QAM) \end{aligned}$$

Since node r_0 is the source and is always transmitting, $PER_0 = 0$, and

$$\begin{aligned} E(P_3^{(64QAM)}) &= (1 - PER_0) PER_2 \cdot P_3(SNR_{0,3}, 64QAM) \\ &\quad + (1 - PER_0)(1 - PER_2) \cdot P_3(SNR_{0,3} + SNR_{2,3}, 64QAM). \end{aligned} \quad (2.19)$$

The packet error rate at node r_3 can be obtained by substituting (2.19), (2.18), and (2.17) into (2.16).

Also note that all nodes in the route do not necessarily perform MRC combining. In Fig. 2.10 for example, node r_2 only performs selection combining. If for all modes, the receiver receives at most one signal for all modes, $|N_i^{(m)}| = 1, \forall m \in M$, then,

$$\begin{aligned}
PER_i &= \prod_{m \in M} PER_i^{(m)}(N_i^{(m)}) = \prod_{\substack{j \in N_i^{(m)} \\ m \in M}} PER_j + (1 - PER_j)P_{j,i} \\
&= \prod_{j=0}^{i-1} (PER_j + (1 - PER_j)P_{j,i}) \quad i \in \{1, 2, \dots, n\}
\end{aligned}$$

This implies that in the situation where received signals use dissimilar modes, MHMRC diversity behaves as MHSC diversity since nodes cannot MRC combine signals using dissimilar modes. In the worst case, a route using MHMRC diversity will perform similar to only using MHSC diversity.

2.4.4 Hybrid Digital Analog Relaying

MHMRC performance may be increased by permitting nodes to relay incorrectly detected signals as analog signals. This increases the number of signals to MRC combine at receivers and may reduce PER. A relaying node will relay a digital signal when correctly detected, and it will relay an analog signal otherwise. We call this an HDAR system. The PER at node r_i can be similarly using (2.13) and (2.14) but the mean packet error rate of the branch using mode m from (2.15) becomes

$$\begin{aligned}
E(P_i^{(m)}) &= \sum_{N \in 2^{N_i^{(m)}} - \phi} \left[\left(\prod_{k \in N_i^{(m)}} PER_k^{1-I_k(N)} \cdot (1 - PER_k)^{I_k(N)} \right) \times P_i \left(\sum_{j \in N_i^{(m)}} SNR_{j,i}, m \right) \right] + \\
&\quad \prod_{k \in N_i^{(m)}} PER_k, \quad (2.19)
\end{aligned}$$

$$\text{where } SNR_{j,i} = \begin{cases} P_t G_{j,i} / \eta_i & j \in N \\ S_{j,i}(N_i^{(m)}, N) & j \in N_i^{(m)} - N \end{cases}$$

When node r_j detects the packet correctly it is able to relay digitally, $j \in N$, and the SNR contribution of the signal received at node r_i from node r_j is $SNR_{j,i} = P_t G_{j,i} / \eta_i$. If node r_j

failed to detect the packet, $j \in N_i^{(m)} - N$, it will resort to analog relaying. The contribution of the analog signal to the SNR at the MRC combiner is given by

$$S_{j,i}(N_i^{(m)}, N) = \begin{cases} \frac{P_t \prod_{k=1}^{|U|-2} a_{u_k} \prod_{k=0}^{|U|-2} G_{u_k, u_{k+1}}}{\eta_i + \sum_{k=1}^{|U|-2} \eta_{u_k} \prod_{k=1}^{|U|-2} a_{u_k} G_{u_k, u_{k+1}}} & \exists s \in N \\ 0 & \text{otherwise} \end{cases} \quad (2.20)$$

In order for node r_j to relay, a digital node transmitting with mode m is required as a source to begin the chain of analog relaying. This node r_s must be upstream to node r_j in the route,

$$s = \max_{l \in N} (l < j),$$

when r_j is relaying an analog signal. However if there is no digital source upstream to node r_j then it cannot relay a signal and the SNR contribution is $S_{j,i}(N_i^{(m)}, N) = 0$. When there exists a digital node upstream to node r_j , $\exists s \in N$, to calculate the SNR contribution in (2.20) we consider a chain of relaying nodes given by the ordered set

$$U(N_i^{(m)}, N) = \{s\} \cup \{l \mid s < l \leq j, l \in N_i^{(m)} - N\} \cup \{i\}.$$

This set of nodes is ordered according to the order of nodes in the route: $U(N_i^{(m)}, N) = (u_0, u_1, \dots, u_{|U|-2}, u_{|U|-1})$ where $u_0 = s$, $u_{|U|-2} = j$, $u_{|U|-1} = i$ and the remaining are intermediate analog relaying nodes. For formatting purposes $U(N_i^{(m)}, N)$ and U are used interchangeably in equation (2.20). In expression (2.20) the amplification factor at any node r_{u_k} is given by

$$a_{u_k} = P_t / (P_t G_{u_{k-1}, u_k} + \eta_{u_k}), \quad k \geq 1. \quad (2.21)$$

Note that $k \geq 1$ since $u_{k=0} = s$ and r_s is the digital source in the chain of analog relaying nodes and does not perform amplification. From the above expression we see that the amplification factor accounts for amplifying the received power ($P_r G_{j,i}$) and noise power (η_i) such that the average output power is P_t [2]. It is assumed all nodes transmit with power P_t . Fig. 2.11 illustrates the concept of amplification at relaying nodes.

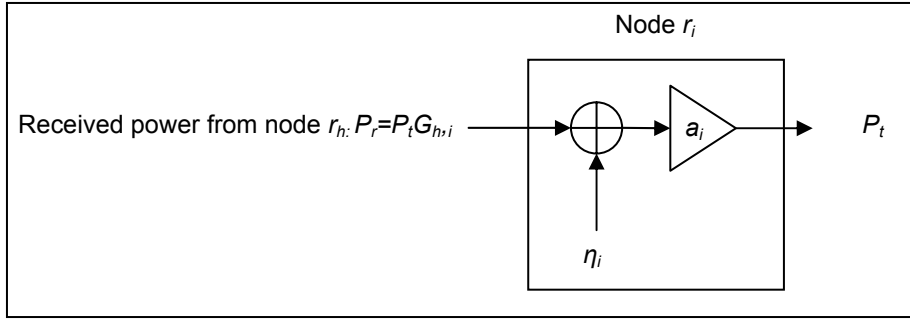


Fig. 2.11 – Amplification in analog relaying

Example (HDAR):

As a simple example, let us again consider the scenario from Fig. 2.10 where we calculate the packet error rate at node r_3 . Steps follow similarly as the MHMRC example up to equation (2.18). Then the power set of $N_3^{(64QAM)}$, written as $2^{N_3^{(64QAM)}} = \{ \phi, \{0\}, \{2\}, \{0, 2\} \}$, is used to determine whether no nodes, only node r_0 , only node r_2 , or both nodes relayed a packet digitally. According to (2.20) we have

$$E(P_3^{(64QAM)}) = \sum_{N \in 2^{N_3^{(64QAM)}} - \phi} A_N + \prod_{k \in N_3^{(64QAM)}} PER_k = A_{N=\{0\}} + A_{N=\{2\}} + A_{N=\{0,2\}} + PER_0 PER_2,$$

$$\text{where } A_N = \left(\prod_{k \in N_3^{(64QAM)}} PER_k^{1-I_k(N)} \cdot (1 - PER_k)^{I_k(N)} \right) \times P_3 \left(\sum_{j \in N_3^{(64QAM)}} SNR_{j,i}, m \right).$$

Since node r_0 is the source, it will always transmit a packet in digital form ($PER_0 = 0$) and

$$E(P_3^{(64QAM)}) = A_{N=\{0\}} + A_{N=\{0,2\}}. \quad (2.22)$$

From above, $A_{N=\{0,2\}}$, the event that both r_0 and r_2 relay digitally, is given by

$$A_{N=\{0,2\}} = (1 - PER_0)(1 - PER_2) \cdot P_3(SNR_{0,3} + SNR_{2,3}, 64QAM). \quad (2.23)$$

This same term appears in the MHMRC example in (2.18). Since these are digital signals we have $SNR_{0,3} = P_t G_{0,3} / \eta_3$ and $SNR_{2,3} = P_t G_{2,3} / \eta_3$. To calculate the event that node r_0 relays the packet digitally and node r_2 relays in analog form we have

$$A_{N=\{0\}} = (1 - PER_0)PER_2 \cdot P_3(SNR_{0,3} + S_{2,3}(N_3^{(64QAM)}, N), 64QAM). \quad (2.24)$$

To calculate $S_{2,3}(N_3^{(64QAM)}, N)$, the SNR of the relayed analog signal from node r_2 ($j = 2$), we first determine the immediate preceding digital relaying node given by

$$s = \max_{l \in N}(l < j) = \max_{l \in N}(l < 2) = 0. \text{ (Since } N = \{0\}.)$$

This means node $r_s = r_0$ is the digital source in the chain of analog relaying nodes. Then the ordered set of nodes is given by

$$U(N_3^{(64QAM)}, N) = \{0\} \cup \{l \mid 0 < l \leq 2, l \in N_3^{(64QAM)} - N\} \cup \{3\} = \{0\} \cup \{2\} \cup \{3\} = (0, 2, 3).$$

To clarify, $u_0 = 0$, $u_1 = 2$, $u_2 = 3$. Then the chain of relaying nodes transmitting with mode $64QAM$ is r_0, r_2, r_3 . Here $|U(N_3^{(64QAM)}, N)| = 3$. We can then calculate the SNR of

the analog signal received at node r_3 from node r_2 as

$$S_{2,3}(N_3^{(64QAM)}, N) = \frac{P_t \prod_{k=1}^{|U|-2} a_{u_k} \prod_{k=0}^{|U|-2} G_{u_k, u_{k+1}}}{\eta_i + \sum_{k=1}^{|U|-2} \eta_{u_k} \prod_{k=1}^{|U|-2} a_{u_k} G_{u_k, u_{k+1}}} = \frac{P_t a_2 G_{0,2} G_{2,3}}{\eta_3 + \eta_2 a_2 G_{2,3}}. \quad (2.25)$$

Here the amplification at node r_2 is $a_2 = P_t / (P_t G_{0,2} + \eta_2)$. This is the amplification factor applied to the signal received from node r_0 at node r_2 . This amplified signal is then relayed to node r_3 .

Finally we can calculate $E(P_3^{(64QAM)})$ by combining (2.25), (2.24), and (2.23) back into (2.20). (2.22), (2.18), and (2.17) can then be combined to obtain PER_3 in (2.16).

Chapter 3

Routing Strategies

Relaying node selection, or routing, is a critical function in multihop networks. The performance of these networks is significantly dependent on the intelligence of routing. Similar to wire-line routing, current wireless routing strategies consider only single point-to-point links in routes as described by Fig. 2.3. These strategies do not consider the benefits of multihop diversity involved in relaying, shown in Fig. 2.6.

In this chapter we use the frame allocation and packet error rate models introduced in the previous chapter to formulate a simple relaying metric and relay node selection algorithms designed to maximize throughput and extend coverage in TDMA networks using multihop diversity. Finally we define a throughput maximization algorithm designed to maximize throughput by selecting modulation and coding modes to better utilize multihop maximal ratio combining when relaying.

3.1 Routing Metric

In a high-data rate system, we would ideally like to maximize the throughput. Thus, a metric to be used for routing can be derived from the throughput expression. We define the end-to-end throughput for a n -hop connection as

$$T_n = F \cdot s_{i-1,i} D_{i-1,i} (1 - PER_n) \quad i \in \{1, 2, \dots, n\}. \quad (3.1)$$

Here $s_{i-1,i}$ is the symbols/frame of the $i-1$ 'th hop, $D_{i-1,i}$ is the modulation efficiency in bits/symbol of the $i-1$ 'th hop and F represents frame frequency with unit frame/sec. PER_n represents the connection packet error rate observed at the destination node, r_n .

Using equations (3.1) and (2.9), the throughput expression can be further expanded to obtain the metric expression for a n -hop connection as

$$C_n = T_n = F \frac{S_c}{\sum_{j=1}^n \frac{D_{i-1,i}}{D_{j-1,j}}} D_{i-1,i} (1 - PER_n) \quad i \in \{1, 2, \dots, n\}.$$

Ignoring constants S_c and F , the metric becomes

$$C_n = \frac{(1 - PER_n)}{\sum_{i=1}^n \frac{1}{D_{i-1,i}}}. \quad (3.2)$$

To facilitate expression of routing algorithms, the metric is rewritten as

$$C(R_d, M_d) = \frac{(1 - PER_n)}{\sum_{i=0}^{n-1} \frac{1}{D_i}}. \quad (3.3)$$

For n -hop connections, $R_d = (r_0 \ r_1 \ \dots \ r_n)$ and $M_d = (m_0 \ m_1 \ \dots \ m_{n-1})$. R_d is a n -hop route used to relay data to node d and is an ordered set consisting of $n+1$ relaying nodes where r_i denotes the i 'th relaying node in the route. The final node in the ordered set is the destination, node d , $r_n = d$. r_0 denotes the source; this will always be the central controller in the downlink scenario. M_d is an ordered set of modes used on hops, where m_i denotes the mode of the i 'th hop between nodes r_i and r_{i+1} . A n -hop connection contains n modes. D_i is simply the modulation efficiency in bits/sym of the i 'th hop between nodes r_i and r_{i+1} using mode m_i for that hop ($D_i = D_{i,i+1}$). PER_n is the packet error rate seen at the destination node, r_n . The PER_n expression may be evaluated using equations (2.11) or (2.12) if we are using multihop (no diversity) or MHSC respectively. Expressions (2.13), (2.14), and (2.15) are used if nodes utilize MHMRC diversity and expressions (2.13), (2.14), (2.19), (2.20), and (2.21) are used if nodes utilize HDAR.

Routing algorithms calculate the metric to evaluate multihop connections in the downlink. Since the metric is derived from the throughput expression, selecting routes generating larger metrics maximizes throughput. A larger metric indicates a connection with greater throughput. In the routing phase, the router will select routes that generate the largest possible metric or maximum throughput.

To perform routing, an effective method to estimate link packet error rates, $P_e(SNR, m)$, is required to calculate routing metrics. Global channel-state (link SNR) updates between all nodes and packet error rate look-up tables (or mathematical functions) for the channel are prerequisites to estimating packet error rates [19]. Fig. 2.1 provides us with packet error rate look-up tables. We also note that channel measurement additionally provides performance gains regardless of varying radio-link quality.

However, a drawback to using channel-state information in routing is the increased traffic overhead involved in updating the AP with the necessary information. For example, a network with M nodes using AMC will require M channel-state updates per unit time (between the AP and all other M nodes). In comparison the same network using routing will require $M(M-1)/2$ updates per unit time (between all $M+1$ nodes including the AP). Using GPS or other location techniques, the number of updates may be reduced if a node limits its updates to only those links to neighboring nodes located within a set distance from itself [18].

3.2 Multihop Routing Algorithms

The routing algorithms in this thesis can find relaying routes that provide maximized throughput for a multihop connection using the metric given by expression (3.3). Here we define two algorithms, adapted from the Bellman-Ford algorithm [1, 8],

capable of finding routes with throughput greater than or equal to optimal 2-hop routes.

The algorithms attempt to efficiently find routes in the network such that routes generate larger metrics and hence throughputs. The algorithms are described as follows,

Algorithm 3.1 - Multihop (MH) Routing

```

 $k = 0$ 
 $N_c^{(0)} = N_m$ 
 $\forall i, R_i^{(0)} = (cc, i), M_i^{(0)} = (m_{cc,i}^{(max)})$ 
while  $|N_c^{(k)}| > 0$  AND  $k < k^{(max)}$ 
     $N_c^{(k+1)} = \{\}$ 
     $\forall i, R_i^{(k+1)} = R_i^{(k)}, M_i^{(k+1)} = M_i^{(k)}$ 
    for all  $s \in N_c^{(k)}$ 
        for all  $d \in N - R_s^{(k)}$ 
            if  $C(R_s^{(k)} \cup \{d\}, M_s^{(k)} \cup \{m_{s,d}^{(max)}\}) > C(R_d^{(k+1)}, M_d^{(k+1)})$  then
                 $R_d^{(k+1)} = R_s^{(k)} \cup \{d\}$ 
                 $M_d^{(k+1)} = M_s^{(k)} \cup \{m_{s,d}^{(max)}\}$ 
                 $N_c^{(k+1)} = N_c^{(k+1)} \cup \{d\}$ 
            end if
        end for
    end for
     $k = k + 1$ 
end while

```

Algorithm 3.2 - Multihop Adaptive Modulation & Coding (MHAM) Routing

```

 $k = 0$ 
 $N_c^{(0)} = N_m$ 
 $\forall i, R_i^{(0)} = (cc, i), M_i^{(0)} = (m_{cc,i}^{(max)})$ 
while  $|N_c^{(k)}| > 0$  AND  $k < k^{(max)}$ 
     $N_c^{(k+1)} = \{\}$ 
     $\forall i, R_i^{(k+1)} = R_i^{(k)}, M_i^{(k+1)} = M_i^{(k)}$ 
    for all  $s \in N_c^{(k)}$ 
        for all  $d \in N - R_s^{(k)}$ 
            for all  $m \in M_s^{(k)} \cup \{m_{s,d}^{(max)}\}$ 

```

```

    if  $C(R_s^{(k)} \cup \{d\}, M_s^{(k)} \cup \{m\}) > C(R_d^{(k+1)}, M_d^{(k+1)})$ 
         $R_d^{(k+1)} = R_s^{(k)} \cup \{d\}$ 
         $M_d^{(k+1)} = M_s^{(k)} \cup \{m\}$ 
         $N_c^{(k+1)} = N_c^{(k+1)} \cup \{d\}$ 
    end if
end for
end for
end for
 $k = k + 1$ 
end while

```

Where,

N = set of all nodes, not including the central controller

N_m = set of all mobile nodes

cc = element symbol denoting the central controller (AP) node

i, s, d = element symbol denoting a particular node

k = iteration

$k^{(max)}$ = maximum iterations limit

$N_c^{(k)}$ = set of nodes which have a route change at iteration n

$R_i^{(k)}$ = ordered set of nodes in relay route to node i at iteration n

$M_i^{(k)}$ = ordered set of modes used on hops in relay route to node i at iteration n

$m_{i,j}^{(max)}$ = hop mode between nodes i and j, selected by expression (2.6)

$C(R, M)$ = routing metric to the destination node in the ordered set R, using the ordered set M of modes used on hops

We define $C=A \cup B=(a_0, a_1, \dots a_{n-1}, b_0, b_1, \dots b_{m-1})$ where A and B are ordered sets containing n and m elements respectively, and the resultant ordered set C contains $n+m$ elements.

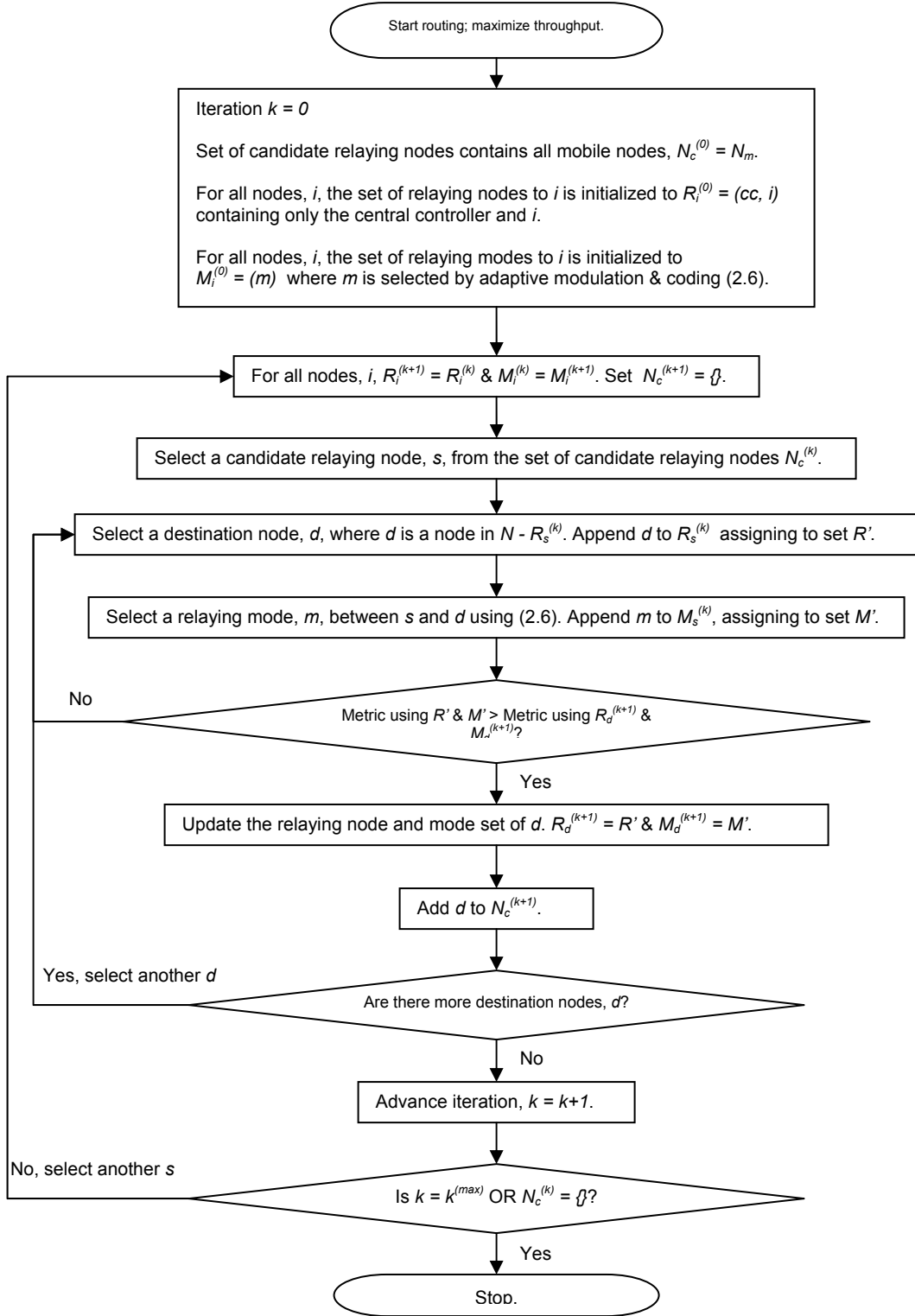


Fig. 3.1 – MH routing flowchart.

Fig. 3.1 illustrates algorithm 3.1 using a flowchart. Initially nodes begin with single-hop routes from the central controller to the node, $R_i^{(0)} = (cc, i) \forall i$. Similarly

the hop modes are selected according to expression (2.6), $M_i^{(0)} = (m_{cc,i}^{(max)}) \forall i$. For every iteration, n , we examine all routes, $R_s^{(k)}$, from the set of candidate relaying nodes, $s \in N_c^{(k)}$, to all other candidate destination nodes, $d \in N - R_s^{(k)}$. Initially the candidate relaying node set $N_c^{(k)}$ contains all mobile nodes, the set N_m . Candidate destination nodes are limited to those nodes not already in the relaying nodes route, $R_s^{(k)}$. A potential route to node d is created by appending node d to the route of the candidate relaying node, written as $R_s^{(k)} \cup \{d\}$. Similarly a potential hop mode set is formed from the candidate relaying nodes set of hop modes, written as $M_s^{(k)} \cup \{m_{s,d}^{(max)}\}$. Any potential route/mode set generating a higher metric than the destinations route/mode set, $R_d^{(k+1)}$ and $M_d^{(k+1)}$, will replace the set for node d on the next iteration. The node will be added to the candidate relaying node set for the next iteration, $N_c^{(k+1)}$. At the beginning of an iteration $N_c^{(k)}$ is set to $N_c^{(k+1)}$ and $N_c^{(k+1)}$ is set to the null set. The next iteration routes/modes are set to the current routes/modes for all nodes, $R_i^{(k+1)} = R_i^{(k)}$ and $M_i^{(k+1)} = M_i^{(k)}$. The next iteration routes/modes are built from the routes/modes from the previous iteration which generated maximum metrics, $R_{i \in N_c^{(k)}}$ and $M_{i \in N_c^{(k)}}$. Since $N_c^{(k)}$ contains only the nodes which had a route change from the previous iteration, we cull previously examined routes and reduce processing complexity. The algorithm will iterate until we have reached our iteration limit $k^{(max)}$ or $N_c^{(k)}$ is the null set at the beginning of an iteration, indicating nodes were not added to process for the next iteration. Potential routes in the next iteration will not provide a greater metric than routes in the current iteration and the algorithm stops

searching. Routes and hop modes used in the current iteration provide maximum throughput for relaying.

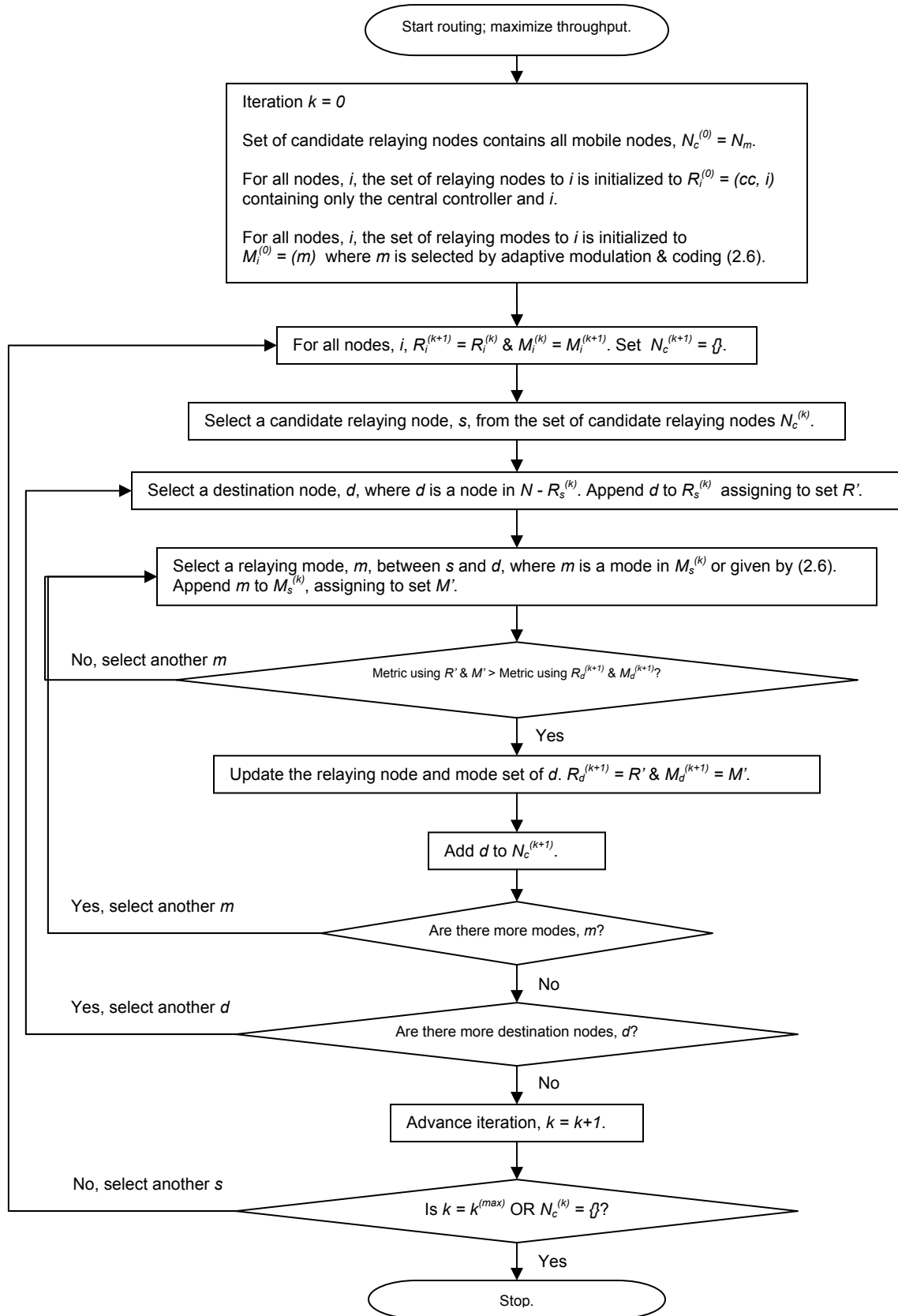


Fig. 3.2 – MHAM routing flowchart.

The second algorithm is an improved version of the first algorithm in that it incorporates adaptive modulation and coding maximization while performing route discovery. Fig. 3.2 describes the algorithm using a flowchart. Algorithm 3.1 automatically selected hop modes between node s and node d , $m_{s,d}^{(\max)}$, according to (2.6). Algorithm 3.2 selects modes to better take advantage of MRC combining at nodes to improve end-to-end throughput. For the last hop, it attempts to use modes from the set of modes which have been used in previous hops in the route, $m \in M_s^{(n)} \cup \{m_{s,d}^{(\max)}\}$. By restricting modes to only those used in previous hops, we reduce processing while using only those modes which may benefit MRC combining at receivers. Increased number of signals of similar mode increases the effectiveness of MRC combining and reduces the packet error rate observed at the destination. Setting a hop mode to lower efficiency modulation will increase frame fragmentation while reducing packet error rate. Conversely, changing to a mode with increased modulation efficiency will reduce frame fragmentation but increase the hop packet error rate. We calculate the metric to evaluate the effect of mode changes factoring both frame fragmentation and packet error rate. The mode generating the maximum metric is added to the mode set for the destination node,

$$M_d^{(k+1)} = M_s^{(k)} \cup \{m\}.$$

3.3 Adaptive Modulation and Coding Maximization (AMCM)

Modulation and coding maximization can occur after the MH algorithm has found routes. Using MH followed by AMCM differs from using MHAM since the two different algorithms may select different routes. MHAM considers modulation and coding maximization while performing routing thereby different routes may be chosen.

However, MHAM is limited to maximizing the mode in the last hop with knowledge of preceding hops (no knowledge of subsequent hops on further iterations) whereas AMCM can maximize knowing the full set of modes. While AMCM can be performed after routes have been selected using MHAM we did not include the results in this thesis since the gains obtained were minimal. The following AMCM algorithm alters hop modes to maximize throughput for the destination, node d , after the route, R_d , has been selected using the MH algorithm.

Algorithm 3.3 - Adaptive modulation and coding maximization (AMCM)

```

 $k = 0$ 
 $h^{(max)} \neq h$ 
 $M_d^{(max)} = M_d^{(0)}$ 
do
  for all  $h = 0$  to  $|M_d^{(0)}| - 1$  and  $h \neq h^{(max)}$ 
    for all  $m \in M_d^{(0)} - m_h^{(k)}$ 
       $M_d^{(k+1)} = M_d^{(k)}$ 
       $m_h^{(k+1)} = m$ 
      if  $C(R_d, M_d^{(k+1)}) > C(R_d, M_d^{(max)})$  then
         $M_d^{(max)} = M_d^{(k+1)}$ 
         $h^{(max)} = h$ 
      end if
    end for
  end for
   $M_d^{(k+1)} = M_d^{(max)}$ 
   $k = k + 1$ 
while  $M_d^{(k)} \neq M_d^{(k-1)}$ 

```

Where,

h = hop index

$h^{(max)}$ = hop index of the mode change generating the maximum metric

$m_h^{(k)}$ = the h 'th mode in the ordered set $M_d^{(k)} = (m_0 \ m_1 \ \dots \ m_{x-1})$

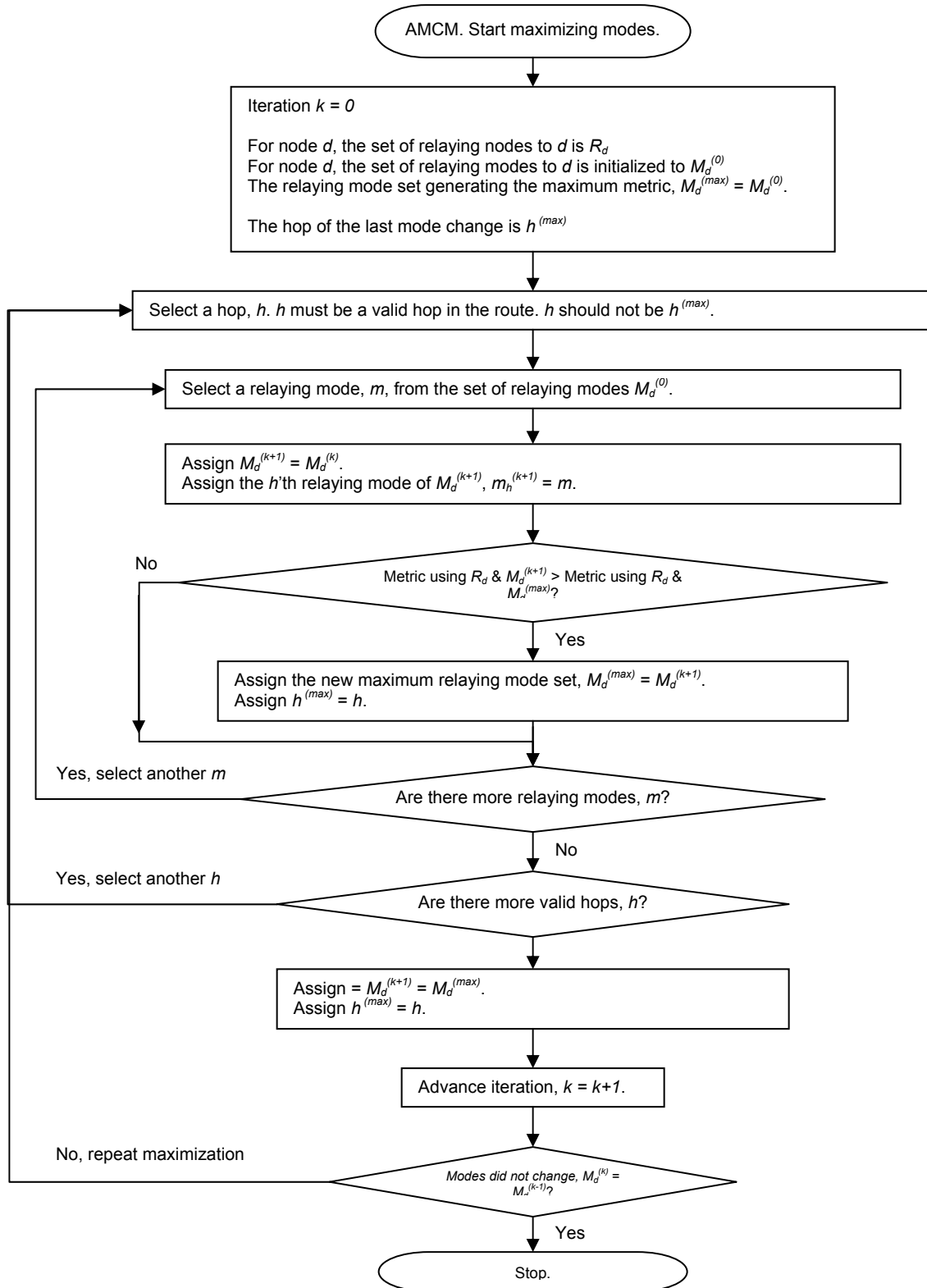


Fig. 3.3 – AMCM flowchart.

Fig. 3.3 illustrates the AMCM algorithm. Every iteration, the algorithm selects the mode for a hop, h , which generates the maximum possible metric for the destination, node d . Only a single mode can be changed per iteration. Candidate modes are limited to the set of modes used in the connection, $m \in M_d^{(0)} - m_h^{(k)}$, thereby reducing processing complexity. When processing candidate modes for a particular hop, h , we avoid using the mode used by the hop in the current iteration, $m_h^{(k)}$. The selected mode generates a metric greater than any other candidate mode change. When the metric can not be increased by mode changes, $M_d^{(k)} = M_d^{(k+1)}$, the algorithm stops, and the selected hop modes generate a maximum metric.

3.4 Examples of Algorithms

The routing algorithms can be viewed as a trellis containing the routes to nodes in the network. The path through the trellis to a node denotes the route in the network generating the maximum metric/throughput for the particular node. Figures 3.4, 3.5, and 3.6 illustrate an example of routing and provide insight into the algorithms. Table 3.1 accompanies the figures and summarizes routing calculations. (These examples and illustrations are arbitrary.)

Table 3.1 – Example routing calculations

Iteration, k	Candidate relaying nodes, $N_c^{(n)}$	Current routes, $R_d^{(n)}$	Next routes, $R_d^{(n+1)}$
0	{A, B, C, D, E}	$R_A = (AP, A)$ $R_B = (AP, B)$ $R_C = (AP, C)$ $R_D = (AP, D)$ $R_E = (AP, E)$	$R_A = (AP, A)$ $R_B = (AP, A, B)$ $R_C = (AP, E, C)$ $R_D = (AP, D)$ $R_E = (AP, E)$
1	{B, C, E}	$R_A = (AP, A)$ $R_B = (AP, A, B)$ $R_C = (AP, E, C)$	$R_A = (AP, A)$ $R_B = (AP, A, B)$ $R_C = (AP, A, E, C)$

		$R_D = (AP, D)$ $R_E = (AP, E)$	$R_D = (AP, E, C, D)$ $R_E = (AP, A, E)$
2	{C, D}	$R_A = (AP, A)$ $R_B = (AP, A, B)$ $R_C = (AP, A, E, C)$ $R_D = (AP, E, C, D)$ $R_E = (AP, A, E)$	$R_A = (AP, A)$ $R_B = (AP, A, B)$ $R_C = (AP, A, E, C)$ $R_D = (AP, E, C, D)$ $R_E = (AP, A, E)$
3	{}	$R_A = (AP, A)$ $R_B = (AP, A, B)$ $R_C = (AP, A, E, C)$ $R_D = (AP, E, C, D)$ $R_E = (AP, A, E)$	

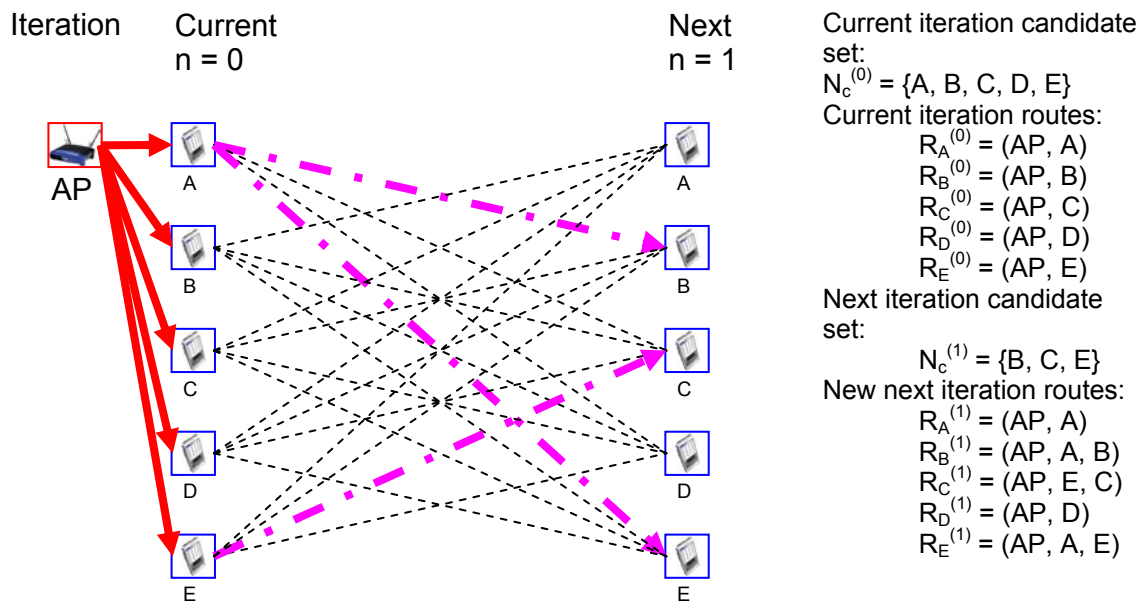


Fig. 3.4 – Routing example: Iteration 1.

The small network contains an AP node and five mobile nodes denoted by A, B, C, D, and E. In the first iteration, $k = 0$, illustrated in Fig. 3.4, all connections contain only the AP and the destination node in the route. Current routes are drawn as thick arrows to nodes. All current routes are single hop. The algorithm evaluates all possible routes from a node to all other nodes using the nodes current route. The nodes examined are determined by the candidate relaying node set $N_c^{(k)}$; initially the set contains all mobile nodes. For the k 'th iteration, we examine routes with $k+1$ hops. Routes that are examined for the iteration are drawn as dashed arrows. Routes to nodes which yield a

larger metric than the nodes current route will be used on the next iteration. These routes are drawn as thick irregular dashed lines. For nodes A and D, we notice that no routes yield a larger metric than their current route. The route $R_A^{(0)} = (AP, A)$ generates a larger metric, $C(R_A^{(0)}, M_A^{(0)}) > C(R_A^{(1)}, M_A^{(1)})$, where $R_A^{(1)}$ can be possible two-hop routes of $R_A^{(1)} = (AP, B, A)$, $R_A^{(1)} = (AP, C, A)$, $R_A^{(1)} = (AP, D, A)$, or $R_A^{(1)} = (AP, E, A)$. For nodes B, C, and E a two-hop route provides a greater metric than the metric of the current route. For example $C(R_B^{(1)}, M_B^{(1)}) > C(R_B^{(0)}, M_B^{(0)})$ where $R_B^{(1)} = (AP, A, B)$. Note also that this route generates a larger metric than other possible two-hop routes $R_B^{(1)} = (AP, C, B)$, $R_B^{(1)} = (AP, D, B)$, and $R_B^{(1)} = (AP, E, B)$.

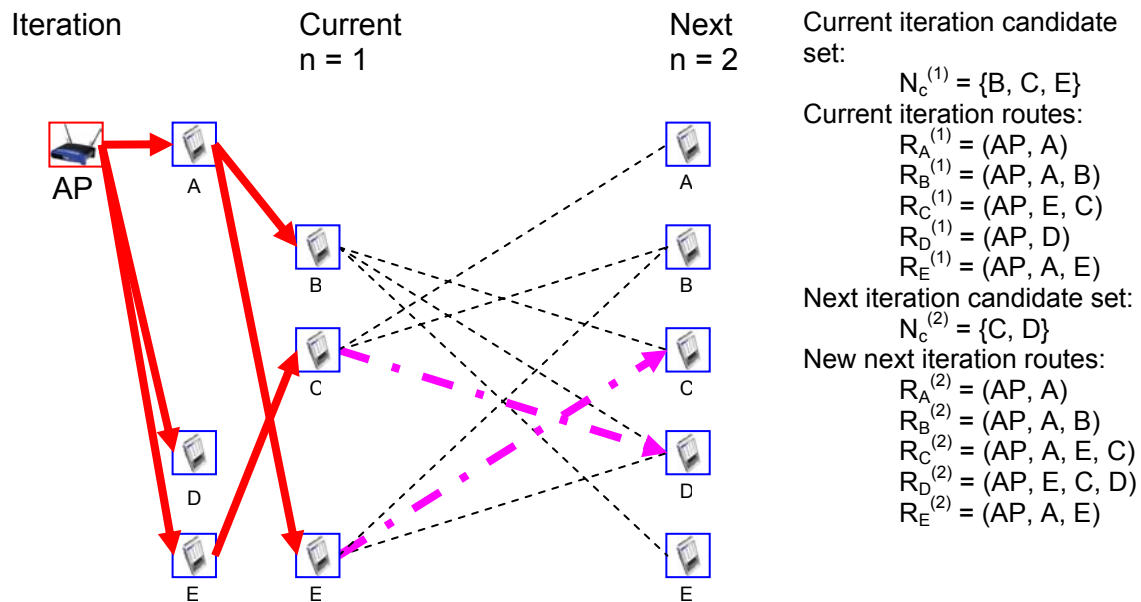


Fig. 3.5 – Routing example: Iteration 2.

Advancing to iteration $k = 1$ in Fig. 3.5, the maximum next generation routes from the previous iteration become the current routes for this iteration. Table 3.1 summarizes the routes. Once more the algorithm examines possible routes, however the candidate relaying node set $N_c^{(1)}$ is reduced to only nodes B, C, and E. These nodes

observed a route change from the previous iteration. The remaining nodes, nodes A and D, are culled from the candidate relaying node set since their routes were examined and have not changed from the previous iteration. Processing complexity is further reduced by limiting the search to only those nodes not used in the relaying nodes route. Thus, we note that node B's route is only evaluated for routes to node C, D, and E. Node A is not evaluated as a destination using node B's route since node A is already used as a relaying node in B's route. Thus we also avoid feedback loops.

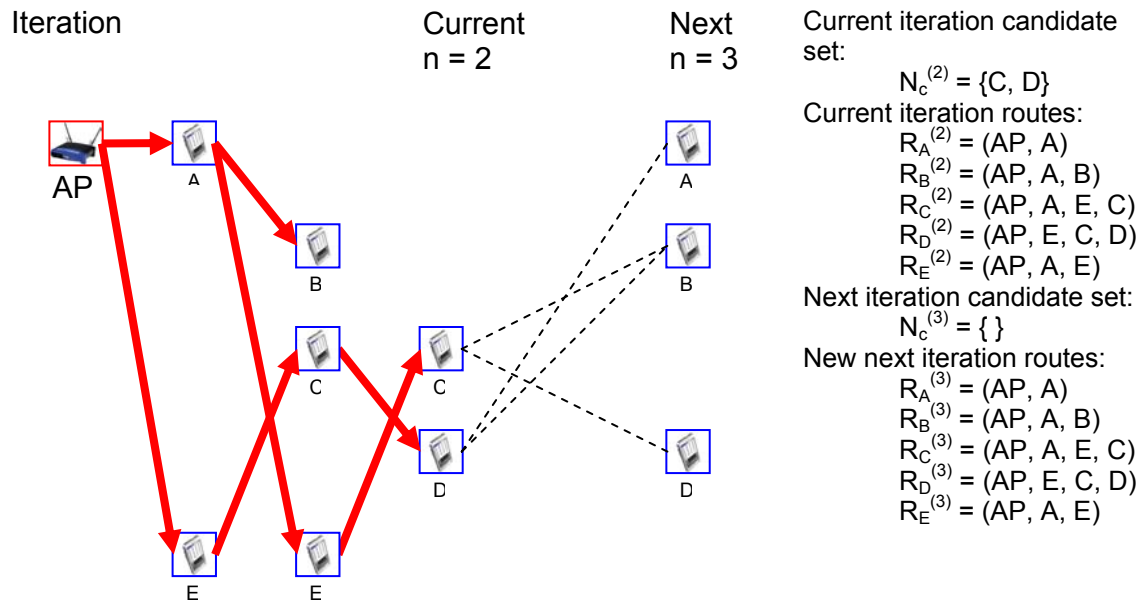


Fig. 3.6 – Routing example: Iteration 3.

By iteration $k = 2$, Fig. 3.6, we have reduced our candidate relaying node set to only nodes C and D which both have 3-hop routes. Examining potential routes does not yield a route generating larger metrics for any node. At this stage, no nodes are added to $N_c^{(3)}$. Advancing to iteration $k = 3$, $N_c^{(3)}$ is a null set and the algorithm stops searching and the network uses the current routes for relaying. Table 3.1 lists the final routes used in the network.

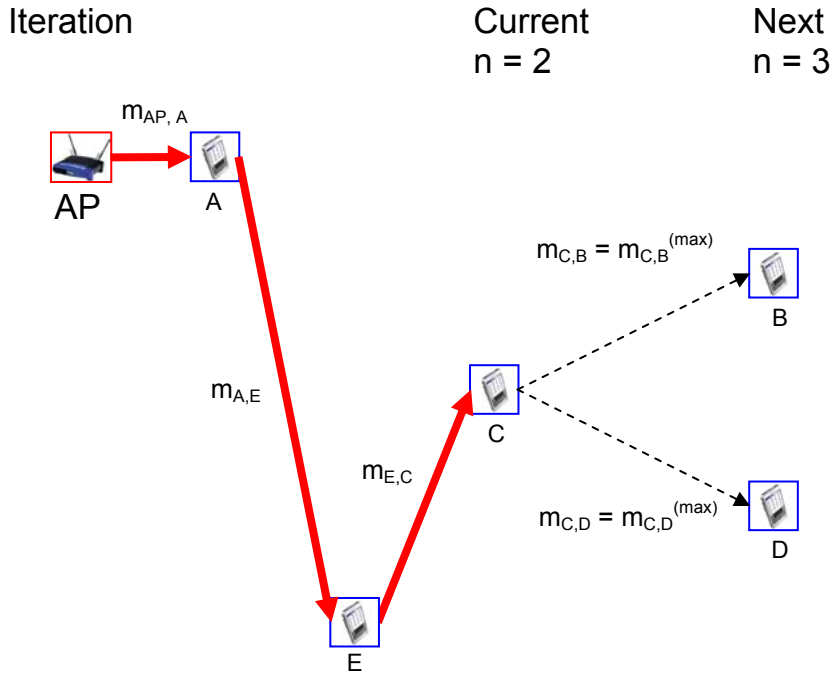


Fig. 3.7 – MH Algorithm 3.1 mode selection.

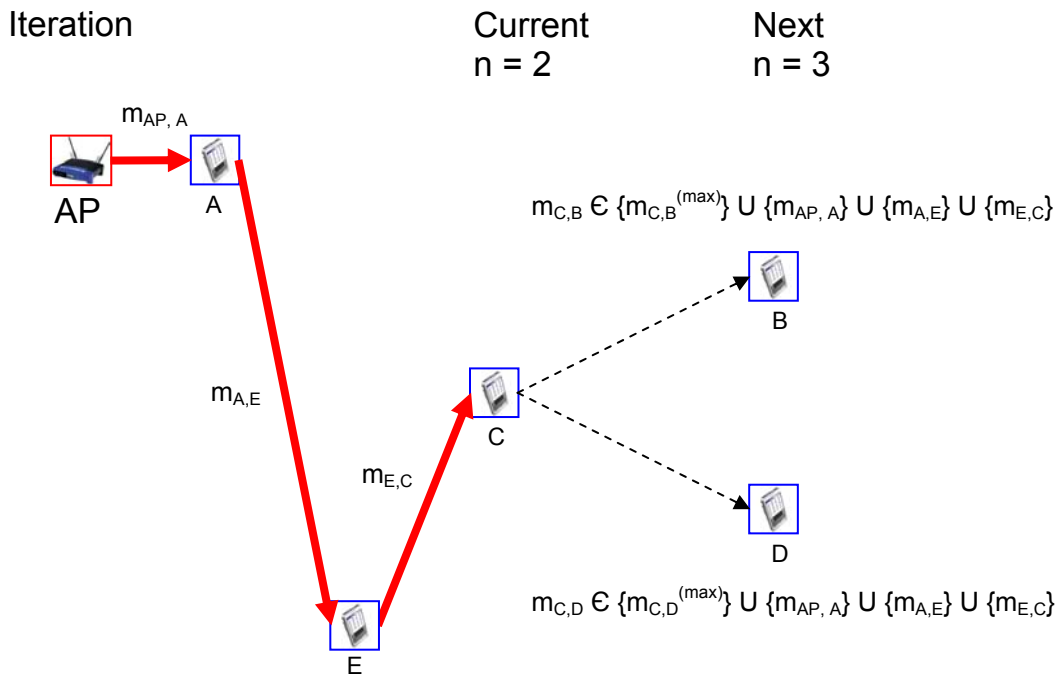


Fig. 3.8 – MHAM Algorithm 3.2 mode selection.

Fig. 3.7 and Fig. 3.8 illustrate the difference between Algorithm 3.1 and Algorithm 3.2 respectively. Both figures show a routing step from iteration $k = 2$, where we use node C's route to create potential new routes to nodes B and D. In Fig. 3.7 the

modes used to examine the last hop to either node B or D is the default mode that maximizes the link data rate according to equation (2.6). In contrast, Fig. 3.8 evaluates multiple possible modes in the last hop including the default mode. The modes used are restricted to the set of modes used in the connection to node C. For example, if the hop modes for the route to C are $M_C^{(2)} = \{m_{AP,A}, m_{A,E}, m_{E,C}\} = \{16QAM, 16QAM, 64QAM\}$ and $m_{C,D}^{(\max)} = 64QAM$, then we try the following modes, m , for the last hop to node D $m \in M_C^{(2)} \cup \{m_{C,D}^{(\max)}\} = \{16QAM, 64QAM\}$. The resultant route and mode sets will be compared to node C's current route and mode set and the set generating the maximum metric will be used for the route and mode set to node D. Routes with multiple mode sets are used to evaluate connections thus Algorithm 3.2 will require more processing Algorithm 3.1.

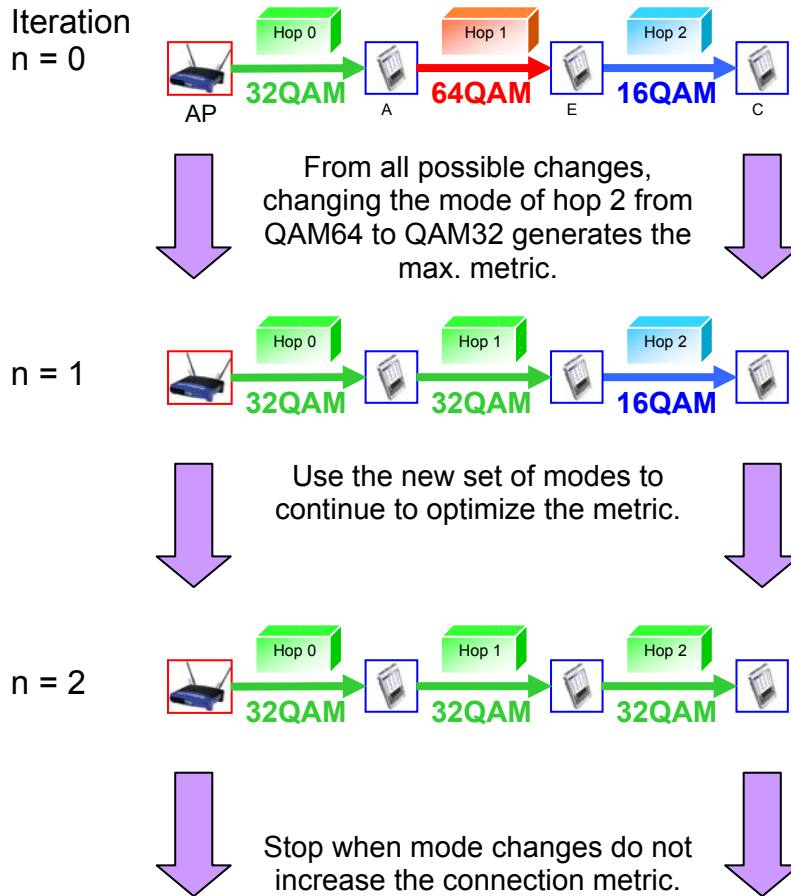


Fig. 3.9 – AMCM example.

An example of the AMCM algorithm, Algorithm 3.3, is illustrated in Fig. 3.9 and Table 2 summarizes the actions. We examine the connection to node C , where the route is $R_C = (AP, A, E, C)$ and the initial hop modes are $M_C^{(0)} = (32QAM, 64QAM, 16QAM)$. Mode sets are written in an abridged form in the table, for example $M_C^{(0)} = (32, 64, 16)$. The modes are originally selected according to Algorithm 3.1 or 3.2. As listed in Table 3.2, candidate mode sets are created by using a mode initially used in the connection for a given hop. In this example a hop mode can be selected to be one of the three modes listed in $M_C^{(0)}$. The set of hop modes generating the maximum metric for the current iteration is used in the next iteration. As an example, for iteration $n = 0$, $C(R_C, M_C^{(\max)}) > C(R_C,$

$M_C^{(0)})$ where $M_C^{(\max)} = (32QAM, 32QAM, 16QAM)$. Changing $m_l = 64QAM$ to $m_l = 32QAM$ generates a larger metric. With this change $M_C^{(\max)}$ generates a larger metric than other potential mode combinations. The algorithm iterates until the current set of modes does not change when advancing to the next iteration. This indicates changes to hop modes do not increase the connection metric further.

Table 3.2 – Example AMCM calculations

Iteration, n	Current hop modes, $M_C^{(n)}$	Hop, h	Candidate mode sets, $M_C^{(n+1)}$	$M_C^{(n+1)} = M_C^{(\max)}$	Mode change hop, $h^{(\max)}$
0	(32, 64, 16)	0	(64, 64, 16) (16, 64, 16)	(32, 32, 16)	1
		1	(32, 32, 16) (32, 16, 16)		
		2	(32, 64, 32) (32, 64, 64)		
1	(32, 32, 16)	0	(64, 32, 16) (16, 32, 16)	(32, 32, 32)	2
		2	(32, 32, 64) (32, 32, 32)		
2	(32, 32, 32)	0	(16, 32, 32) (64, 32, 32)	(32, 32, 32)	
		1	(32, 16, 32) (32, 64, 32)		

Chapter 4

Simulation Model

This chapter describes the various parameters and methods used to simulate the HiperLAN/2 network and multihop scenarios. The first section discusses propagation environment related assumptions and parameters, followed by a section on the network model including implementation of adaptive modulation and coding. Finally we present a section describing a basic step-by-step simulation using flow charts.

4.1 Environment Parameters and Assumptions

The following environmental assumptions and parameters are based on a typical HiperLAN/2 network in indoor environments operating in the 5.3 GHz spectrum [17, 21].

- Path-loss propagation exponent: $\alpha = 3.4$
- Lognormal shadowing standard deviation: $\sigma = 5.1$ dB
- ETSI-A channel: Non-Line-of-Sight (NLOS) 50ns RMS delay spread
- RF carrier: $f = 5.3$ GHz
- Number of frequency channels: 12
- Noise power: $\eta = -90$ dBm
- No power control, node transmit power: $P_t = 23$ dBm
- Omni-directional antennas with a gain of 1: $g_t = 1$ and $g_r = 1$ for both transmitter and receiver respectively
- Hexagonal cellular structure: 12-cell clusters, cell sizes vary from 30 m to 170 m
- Interference originating from the first-tier co-channel cells
- Interference power is constant during transmission

HiperLAN/2 networks employ a feature known as Dynamic Frequency Selection (DFS) [34] which allows access points to dynamically select a channel with the least measured interference. Using DFS we assume a HiperLAN/2 network will form a frequency plan that results in the least measured co-channel interference [14]. For

simulation purposes a hexagonal cellular structure is used and we consider constant interference originating from a randomly placed user in each first tier co-channel cell.

4.2 Network Parameters and Assumptions

The relaying model and network parameters are a key factor in determining network performance. We provide a list of network and relaying assumptions and determine how we calculate throughput performance. Adaptive modulation and coding for HiperLAN/2 networks is also presented.

The network is simulated using the following assumptions:

- 64 users uniformly distributed throughout cell
- Continuous traffic
- Infinite buffer sizes at nodes
- Digital relaying is used except when using HDAR
- Relaying algorithms can discover routes with unlimited number of hops
- Unlimited destination nodes supported by a relaying node
- Hops share the same frequency channel
- Hops are allocated time symbols according to (2.9)
- Adaptive Modulation and Coding per hop
- Downlink scenario

Here we assume that nodes always have data to receive from the AP hence we use a continuous traffic model where all nodes are equally served. The traffic model used has no effect on routing algorithms presented earlier. Using the continuous traffic model we can calculate the average aggregate throughput as,

$$T_N = \frac{\sum_{d \in N} T_d}{|N|} = \frac{\sum_{d \in N} F \cdot S_c \cdot C(R_d, M_d)}{|N|} \quad (4.1)$$

Here N is the set of mobile nodes in the network and T_d is the throughput of node d . T_d is simply calculated using the metric at node d . We use $F = 1/2$ frame/msec and $S_c = 500$

symbols/frame corresponding to transmitting one full HiperLAN/2 frame. Throughput calculation excludes factors such as overhead per frame or relaying overhead.

Adaptive modulation and coding is implemented using the packet error rate model for ETSI-A channels in Fig. 2.1 and throughput expression (2.5). $F = 1/2$ frame/msec and $S_l = 500$ symbols/frame. We obtain results in Fig. 4.1 showing the throughput of a link as a function of SNR for various modes.

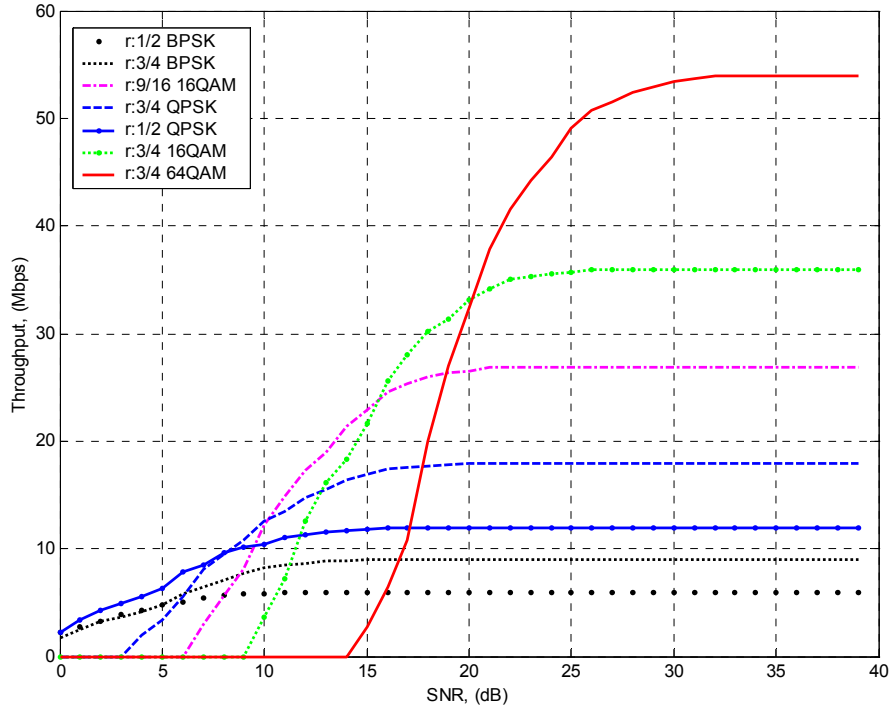


Fig. 4.1 – Throughput vs. SNR for various modes

From these results we obtain SNR ranges for which to use a mode to maximize the link throughput. For example, if the link SNR falls between a range of 8.09 dB and 10.25 dB we select mode r:3/4 QPSK. The mode selection settings for given SNR are listed in Table 4.1. Note that this table satisfies the adaptive modulation scheme given by

expression (2.6). The table also lists the modulation efficiency, D , in information bits/OFDM symbol, corresponding to the particular mode.

Table 4.1 – Adaptive modulation and coding settings

SNR (dB)	Mode, m	D , (info. bits/OFDM symbol)
< 8.09	r:1/2 QPSK	48
< 10.25	r:3/4 QPSK	72
< 15.57	r:9/16 16QAM	108
< 20.17	r:3/4 16QAM	144
>= 20.17	r:3/4 64QAM	216

4.3 Simulation Algorithm

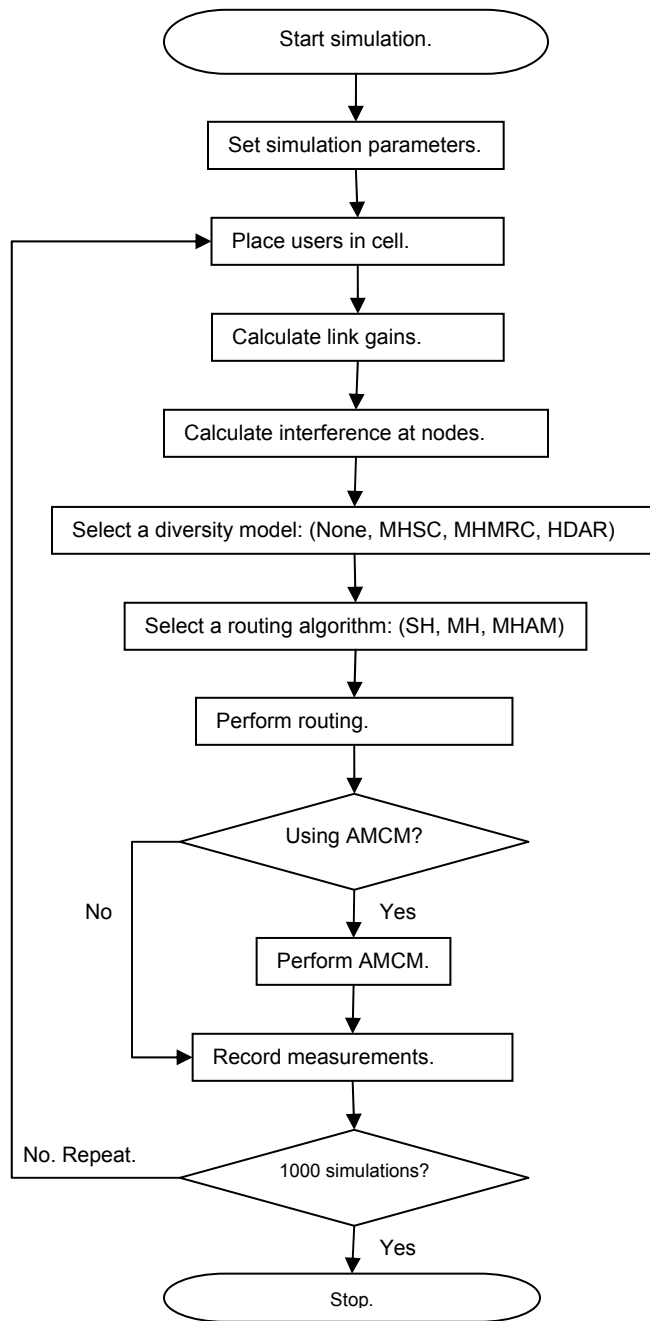


Fig. 4.2 – Simulation flowchart

Chapter 5

Simulation Results

In this chapter we present simulation results for the various multihop schemes and algorithms presented in the previous chapters. The objective of these simulations is to determine the potential coverage extension and throughput performance increase obtainable by using various combinations of multihop diversity and algorithms as compared to singlehop systems.

In our first section we discuss the performance of 2-hop relaying with various forms of diversity followed by 2-hop relaying in a cellular system using our various routing and diversity schemes. Finally we discuss the multihop network and compare it to 2-hop systems.

5.1 The Effect of Diversity in 2-hop Relaying

In this section we evaluate the performance of multihop diversity schemes such as MH (no diversity), MHSC, MHMRC and HDAR for 2-hop relaying by evaluating throughput as we vary distance between relaying node r_1 and destination r_2 , shown in Fig. 5.1. This corresponds to varying values of β , $0 < \beta < 1$, where $\beta = d_{0,1}/d_{0,2}$. Link modes ($m_{0,1}$, $m_{1,2}$, or $m_{0,2}$) between nodes are selected using AMC according to Table 4.1. Shadow fading and interference is not included.

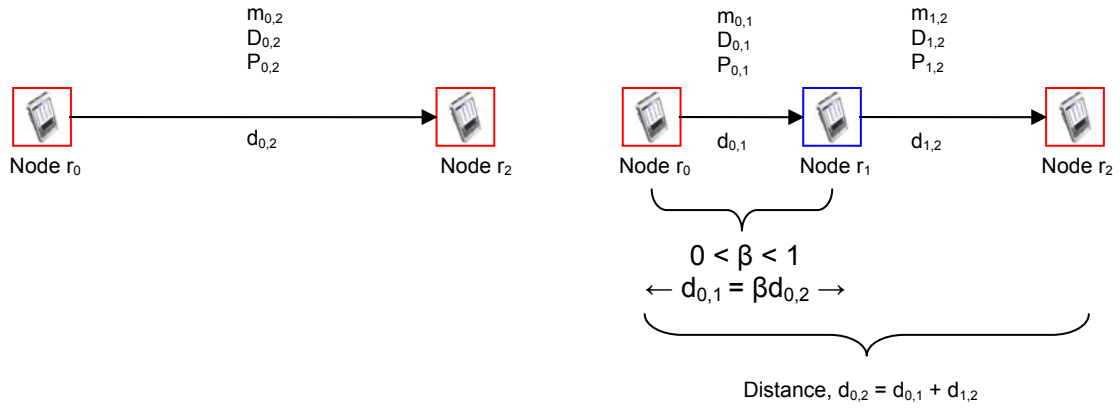


Fig. 5.1 – 2-hop relaying scenario

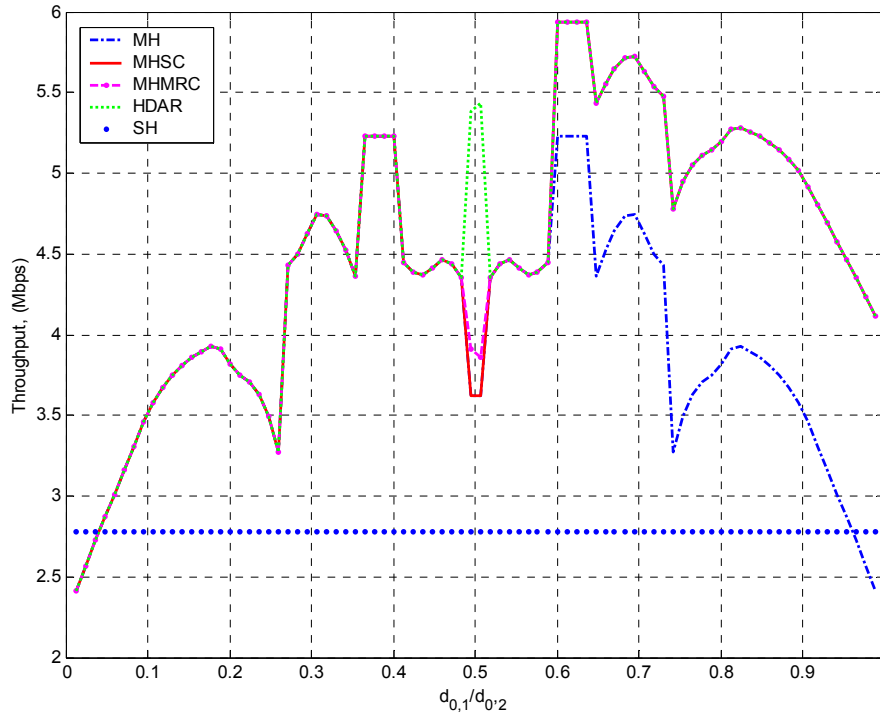


Fig. 5.2 – 2-hop simulation, $m_{0,2} = r:1/2$ QPSK, $SNR_{0,2} = 0.46$ dB

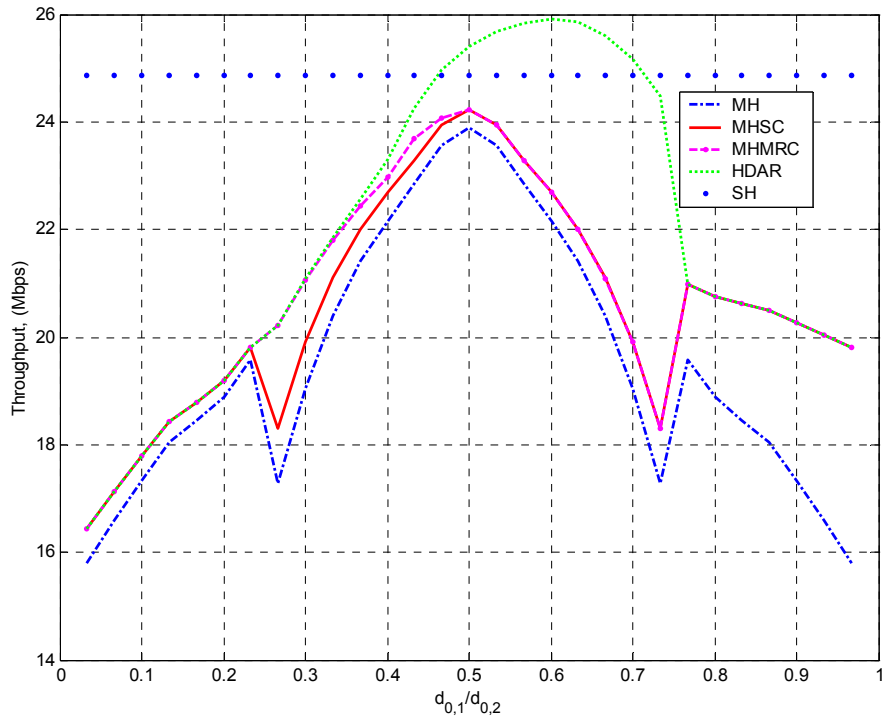


Fig. 5.3 – 2-hop simulation, $m_{0,2} = r:3/4$ 16QAM, $SNR_{0,2} = 15.8$ dB

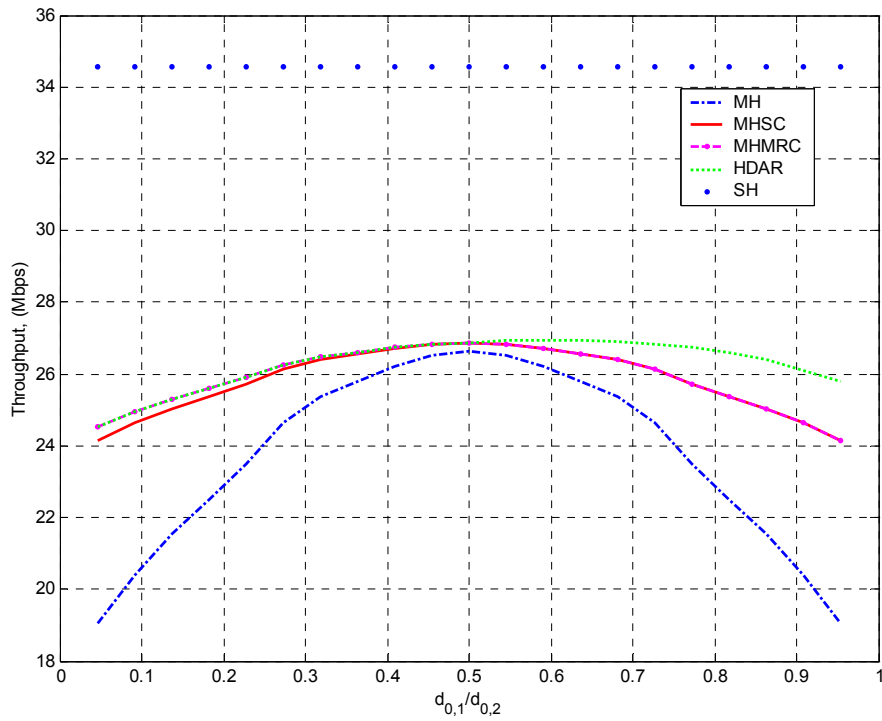


Fig. 5.4 – 2-hop simulation, $m_{0,2} = r:3/4$ 64QAM, $SNR_{0,2} = 20.41$ dB

Fig. 5.2, 5.3, and 5.4 show the results for distance $d_{0,2}$ corresponding to using $r:1/2$ QPSK, $r:3/4$ 16QAM, or $r:1/2$ 64QAM for the singlehop link mode, $m_{0,2}$, respectively. The sharp transitions in the figures are a result of AMC changing hop modes to maximize link throughput. From the figures we see that 2-hop relaying can offer throughput increases over singlehop (SH) when the link SNR is equal to or less than that required to support $r:3/4$ 16QAM mode. However in Fig. 5.4, the link SNR is sufficient for low packet error rates when using $r:1/2$ 64QAM such that relaying only causes frame segmentation (loss of time resources due to relaying) reducing throughput below that of singlehop relaying. Thus relaying only provides benefits for users suffering from low SNR. At higher SNR levels possible gains may be achieved if the system supports modulation and coding modes greater than $r:1/2$ 64QAM.

For users with low SNR, relaying even without diversity can outperform a SH system as seen in Fig. 5.2 where MH outperforms SH by 2.45 Mbps or 88%. MHSC outperforms SH by 3.16 Mbps or 114%. MHMRC and HDAR perform similarly as MHSC when both hops use different modes but perform better when modes are the same, at a ratio of $\beta = 0.5$. HDAR generates 5.38 Mbps throughput compared to throughput of 3.91 Mbps using MHMRC and 3.62 Mbps using MHSC. Since a relaying node using MHMRC only relays when the received signal is decoded correctly, the destination node can not perform MRC combining when a signal is not relayed. It only receives a weaker version of the signal from the source node with small likelihood of being decoded correctly. Thus the lack of relayed signals, reducing sources of diversity, seriously hampers MHMRC performance particularly when the relaying node is near to the destination. Since HDAR relays incorrectly decoded signals in analog form with noise,

we have greater sources of diversity. The diversity gain seen by MRC combining, albeit with noisier signals, provides greater performance. As seen from Fig. 5.3 only relaying with HDAR provides performance greater than SH. If the link SNR between source and destination can support $r:3/4$ 16QAM, only HDAR can provide reduced packet error rates such that throughput is greater than SH. Other forms of diversity do not reduce packet error significantly to overcome the loss of time resources due to frame segmentation. We also note that MHMRC performs slightly better than MHSC for $0.26 < \beta < 0.5$. During this period the relaying node decodes the signal correctly enough of the time to relay a signal allowing for MRC combining at the destination. From $0.5 < \beta < 0.73$ MHMRC does not provide a gain compared to MHSC since the limiting factor is the probability of decoding error at the relaying node. The worst case of only receiving a single signal at the destination dominates performance. A similar conclusion can be drawn from Fig. 5.4 for $\beta > 0.5$ region. We also note that HDAR performs better than MHMRC in this region due to analog relaying hence in the worst case we still have two signals to MRC combine.

One final observation is the increased performance of MHSC when the relaying node is closer to the destination. This can be explained for the general scenario when using 2-hop relaying with AMC.

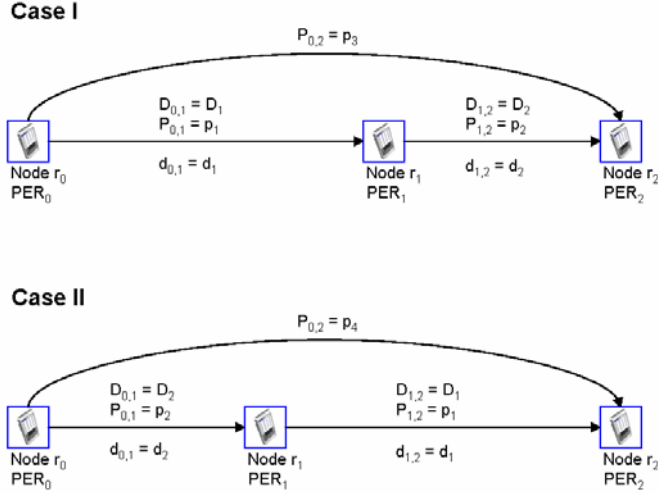


Fig. 5.5 – Generic 2-hop relaying using AMC and MHSC diversity.

Fig. 5.5 illustrates two generic relaying scenarios. In the first scenario relaying node r_1 is distance d_1 from source node r_0 and distance d_2 from destination node r_2 . The hop distances are switched in the second scenario. In general $d_1 \geq d_2$. We will prove that the first scenario where a relaying node is situated nearer to the destination generates an increased metric (hence throughput) for the destination. For scenario I we have

$$\begin{aligned}
 PER_0 &= 0, \\
 PER_1 &= [PER_0 + (1 - PER_0)P_{0,1}] = p_1, \\
 PER_2 &= [PER_0 + (1 - PER_0)P_{0,2}][PER_1 + (1 - PER_1)P_{1,2}] = p_3[p_1 + (1 - p_1)p_2], \\
 \text{and } C_2^I &= \frac{(1 - PER_2)}{\frac{1}{D_{0,1}} + \frac{1}{D_{1,2}}} = \frac{1 - p_3[p_1 + (1 - p_1)p_2]}{\frac{1}{D_1} + \frac{1}{D_2}}.
 \end{aligned}$$

For scenario II,

$$\begin{aligned}
 PER_0 &= 0, \\
 PER_1 &= [PER_0 + (1 - PER_0)P_{0,1}] = p_2, \\
 PER_2 &= [PER_0 + (1 - PER_0)P_{0,2}][PER_1 + (1 - PER_1)P_{1,2}] = p_4[p_2 + (1 - p_2)p_1], \\
 \text{and } C_2^{II} &= \frac{(1 - PER_2)}{\frac{1}{D_{0,1}} + \frac{1}{D_{1,2}}} = \frac{1 - p_4[p_2 + (1 - p_2)p_1]}{\frac{1}{D_1} + \frac{1}{D_2}}.
 \end{aligned}$$

Since hops use adaptive modulation and coding (2.6), the mode used for the first hop in scenario I is a lower or equal mode used for the first hop in scenario II, $m_1'' \geq m_1'$, due to decreased SNR of the signal between nodes r_0 and r_1 (increased distance) in scenario I. Considering only distance attenuation, the SNR of the received signal at destination r_2 is $SNR_{0,2}^I = SNR_{0,2}'' = \gamma$. It is obvious that $P_e(\gamma, m_1'') \geq P_e(\gamma, m_1')$ or $p_4 \geq p_3$. Assuming $C_2^I \geq C_2''$ we have

$$\frac{1 - p_3[p_1 + (1 - p_1)p_2]}{\frac{1}{D_1} + \frac{1}{D_2}} \geq \frac{1 - p_4[p_2 + (1 - p_2)p_1]}{\frac{1}{D_1} + \frac{1}{D_2}}$$

This expression can be simplified to $p_4 \geq p_3$ which is true. Thus $C_2^I \geq C_2''$ and scenario I generates greater metric and throughput than scenario II. We can conclude that a 2-hop connection using MHSC diversity and AMC generates increased throughput when the second hop distance is less than the first hop distance. A lower mode is selected for the first hop when the distance is large. This decreases the error rate of the first hop signal received at the destination and reduces the overall packet error rate at the destination.

5.2 2-hop Relaying Networks

In this section we discuss the network performance of 2-hop relaying systems. We can construct 2-hop relaying networks by using our routing algorithms with $k^{(max)} = 1$ iteration(s). Fig. 5.6 and 5.7 show the average aggregate throughput as it varies for different cell sizes for various diversity and routing schemes. Throughout this chapter we will use abbreviations for the various combinations of schemes. In the figures MH and

MHAM indicate the use of routing algorithm 3.1 or 3.2 respectively, and AMCM indicates the use of algorithm 3.3 after routing. SH is singlehop routing. SC, MRC, HDAR indicates the diversity/metric used whether it is selection combining, maximal ratio combining using digital relaying, or maximal ratio combining using hybrid digital analog relaying respectively.

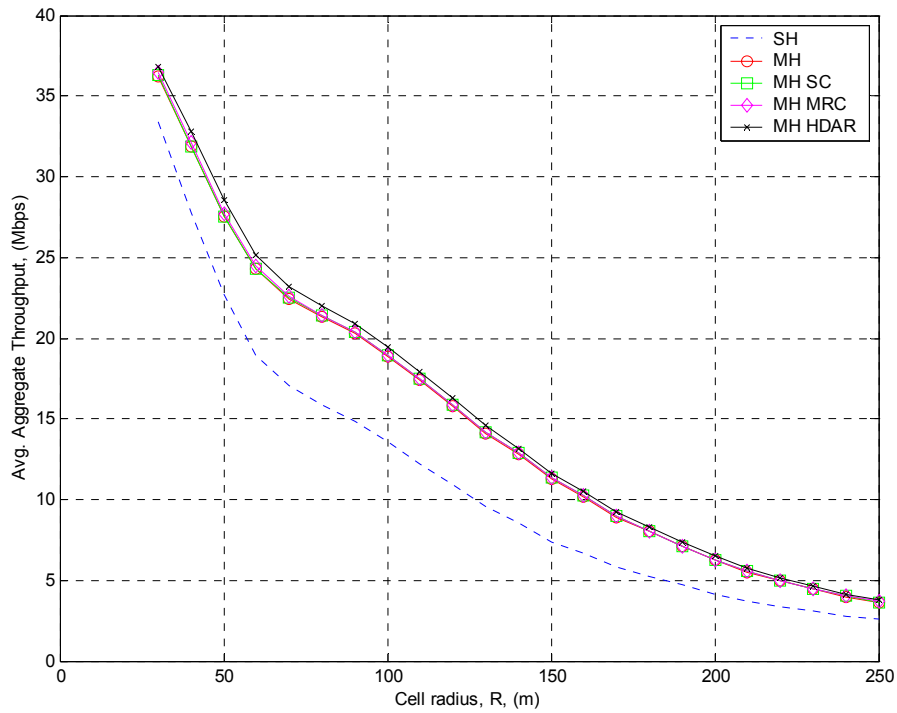


Fig. 5.6 – 2-hop average aggregate throughput as a function of cell radius

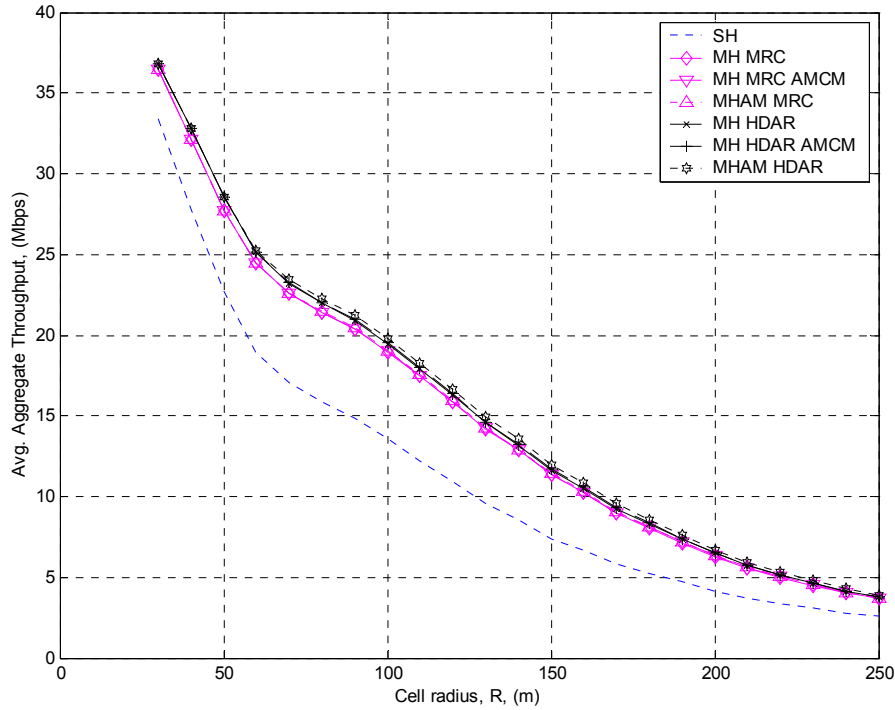


Fig. 5.7 – 2-hop average aggregate throughput as a function of cell radius

A summary of the results for 100 m and 200 m cells is given in Table 5.1.

Table 5.1 – 2-hop throughput performance

Scheme	Average (Mbps)		Minimum (Mbps)	
	100 m	200 m	100 m	200 m
SH	13.60	4.16	0	0
MH	18.88	6.25	5.80	0
MH SC	18.96	6.29	5.89	0
MH MRC	18.96	6.29	5.90	0
MH MRC AMCM	19.01	6.32	5.92	0
MHAM MRC	19.04	6.36	5.94	0
MH HDAR	19.45	6.48	6.12	0
MH HDAR AMCM	19.52	6.53	6.17	0
MHAM HDAR	19.80	6.71	6.50	0

MHAM HDAR yields the greatest gains with a throughput 6.20 Mbps greater than singlehop in a 100 m cell; however all the relaying schemes are within 1 Mbps of each other. We also note that the MHAM network outperforms the MH/AMCM network. This implies joint modulation and coding maximization and routing outperforms disjoint

routing and maximization. However, the true strength of relaying can be seen if we observe the average minimum aggregate throughput. This can be perceived as the minimum throughput a user might experience on average. Fig. 5.8 and 5.9 show the average minimum throughput as a function of cell radius.

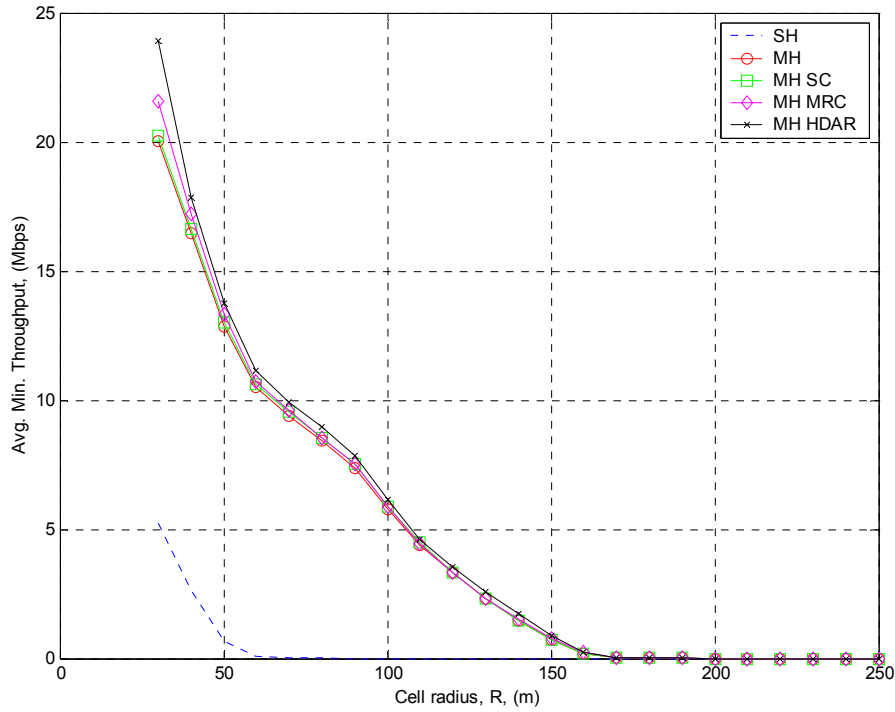


Fig. 5.8 – 2-hop minimum aggregate throughput as a function of cell radius

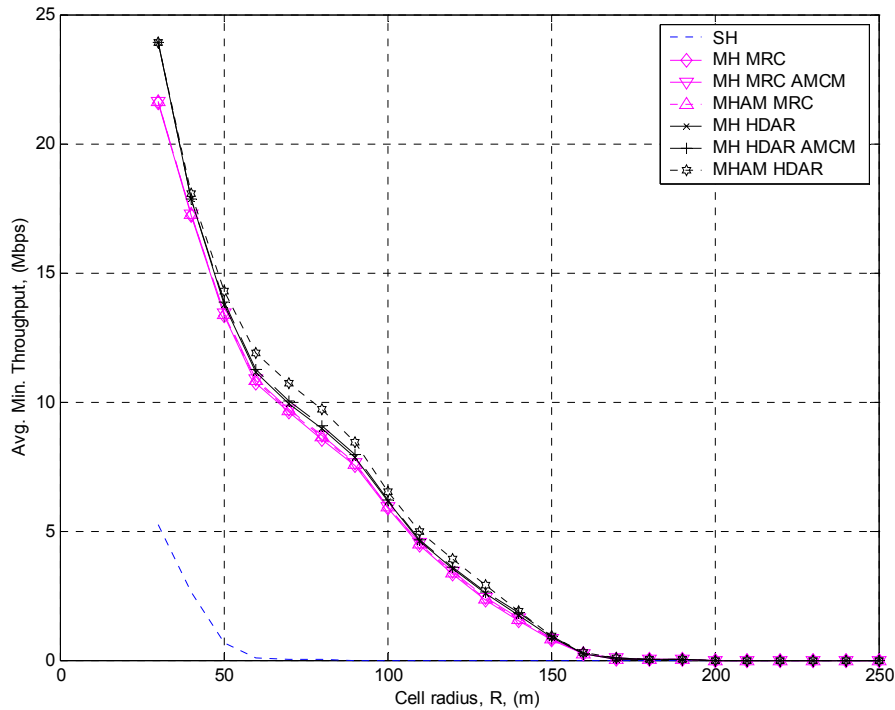


Fig. 5.9 – 2-hop minimum aggregate throughput as a function of cell radius

At 30 m we observe that singlehop can only guarantee a minimum user throughput of 5.24 Mbps whereas multihop (MH) and MHAM HDAR guarantee a minimum of 20.00 Mbps and 23.93 Mbps respectively. We also note diversity can offer gains of almost 4 Mbps over multihop without diversity. By using relaying we can more than triple our cell radius to more than 100 m and still guarantee coverage for all users with throughput around 5 Mbps as opposed to a singlehop network that can guarantee 5 Mbps with cell radius of around 30 m. Table 5.1 summarizes the results for 100 m and 200 m cells. Furthermore, if the network only uses singlehop with cell radius of 85 m or greater the minimum guaranteed throughput has dropped to 0 Mbps. Using relaying the minimum guaranteed throughput drops to 0 at 200 m and greater. Fig. 5.10 shows outage probability versus cell radius where outage probability is the probability that a user's throughput is 0 Mbps (users cannot communicate with the AP). At 100 m singlehop

networks experience 17% outage while multihop networks offer full coverage up to 140 m cell radius (0% outage). Using a cell size of 200 m we have a 23% or lower probability of outage using relaying compared to 74% outage when not using relaying.

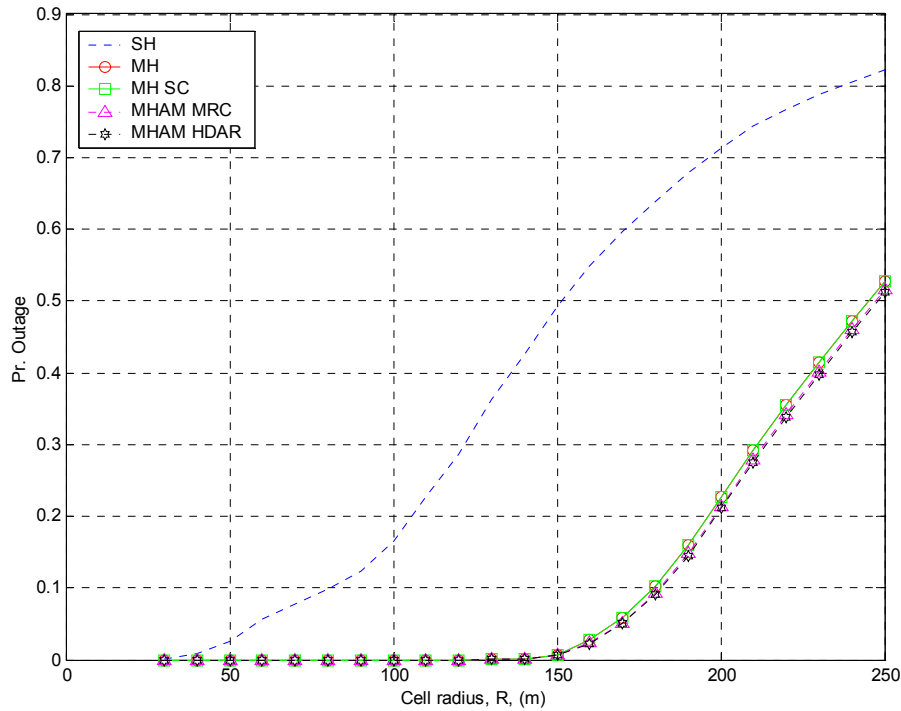


Fig. 5.10 – 2-hop outage probability as a function of cell radius

The gains obtained by relaying however do incur a cost to the network. Since we use mobile nodes, relaying increases the load on wireless terminals and will result in faster battery drain. Fig. 5.11 and Fig. 5.12 illustrate the maximum load that nodes may experience. Here we define load as the number of connections that a node must provide relaying service for.

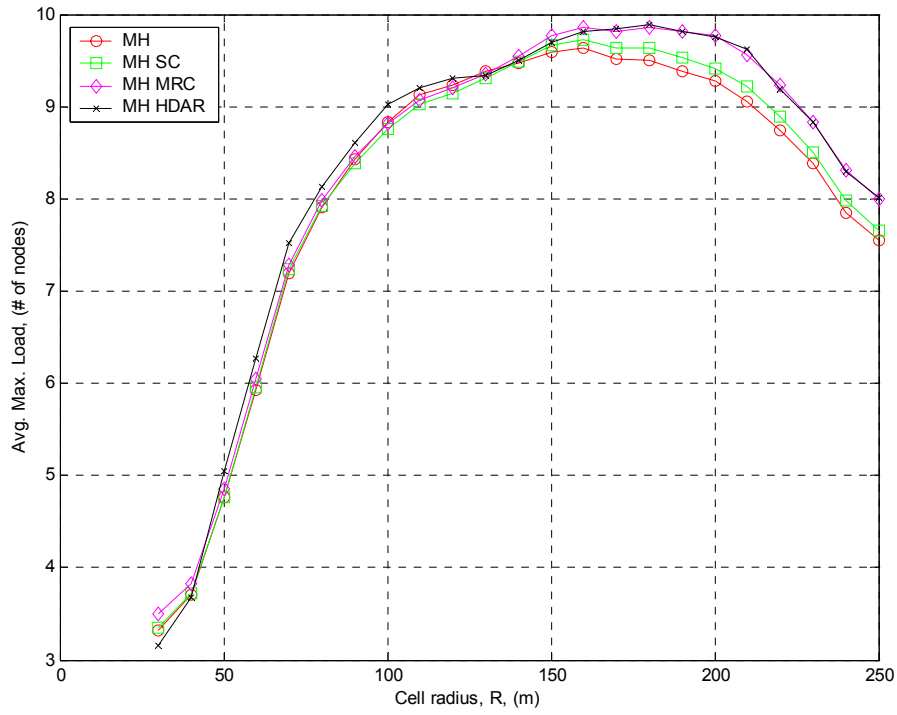


Fig. 5.11 – 2-hop maximum load as a function of cell radius

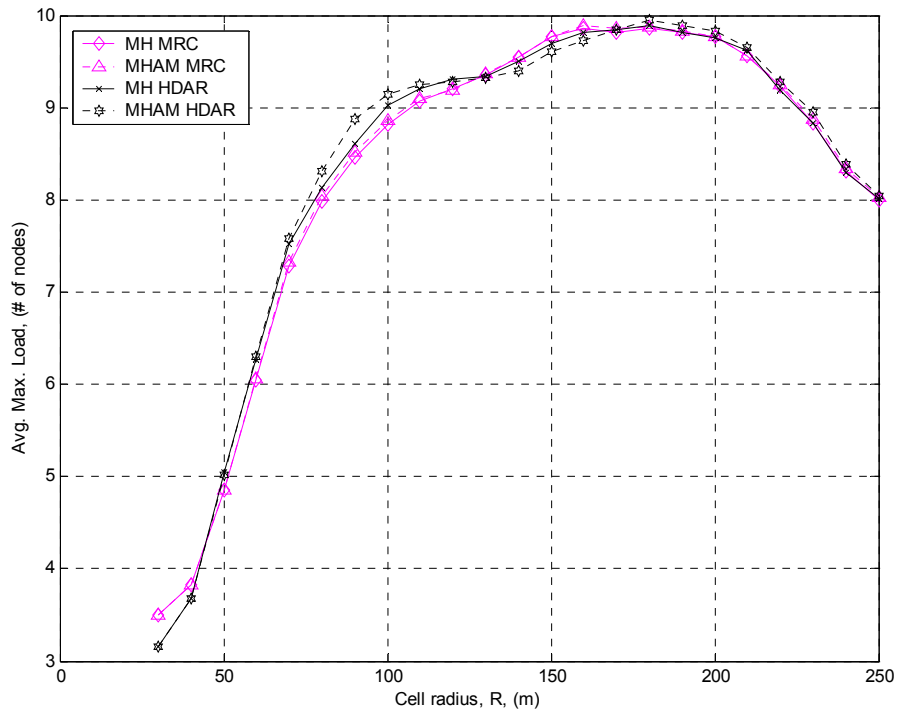


Fig. 5.12 – 2-hop maximum load as a function of cell radius

From the figures we observe that the maximum load may increase to almost supporting 10 relaying connections at a cell radius of 180 m. The load decreases for larger cells since an increasing number of nodes may be located such that even relaying cannot help them. Relaying is used to a lesser extent as more users exist outside the relaying coverage region and we observe a decrease in load.

5.3 Multihop Relaying Networks

In the previous section we observed 2-hop relaying could more than triple our coverage area (triple our cell radius) compared to that of singlehop networks yet offer equal performance. However the performance degrades the larger the cell becomes due to decreased link quality of hops. It may become necessary to use multiple hops when relaying to ensure hops maintain sufficient link quality for communication. By changing the value for $k^{(max)}$ in our routing algorithm we can create networks of a maximum $k^{(max)}+1$ hops. In Fig. 5.13 and 5.14 we investigate how this parameter affects the average minimum throughput for the MH and MHAM HDAR schemes.

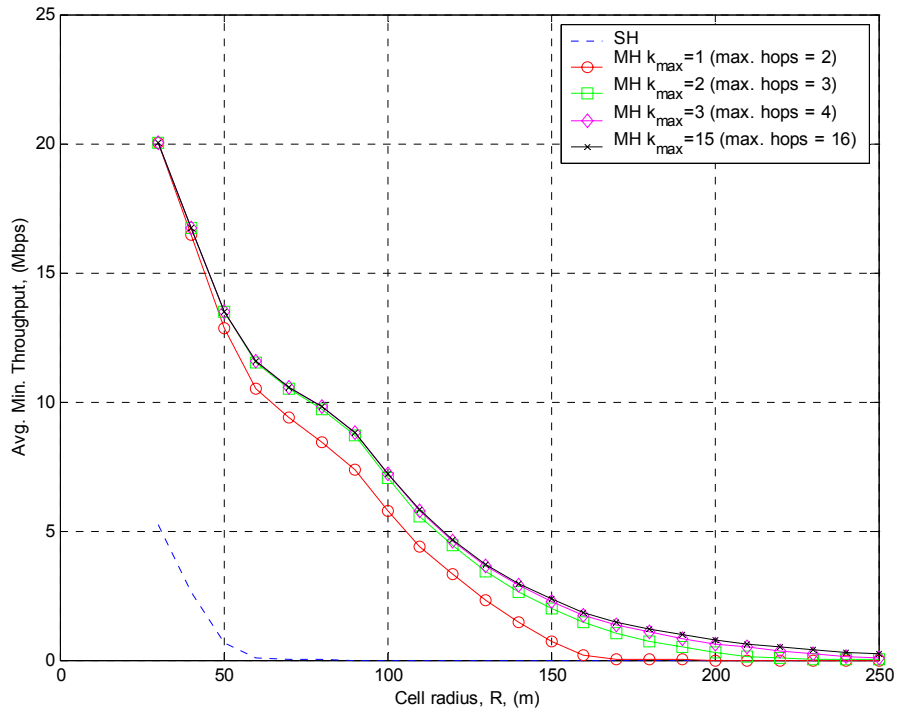


Fig. 5.13 – The effect of $k^{(max)}$ on avg. min. throughput for MH

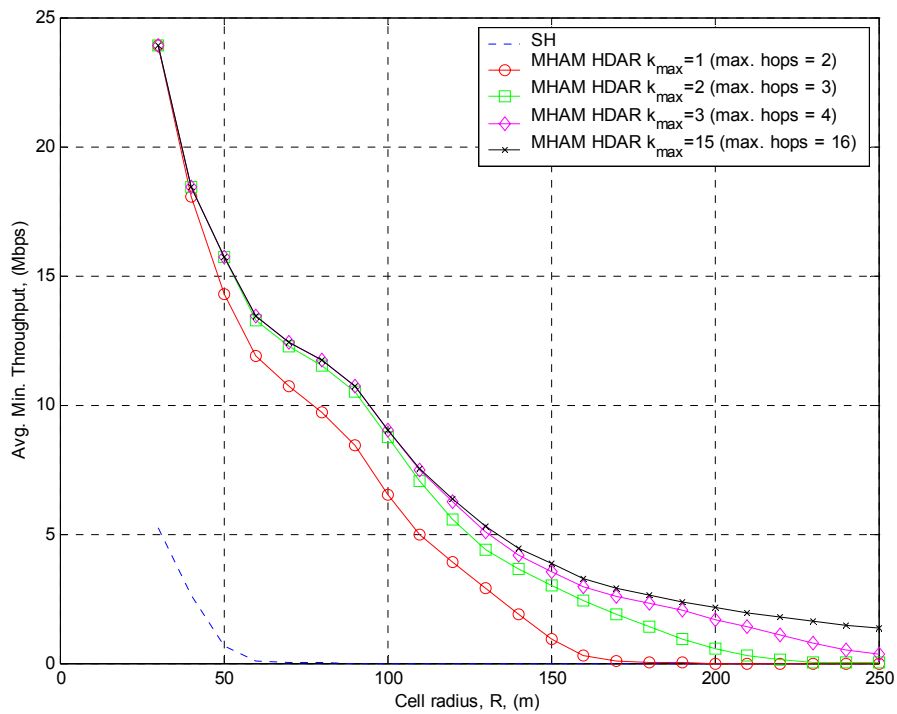


Fig. 5.14 – The effect of $k^{(max)}$ on avg. min. throughput for MHAM

From Fig. 5.13 we can see that by allowing $k^{(max)}=2$, networks of 3 hops, the minimum throughput is increased by more than 1 Mbps for 100 m cells using MH. For MHAM, Fig. 5.14, the increase is greater than 2 Mbps when $k^{(max)}=2$. We also note that $k^{(max)}=3$ offers gains over $k^{(max)}=2$ in larger cell sizes. Regardless of the scheme used, increasing $k^{(max)}$ further to allow for networks with more hops offers diminishing returns. Routes with an increased number of hops will increase frame segmentation hence the gains are small or nonexistent.

Throughout the remainder of this section we will evaluate the performance of our routing algorithms with $k^{(max)} = 15$; virtually unlimited hop multihop networks. The avg. aggregate throughput for the various schemes is shown in Fig. 5.15 and Fig. 5.16.

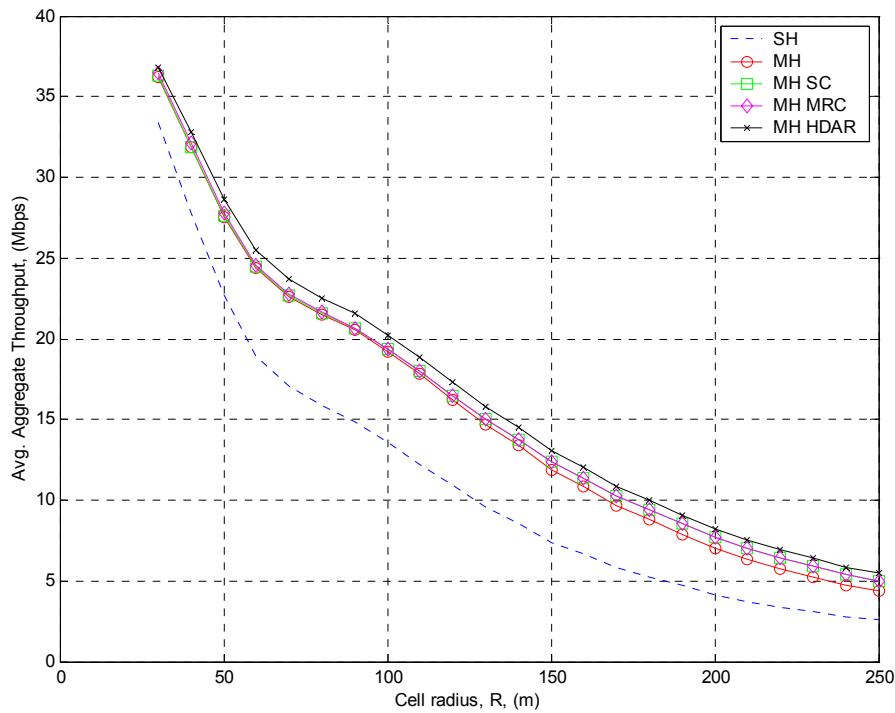


Fig. 5.15 – Multihop average aggregate throughput as a function of cell radius

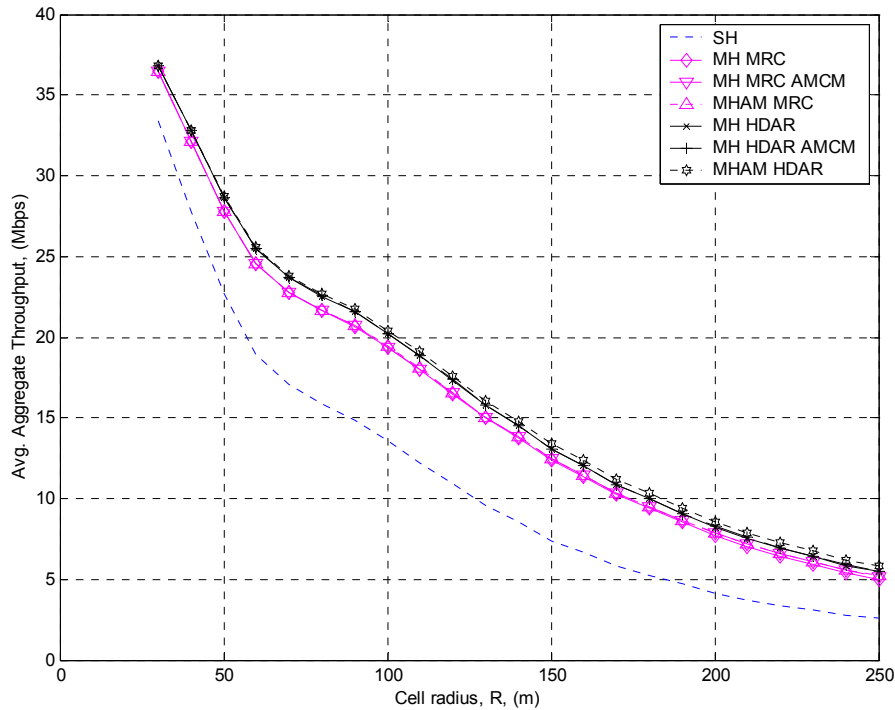


Fig. 5.16 – Multihop average aggregate throughput as a function of cell radius

In order to compare multihop to 2-hop relaying networks we are particularly interested in observing the gains multihop offers at cell radius of 100 m and 200 m. Table 5.2 summarizes the results.

Table 5.2 – Multihop throughput performance

Scheme	Average (Mbps)		Minimum (Mbps)	
	100 m	200 m	100 m	200 m
SH	13.60	4.16	0	0
MH	19.20	7.06	7.23	0.77
MH SC	19.36	7.72	7.59	1.24
MH MRC	19.36	7.73	7.59	1.25
MH MRC AMCM	19.40	7.84	7.76	1.51
MHAM MRC	19.41	7.86	7.78	1.53
MH HDAR	20.24	8.25	8.50	1.63
MH HDAR AMCM	20.25	8.29	8.57	1.72
MHAM HDAR	20.41	8.58	9.02	2.14

The average throughput of multihop systems has increased by 0.3 Mbps and greater at cell radius of 100 m compared to 2-hop networks (see Table 5.1). More

importantly the guaranteed minimum throughput, Fig. 5.17 and Fig. 5.18, has increased by more than 1 Mbps. Even using larger 250 m cells the average minimum throughput is greater than 0. Using multihop with diversity we can guarantee a minimum throughput of 5 Mbps using 130 m cells that equals or exceeds the minimum throughput for singlehop networks at 30 m; more than quadrupling our cell radius.

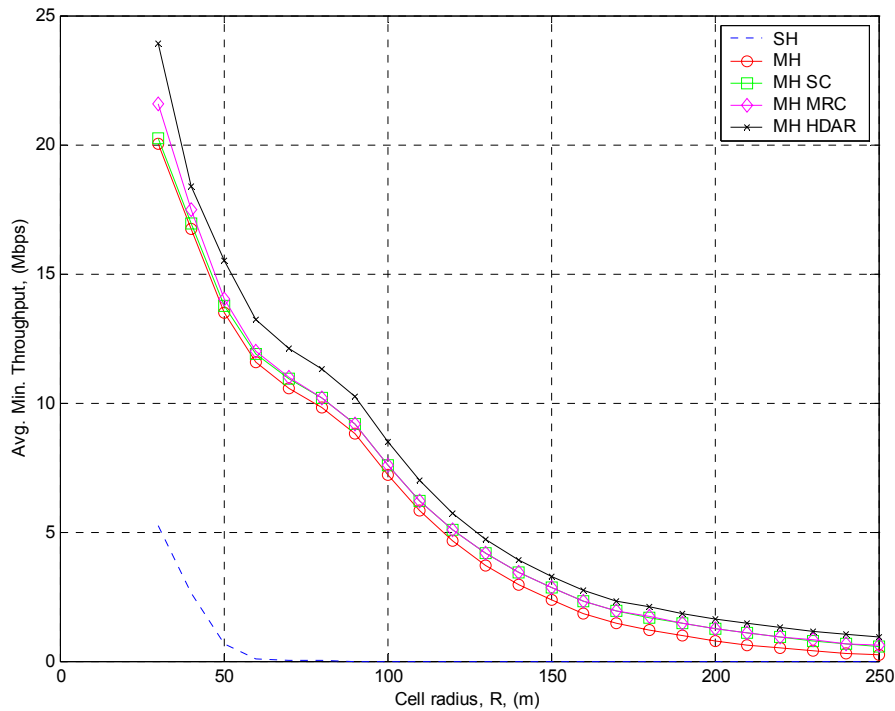


Fig. 5.17 – Multihop minimum aggregate throughput as a function of cell radius

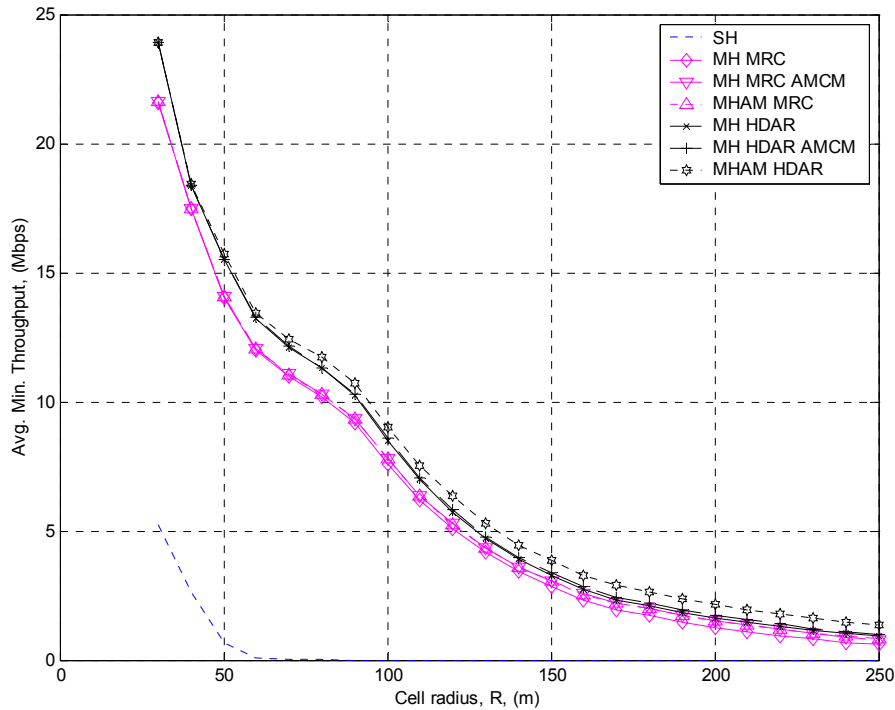


Fig. 5.18 – Multihop minimum aggregate throughput as a function of cell radius

The cumulative distribution functions of throughput at 100 m and 200 m are depicted in Fig. 5.19 and Fig. 5.20. We note that the probability of outage is 0 when using multihop relaying even for large coverage areas such as 200 m cells. In addition, we can conclude from the figures that these relaying schemes only increase the performance of users with low data-rates or poor links to the AP.

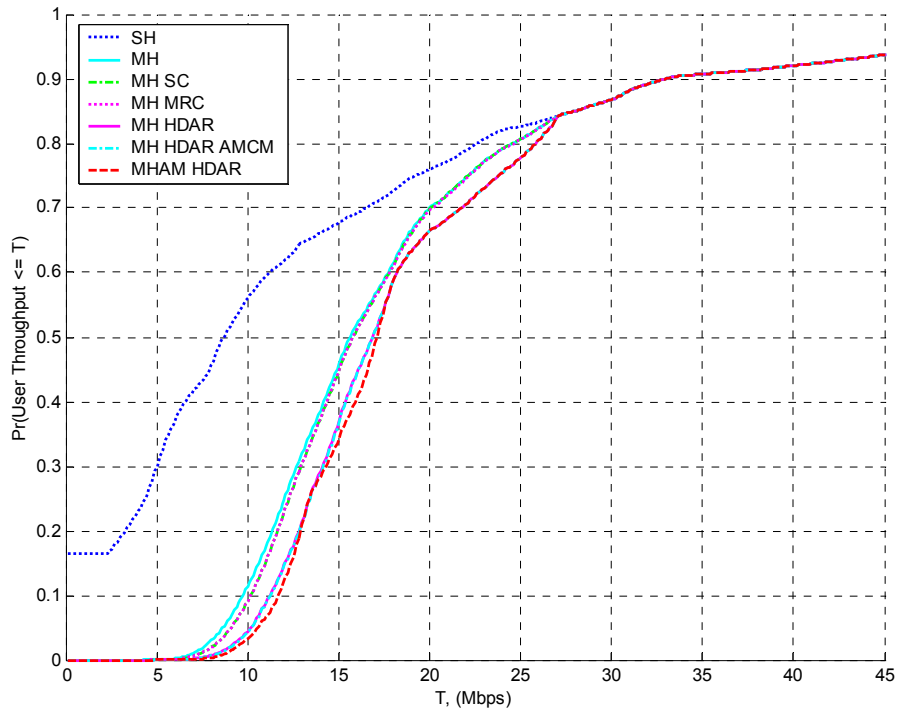


Fig. 5.19 – CDF of throughput for 100 m cells

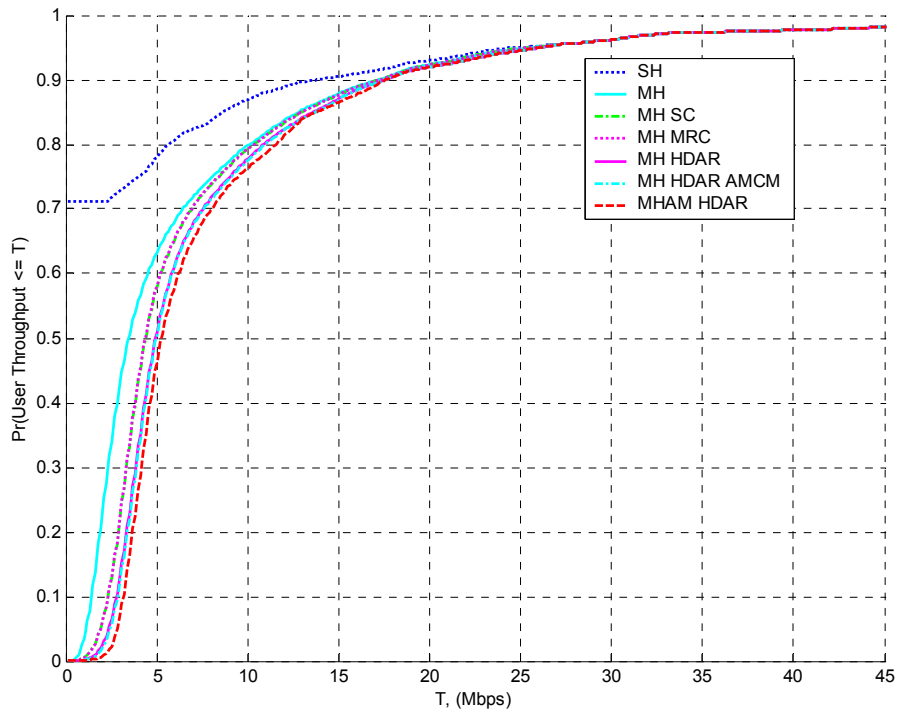


Fig. 5.20 – CDF of throughput for 200 m cells

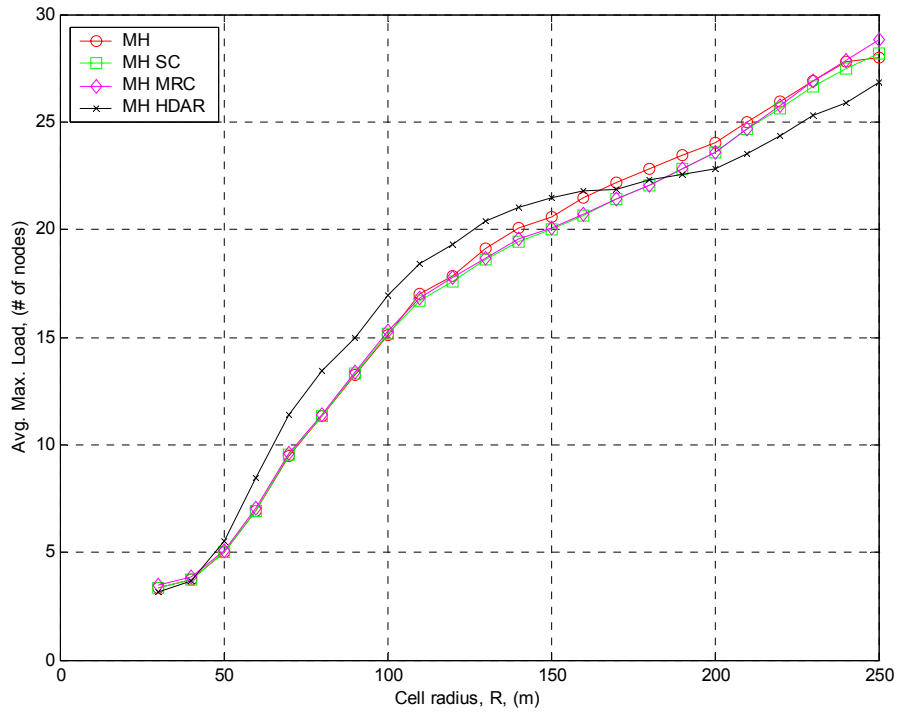


Fig. 5.21 – Multihop maximum load as a function of cell radius

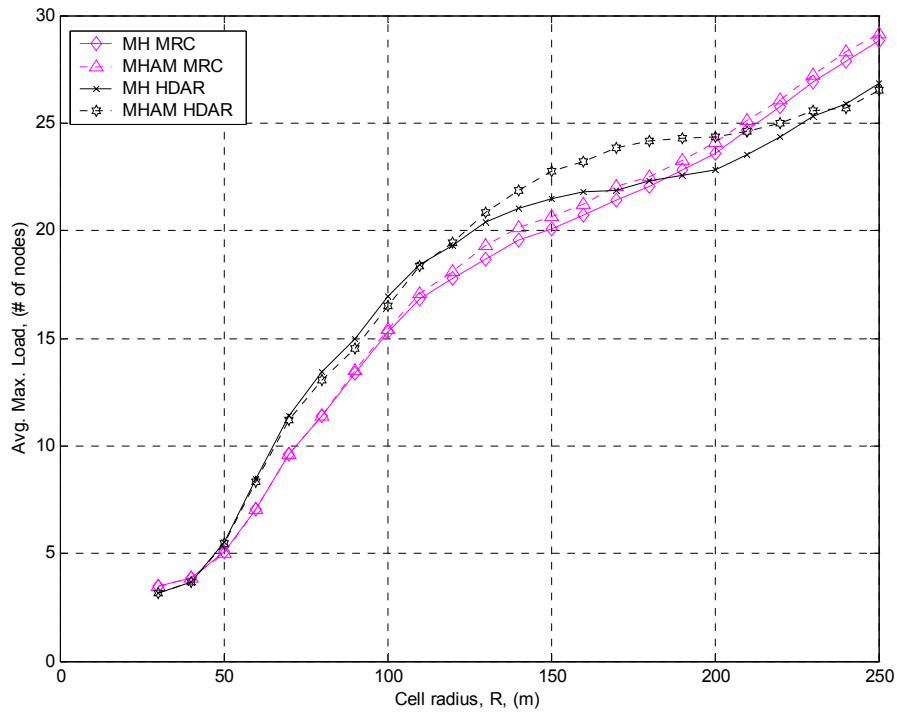


Fig. 5.22 – Multihop maximum load as a function of cell radius

However, to offer coverage for extremely large areas requires using many hops and results in high loads on wireless nodes, as seen in Fig. 5.21 and Fig. 5.22. At 100 m and 200 m we observe that the maximum load exceeds 15 and 22 connections respectively as opposed to 2-hop relaying where the load exceeded 8 and 9 connections respectively. Fig. 5.23 and Fig. 5.24 show the probability distribution function of the number of hops used in routes for 100 m and 200 m cells respectively.

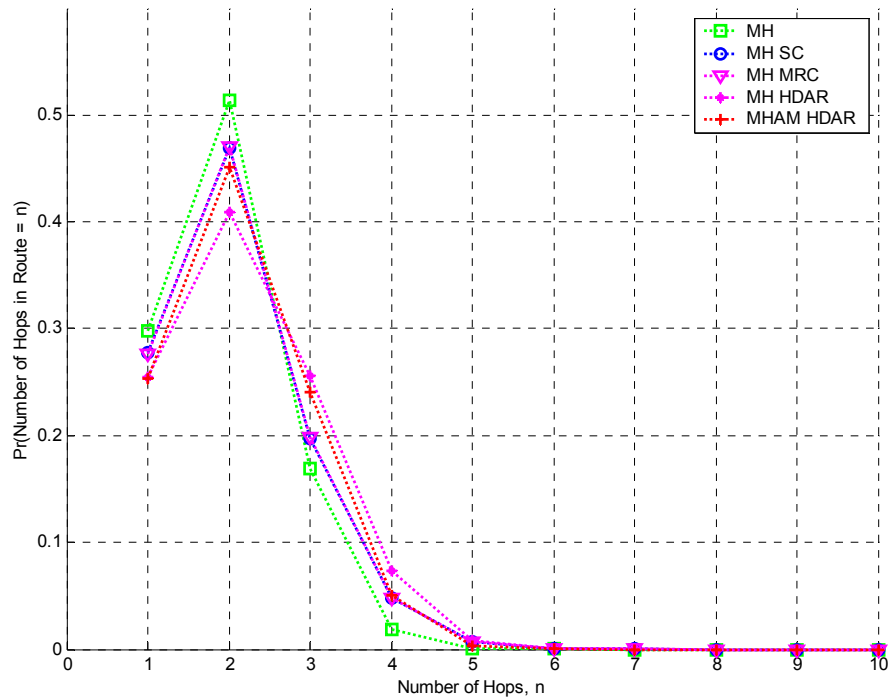


Fig. 5.23 – PDF of number of hops for 100 m cells

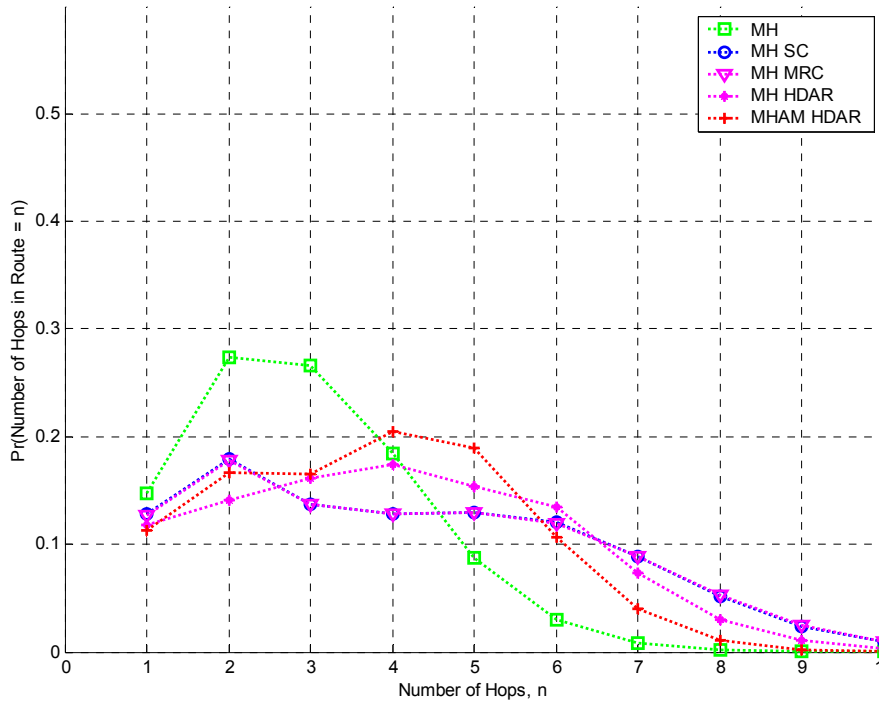


Fig. 5.24 – PDF of number of hops for 200 m cells

Throughout our results, neither MHAM nor AMCM provide much benefit for MRC when only using digital relaying (MHAM MRC or MH MRC AMCM). This is due to reduced sources of diversity when using only digital relaying thus altering hop modes is not as beneficial. However, MHAM provides a distinct performance advantage when used with HDAR. The throughput is increased while connections require a reduced number of hops as compared to MH HDAR, as seen in Fig. 5.23 and 5.24. This is due to the increased MRC combining when using MHAM therefore less number of hops are required to achieve higher throughput. The reduced number of hops may also reduce potential delay and overhead associated with relaying.

The previous results and figures provide a coarse picture of network performance. We can examine the performance for 100 m and 200 m cells in more detail to discern the difference between the various schemes. In Table 5.3, results are categorized by the

singlehop mode, the mode that would be selected by equation (2.6) or Table 4.1 (this categorizes nodes by distance from the AP or more specifically the SINR of the link between node and AP). Average aggregate throughput, average number of hops in routes, and average load is listed in the table.

Table 5.3 – Averages categorized by mode between AP and destination

Mode	Scheme	Throughput (Mbps)		# hops		Load	
		100 m	200 m	100 m	200 m	100 m	200 m
r:1/2 QPSK	SH	4.21	0.99	1	1	0	0
	MH	13.11	4.26	2.35	3.19	0.24	1.32
	MH SC	13.31	4.86	2.54	4.63	0.40	2.82
	MH MRC	13.31	5.00	2.54	4.65	0.40	2.85
	MH HDAR	14.50	5.56	2.70	4.47	0.51	2.68
	MH HDAR AMCM	14.53	5.61	2.70	4.47	0.51	2.68
	MHAM HDAR	14.77	5.95	2.58	4.12	0.42	2.28
r:3/4 QPSK	SH	11.16	11.15	1	1	0	0
	MH	15.87	13.30	1.99	1.54	0.33	2.82
	MH SC	16.16	13.51	2.07	1.65	0.50	2.93
	MH MRC	16.18	13.53	2.08	1.65	0.50	2.89
	MH HDAR	17.31	14.00	2.30	1.77	0.67	2.88
	MH HDAR AMCM	17.33	14.05	2.30	1.77	0.67	2.88
	MHAM HDAR	17.48	14.20	2.26	1.80	0.58	3.25
r:9/16 16QAM	SH	18.36	18.44	1	1	0	0
	MH	19.88	19.00	1.41	1.18	0.82	4.45
	MH SC	20.02	19.07	1.49	1.23	1.02	4.40
	MH MRC	20.06	19.08	1.50	1.23	1.02	4.42
	MH HDAR	20.77	19.37	1.62	1.29	0.99	4.60
	MH HDAR AMCM	20.77	19.38	1.62	1.29	0.99	4.60
	MHAM HDAR	20.79	19.40	1.62	1.29	0.95	5.36
r:3/4 16QAM	SH	29.01	29.04	1	1	0	0
	MH	29.04	29.04	1.02	1.01	2.13	7.01
	MH SC	29.04	29.04	1.03	1.01	2.23	6.37
	MH MRC	29.04	29.05	1.03	1.01	2.25	6.28
	MH HDAR	29.07	29.06	1.06	1.02	2.36	6.04
	MH HDAR AMCM	29.07	29.06	1.06	1.02	2.36	6.04
	MHAM HDAR	29.07	29.06	1.06	1.02	2.57	6.38
r:3/4 64QAM	SH	47.38	47.56	1	1	0	0
	MH	47.38	47.56	1	1	4.37	10.79
	MH SC	47.38	47.56	1	1	4.17	9.30
	MH MRC	47.38	47.56	1	1	4.19	9.08
	MH HDAR	47.38	47.56	1	1	4.75	8.80
	MH HDAR AMCM	47.38	47.56	1	1	4.75	8.80
	MHAM HDAR	47.38	47.56	1	1	4.49	8.43

We can see that multihop provides significant throughput gains when using lower modulation and coding levels. A mobile that would use r:1/2 QPSK for the link between

itself and the AP can only average 4.21 Mbps in a singlehop network with 100 m cell size, but in a multihop network using HDAR that same user can achieve upwards of 14 Mbps, more than tripling its throughput. However, throughput gains are not as great for users with better quality links to the AP. Users with a $r:3/4$ 64QAM link do not see any benefit from relaying; confirming results from section 5.1 where it was shown using simple 2-hop relaying that users with better quality links do not benefit from relaying. These same nodes with excellent links to the AP also bear the highest loads supporting upwards of four wireless terminals with relaying service. The load on nodes reduces as the node is situated further from the AP. This indicates a tree-like relaying topology where the nodes with the best links to the AP form the roots of the tree and intermediate nodes form branches. The nodes furthest away from the AP, benefiting most from relaying, form the leaves. Figure 5.25 up to 5.29 shows this topology from simulation snapshots for various schemes. It would appear that the schemes presented in this thesis are suited for networks using fixed relaying terminals where we can exploit the infrastructure to improve network performance.

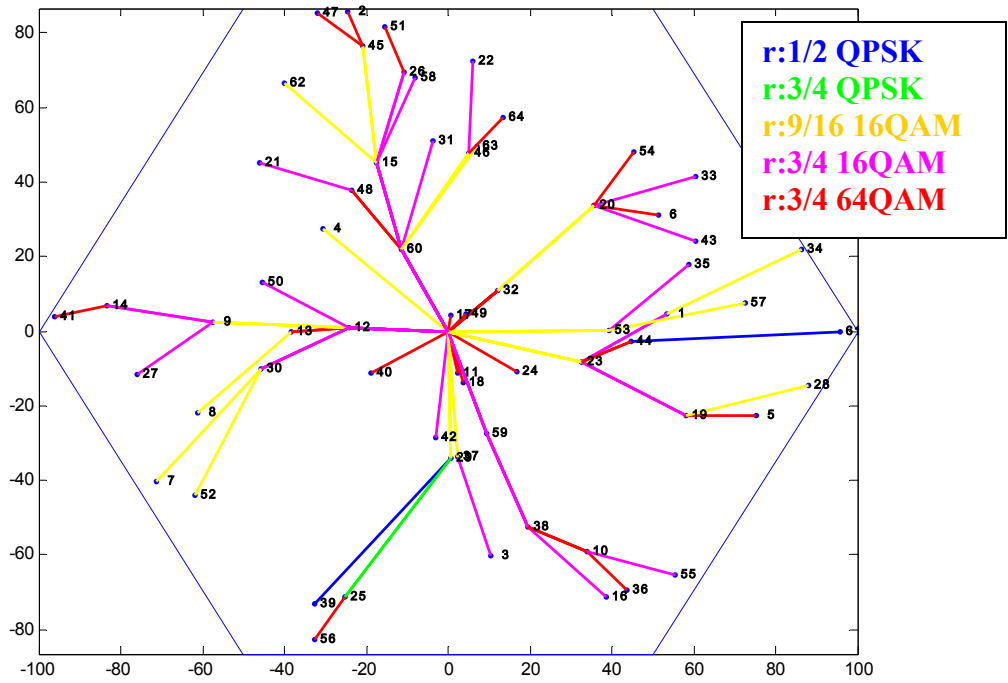


Fig. 5.25 – Example topology of a MH network

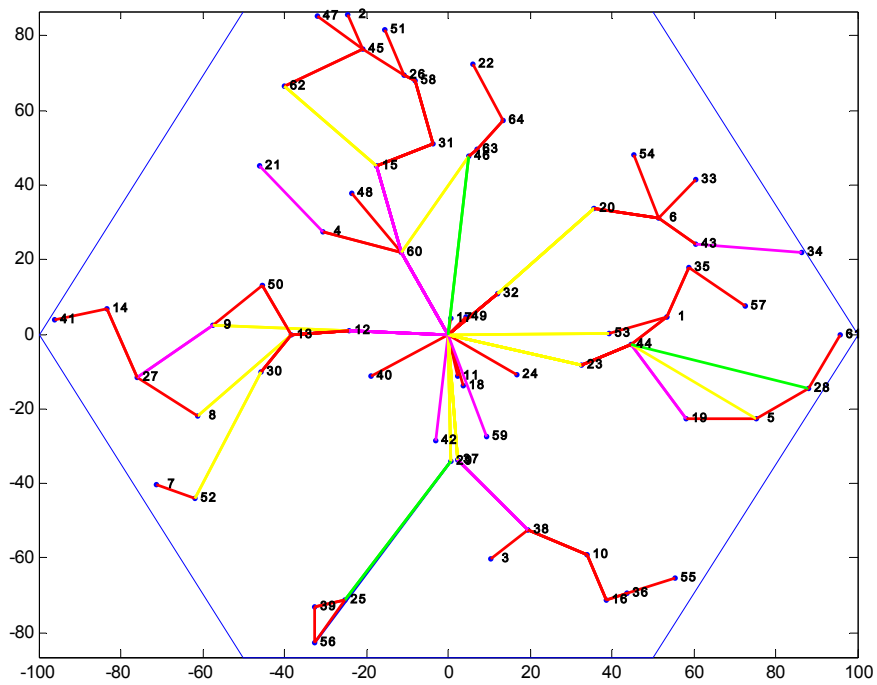


Fig. 5.26 – Example topology of a MH SC network

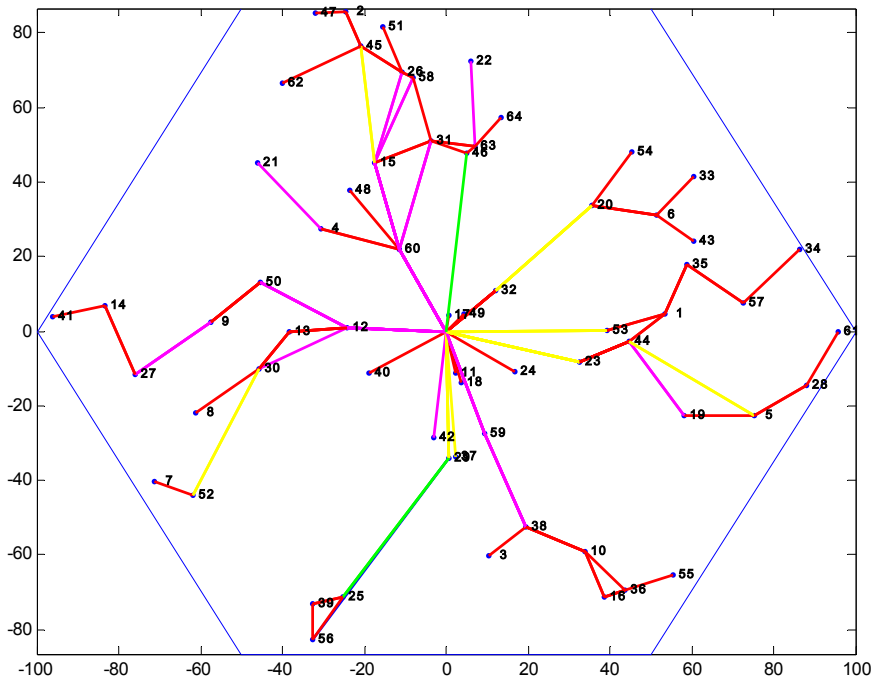


Fig. 5.27 – Example topology of a MH MRC network

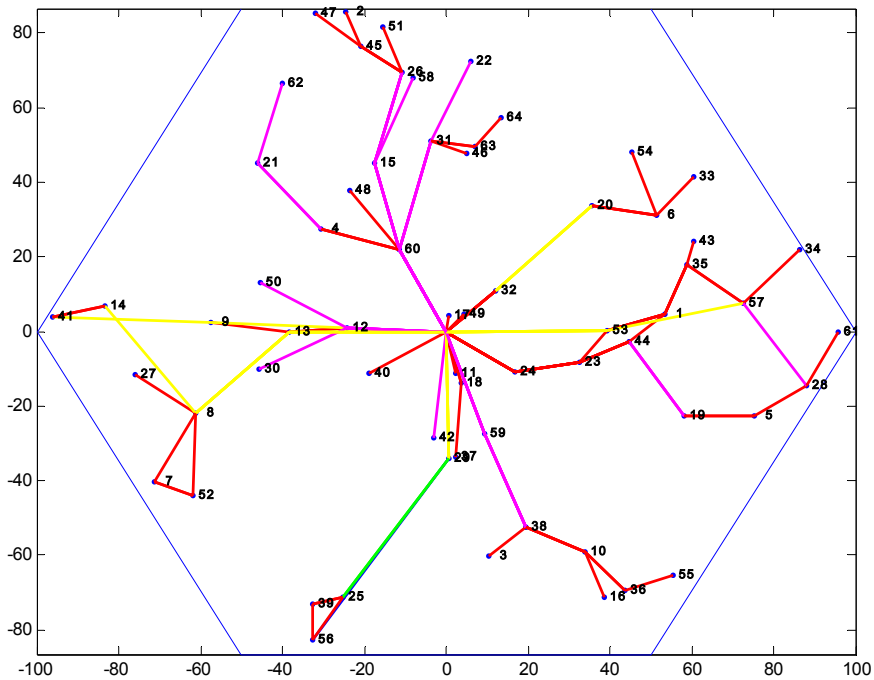


Fig. 5.28 – Example topology of a MH HDAR network

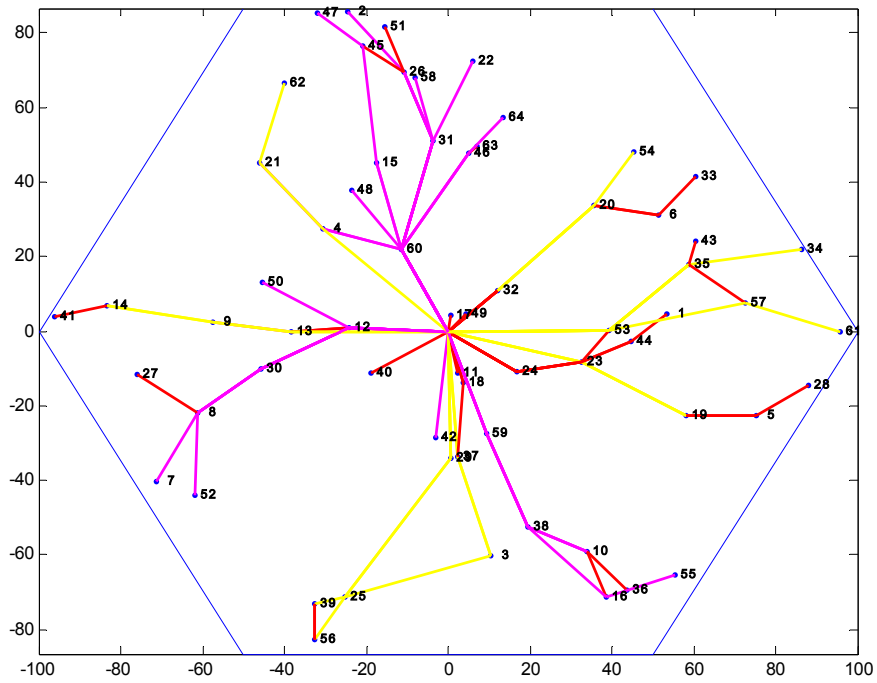


Fig. 5.29 – Example topology of a MHAM HDAR network

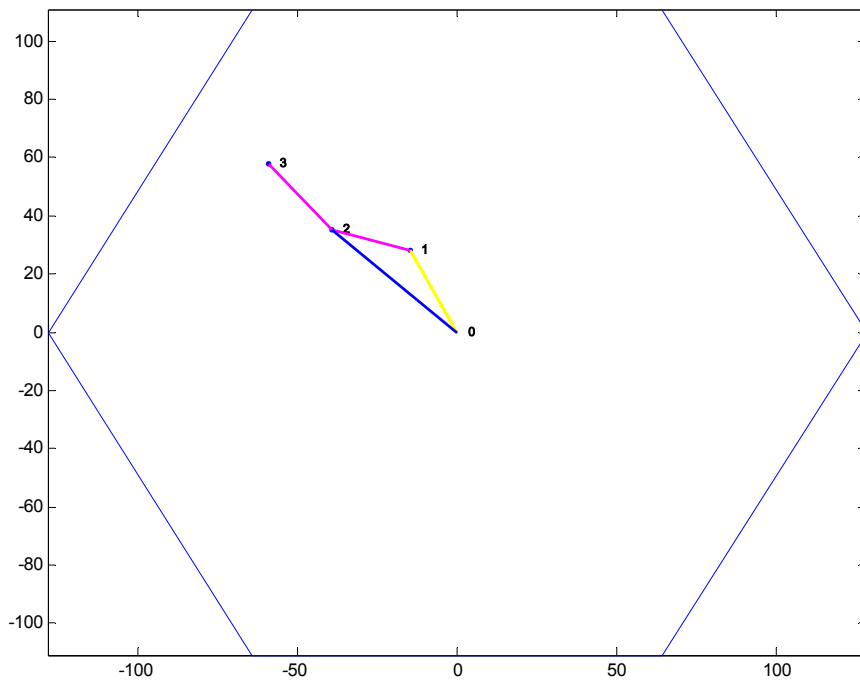


Fig. 5.30 – Example of a cycle in the topology of a MH SC network

In the topology figures where diversity is being used we can also notice “cycles.” Fig. 5.31 shows an example of a cycle. The route to a destination node (node 3) may not use a relaying node’s (node 2) own relaying route when the relaying node itself is the destination (node 2 uses node 1 as a relaying node in its route but node 1 is not used to relay to node 3). Here let us denote the routes generating maximum metrics to nodes i and j as R_i and R_j respectively. If route R_i includes node j as a relaying node, then $R_i = (R_j, \dots, i)$ is not certain. When relaying to node i a different route to node j other than R_j may be used, $R_i = (0, \dots, j, \dots, i)$. The nodes selected to relay up to node j are maximized for the connection to node i .

This concept is clarified from an example using MH SC diversity depicted in Fig. 5.31. Node 0 is the AP and the other nodes are wireless terminals. Routes for mobile nodes, where R_i denotes the route for node i , are $R_1 = (0, 1)$, $R_2 = (0, 1, 2)$, and $R_3 = (0, 2, 3)$. The modes used on the hops, where M_i denotes the set of hop modes to node i , are $M_1 = (r:9/16 \text{ 16QAM})$, $M_2 = (r:9/16 \text{ 16QAM}, r:3/4 \text{ 16QAM})$, $M_3 = (r:1/2 \text{ QPSK}, r:3/4 \text{ 16QAM})$. These connections (routes and hop modes) generate maximal metrics for all the nodes in this example. An alternative (but poorer performing) route to node 3, $R'_3 = (R_2, 3) = (0, 1, 2, 3)$ and $M'_3 = (M_2, r:3/4 \text{ 16QAM}) = (r:9/16 \text{ 16QAM}, r:3/4 \text{ 16QAM}, r:3/4 \text{ 16QAM})$, uses the route to node 2 using R_2 and M_2 to relay to node 3. In comparison R_3 uses node 2 as a relaying node but does not use R_2 when relaying to node 3.

From the example we have:

$$\begin{aligned}
P_{0,1}^{(9/16_16QAM)} &= 0.1508, & P_{0,2}^{(9/16_16QAM)} &= 0.8368, & P_{0,2}^{(1/2_QPSK)} &= 0.2421, & P_{0,3}^{(9/16_16QAM)} &= 1, \\
P_{0,3}^{(1/2_QPSK)} &= 0.7284, \\
P_{1,2}^{(3/4_16QAM)} &= 0.1524, & P_{1,3}^{(3/4_16QAM)} &= 1,
\end{aligned}$$

and $P_{2,3}^{(3/4-16QAM)} = 0.3054$.

Using R_3 and M_3 to relay to node 3 we have:

$$PER_0 = 0,$$

$$PER_2 = [PER_0 + (1 - PER_0)P_{0,2}^{(1/2-QPSK)}] = 0.2421,$$

$$\text{and } PER_3 = [PER_0 + (1 - PER_0)P_{0,3}^{(1/2-QPSK)}][PER_2 + (1 - PER_2)P_{2,3}^{(3/4-16QAM)}] = 0.3450.$$

The metric to node 3 is

$$C(R_3, M_3) = \frac{(1 - PER_3)}{\frac{1}{D_{0,2}} + \frac{1}{D_{2,3}}} = \frac{(1 - 0.3450)}{\frac{1}{48} + \frac{1}{144}} = 23.58.$$

For the alternative connection using R'_3 and M'_3 we have:

$$PER'_0 = 0,$$

$$PER'_1 = [PER'_0 + (1 - PER'_0)P_{0,1}^{(9/16-16QAM)}] = 0.1508,$$

$$PER'_2 = [PER'_0 + (1 - PER'_0)P_{0,2}^{(9/16-16QAM)}][PER'_1 + (1 - PER'_1)P_{1,2}^{(3/4-16QAM)}] = 0.2345,$$

$$\begin{aligned} \text{and } PER'_3 &= [PER'_0 + (1 - PER'_0)P_{0,3}^{(9/16-16QAM)}][PER'_1 + (1 - PER'_1)P_{1,3}^{(3/4-16QAM)}] \times \\ &\quad [PER'_2 + (1 - PER'_2)P_{2,3}^{(3/4-16QAM)}] \\ &= [PER'_2 + (1 - PER'_2)P_{2,3}^{(3/4-16QAM)}] = 0.4683. \end{aligned}$$

Then the metric to node 3 is

$$C(R'_3, M'_3) = \frac{(1 - PER'_3)}{\frac{1}{D_{0,1}} + \frac{1}{D_{1,2}} + \frac{1}{D_{2,3}}} = \frac{(1 - 0.4683)}{\frac{1}{48} + \frac{1}{144} + \frac{1}{144}} = 13.49.$$

In this example R_3 generates a metric greater than R'_3 , $C(R_3, M_3) > C(R'_3, M'_3)$. While

R'_3 uses a route to node 2 maximizing the metric to node 2, it is not the route to node 3 generating the maximum metric. Using R'_3 incurs loss of time resources due to an additional hop to node 1 and does not provide a reduction in PER since the signal from node 1 to node 3 has a high error rate. By using route R_3 to relay to node 3 and route R_2 to

relay to node 2 it would appear there is a “cycle” however, as we can see from this example, the throughputs are maximized.

Chapter 6

Discussion and Conclusions

6.1 Summary

In this thesis we presented various multihop diversity schemes and multihop algorithms and investigated potential benefits to infrastructure based networks. Results show significant benefits in high data rate coverage can be achieved by multihop relaying algorithms using multihop diversity. The following conclusions may be drawn from our results:

- 2-hop relaying (with or without diversity) significantly benefits the wireless terminals with low quality links to the access point significantly. The benefits due to relaying are less for the terminals with better quality links. Terminals able to use the highest modulation and coding level do not benefit.
- Multihop maximal ratio combining using digital relaying has little gains compared to multihop selection combining due to two main reasons: (1) the high packet error rates at relaying terminals reduces the number of signals available for MRC combining and (2) the links between terminals which are further apart will have very weak SNR compared to those terminals close by and will not contribute significantly to reduce packet error rate.
- Multihop maximal ratio combining does provide gains in a hybrid digital and analog relaying network where incorrectly detected signals are relayed in analog form.

- Multihop selection combining was also shown to perform better when the relaying terminal is located closer to the destination in a TDMA system using adaptive modulation and coding.
- 2-hop relaying networks can extend coverage of networks to twice that of a singlehop network. This implies substantially increased throughput performance for users at the edges of the network.
- Multihop relaying networks can extend coverage to nearly triple that of singlehop networks. They can also significantly reduce the probability of outage even for larger cell sizes.
- The majority of performance gain can be achieved with networks of only 2 or 3 hops ($k^{(max)}=1$ and $k^{(max)}=2$) depending on the size of the cell.
- Advanced joint routing and modulation and coding maximization was found to benefit HDAR systems. Disjoint algorithms were less effective. Joint routing and modulation & coding maximization improves throughput gains and reduces the number of hops and load.
- The heavy load characteristics of the networks and the tree-like topology suit these schemes for relaying using fixed terminals.

6.2 Further Discussions

According to our results, 2-hop and multihop relaying can appreciably increase system throughput and extend coverage in the downlink scenario. However before the network can offer relaying service for users, they must register and enter the network. Terminals located beyond the communication range of the access point will require the

assistance of intermediate wireless routers in order to initially enter the network and to establish uplink as well as downlink routes.

While relaying showed great benefits in our simple indoor environment, it would be interesting to see how our system performs in a more advanced propagation environment using different environmental parameters. For example, we assumed similar channel characteristics for all hops but this may not be the case in practice as a multitude of factors in an indoor environment results in very different channels between terminals. For example, at times we may have Ricean channels when relaying terminals have a LOS. This may result in improved error rates when using relaying. Furthermore, when using multihop diversity the channels between the previous terminals in a route and the receiving terminal may have different multipath characteristics. Additional packet error rate models for these channel models need to be investigated and included in routing calculations to more accurately select optimal routes.

One other issue is that our throughput evaluation was based on a continuous traffic model. The traffic model itself does not affect routing calculations since frame segmentation is orthogonal in the coverage region of an access point. While the traffic model will not affect the aggregate throughput, it will affect individual terminal throughput performance. Given a particular traffic model there will exist an optimal number of terminals where we see gains from relaying yet do not generate too much traffic which the network cannot support. In our thesis, coverage extension and throughput enhancement was obtained by using 64 wireless terminals in the cell. Reduced numbers of terminals in a cell may allow higher throughput per terminal (resources are divided for a smaller number of users) but relaying may suffer due to the

potential lack of candidate relaying terminals and reduce the aggregate throughput and the coverage area. In contrast, having increased number of terminals may increase aggregate throughput and coverage up to a limit since additional hops in routes will reduce the amount of information we can transmit due to frame segmentation.

We also note that our relaying schemes used “best-effort” relaying where transmissions on hops occur regardless if terminals following a transmission have already correctly detected a packet. A further improvement to the scheme would be to include some form of signaling to abort transmission of a packet if a terminal downstream in the route has already received it. For example, if the destination is able to decode a packet after only the first hop transmission, subsequent relaying terminals need not relay the packet. This may reduce power consumption and potentially increase capacity. However, the benefits of an early abort scheme may be minimal as the probability of a terminal correctly decoding the packet earlier than intended may be insignificant (high modulation and coding level and/or poor link). The signaling overhead and complexity of such an early abort scheme may outweigh the benefits.

Another closely related issue to traffic models and scheduling is frame scheduling. Using proper scheduling it will be possible to support increasing number of users at their requested traffic loads. Scheduling may also reduce relaying overhead due to processing of hops (see section 2.4). These issues need to be investigated in more detail for networks using mobile relaying.

Finally we note that our relaying schemes created tree-like topologies and as such would be well suited for fixed relaying networks. It is perceived that networks using wireless terminals would subject users to faster battery drain due to increased relaying

loads; particularly affecting users with good links to the access point. However, we did not consider the fact that as more hops are used the modes used per hop may be more spectrally efficient thus terminals may not be required to transmit for as long thereby conserving battery power. It is also worth noting that transmission using multihop relaying will use the same energy as singlehop relaying due to frame segmentation. Multihop relaying will only distribute transmission energy requirements from the access point to wireless terminals. Nevertheless, using fixed terminals for the sole purpose of relaying (does not generate own traffic) could alleviate load from wireless terminals and ensure we have a sufficient number of terminals to maximize the benefits of relaying. Furthermore if power control were used, particularly for links between terminals that have excellent channel conditions, power conservation and reuse of the channel may be possible which may improve the capacity dramatically.

6.3 Thesis Contributions

The major contributions of this thesis can be summarized as follows:

- Diversity schemes and the corresponding packet error rate expressions.
- A novel multihop routing scheme that factors multihop diversity and adaptive modulation & coding in calculations.
- A novel adaptive modulation & coding maximization algorithm that selects modulation & coding on hops to maximize throughput.
- A simulation analysis of multihop diversity in 2-hop relaying showing increased gains for wireless terminals with poor links to the access point.

- A simple analytical proof verifying that multihop selection combining provides increased throughput when the relaying node is located nearer to the destination rather than the source.
- A simulation analysis of 2-hop and multihop networks using the various routing schemes showing significantly increased throughput and coverage.

6.4 Future Work

This thesis raises a number of interesting issues and ideas that may warrant further investigation including:

- Evaluation of more powerful diversity combining techniques such as Chase code combining of packets [4].
- Investigation of combining schemes for dissimilar modulation and coding levels (i.e. combining $r:1/2$ QAM and $r:9/16$ 16QAM) to increase performance. In this thesis we only investigated maximal ratio combining signals of the same mode.
- Evaluation of multiroute diversity and performance comparison to multihop diversity. Multiroute diversity occurs when the copy of data reaches the destination through concurrent parallel relaying routes (as opposed to multihop diversity where there is one relaying route but we benefit from leakage of the signal to all following nodes in the route).
- Combination of multiroute and multihop relaying to create maximum flow routing schemes
- Inclusion of antenna directivity in routing calculations and evaluation of performance

- Investigation of smart channel allocation schemes to allow for concurrent relaying possibly increasing capacity dramatically.
- Investigation of joint power control and adaptive modulation and coding schemes for relaying.
- Topology-independent scheduling of frames for relaying and evaluation of reduction in packet delay. Topology-independent scheduling is especially desirable in mobile networks and can also increase the minimum throughput [5, 15].
- Investigation of mobility in relaying.
- Realistic traffic models and performance evaluation of the network using varying number of relaying nodes.
- Extension of routing to fixed terminal relaying and comparison of performance to wireless terminal relaying networks.
- Investigation of routing in a mobile environment and effects on performance.

References

- [1] R. Bellman, "On a routing problem," *Q. Appl. Math.*, pp.87-90, 1958.
- [2] J. Boyer, Multihop Wireless Communications Channels, *Masters thesis*, Carleton University, 2001.
- [3] J. Boyer, D. Falconer, and H. Yanikomeroglu, "A theoretical characterization of multihop wireless communications channels with diversity," *IEEE GLOBECOM*, November 2001.
- [4] D. Chase, "Code combining - A maximum-likelihood decoding approach for combining an arbitrary number of packets," *IEEE Trans. on Communications*, vol. 33, no. 5, pp. 385-393, 1985.
- [5] I. Chlamtac and A. Farago, "Making transmission schedules immune to topology changes in multi-hop packet radio networks," *IEEE/ACM Trans. Networking*, vol. 2, pp. 23-29, Feb. 1994.
- [6] Z. Dawy, S. Davidovic, and I. Oikonomidis, "Coverage and capacity enhancement of CDMA cellular systems via multihop transmission," *IEEE Globecom, December 2003*, San Francisco, December 2003.
- [7] N. Esseling, E. Weiss, A. Krämling, and W. Zirwas, "Supporting cost efficient public 5GHz-W-LAN roll out with a multi hop HiperLAN/2 concept," *IEEE Vehicular Technology Conference (VTC'S02)*, pp. 1180-1184, May 2002.
- [8] L. R. Ford, "Network Flow Theory," *Technical Report P-923*, Rand Corp., Santa Monica, CA, 1956
- [9] J. Habetha, S. Mangold, and J. Weigert, "802.11a versus HiperLAN/2 – A comparison of decentralized and centralized MAC protocols for multihop ad hoc radio network," *Systemics Cybernetics and Informatics Conference (SCIC'01)*, July 2001.
- [10] S. Hares, H. Yanikomeroglu, and B. Hashem, "A relaying algorithm for multihop TDMA TDD networks using diversity," *IEEE Vehicular Technology Conference (VTC'F03)*, October 2003.
- [11] S. Hares, H. Yanikomeroglu, and B. Hashem, "Diversity- and AMC (Adaptive modulation and coding)-aware routing in TDMA multihop networks," *IEEE GLOBECOM*, December 2003.
- [12] G. R. Hiertz and J. Habetha, "A new MAC protocol for a wireless multi-hop broadband system beyond IEEE 802.11," *World Wireless Research Forum (WWRF) meeting no. 9*, July 2003.

- [13] H. Hu and H. Yanikomeroglu, Performance Analysis of Cellular Networks with Digital Fixed Relays, *Masters thesis*, Carleton University, 2003.
- [14] J. Huschke and G. Zimmermann, "Impact of decentralized adaptive frequency allocation on the system performance of HIPERLAN/2," *IEEE Vehicular Technology Conference (VTC'S00)*, pp. 895-900, May 2000
- [15] J. Ju and V. Li, "An optimal topology-transparent scheduling method in multihop packet radio networks," *IEEE/ACM Trans. Networking*, vol. 6, pp. 298–306, June 1998.
- [16] J. Khun-Jush, P. Schramm, U. Wachsmann, and F. Wenger, "Structure and performance of the HiperLAN/2 physical layer," *IEEE Vehicular Technology Conference (VTC'F99)*, pp. 2667-2671, September 1999.
- [17] J. Kivinen, X. Zhao, and P. Vainikainen, "Empirical characterization of wideband indoor radio channel at 5.3 GHz," *IEEE Trans. on Antennas and Propagation*, vol. 49, no. 8, pp. 1192-1203, 2001.
- [18] Y. Ko and N. H. Vaidya, "Location-aided routing (LAR) in mobile ad hoc networks," *MobiCom*, pp. 66-74, 1998.
- [19] M. Lampe, H. Rohling, and W. Zirwas, "Misunderstandings about link adaptation for frequency selective fading channels," *Personal, Indoor and Mobile Radio Communications (PIMRC)*, vol. 2, pp. 710-714, September 2002.
- [20] H. Li and D. Yu, "Comparison of ad hoc and centralized multihop routing", *Wireless Personal Multimedia Communications (WPMC'02)*, vol. 2, pp. 791-795, October 2002.
- [21] J. Medbo, H. Hallenberg, and J.-E. Berg, "Propagation characteristics at 5 GHz in typical radio-LAN scenarios," *IEEE Vehicular Technology Conference (VTC'S99)*, pp. 185-189, May 1999.
- [22] J. Medbo and P. Schramm, "Channel Models for HIPERLAN 2," ETSI/BRAN document no. 3ERI085B, 1998.
- [23] J. G. Proakis, *Digital Communications*, McGraw-Hill, New York, Fourth Edition, 2001.
- [24] T. S. Rappaport, *Wireless Communications: Principles and Practice*, Prentice Hall PTR, 1996.
- [25] T. Sunaga and R. Sampei, "Performance of multi-level QAM with post-detection maximal ratio combining space diversity in land-mobile radio communications," *IEEE Trans. on Vehicular Technology*, vol. 42, no. 3, pp. 294-301, 1993.

- [26] V. Sreng, H. Yanikomeroglu, and D. Falconer, "Coverage enhancement through two-hop relaying in cellular radio systems", *IEEE Wireless Communications and Networking Conference (WCNC'02)*, pp. 17-21, March 2002.
- [27] M. Schwartz, W.R. Bennett, and S. Stein, *Communication Systems and Techniques*, McGraw-Hill Inc., New York, 1966.
- [28] S. Xu and T. Saadawi, "Does the IEEE 802.11 MAC protocol work well in multihop wireless ad hoc networks?" *IEEE Communications Magazine*, vol. 39, pp. 130-137, June 2001.
- [29] H. Viswanathan and S. Mukherjee, "Performance of cellular networks with relays and centralized scheduling", *IEEE Vehicular Technology Conference Fall 2003 (VTC'F03)*, October 2003.
- [30] H. Wu, C. Qiao, S. De, and O. Tonguz, "Integrated cellular and ad hoc relaying systems: iCAR", *IEEE Journal on Selected Areas in Communications (JSAC)*, vol. 19, no. 10, pp. 2105-2115, 2001.
- [31] H. Yanikomeroglu, "Fixed and mobile relaying technologies for cellular networks", *Second Workshop on Applications and Services in Wireless Networks (ASWN'02)*, pp. 75-81, July 2002.
- [32] H. Yanikomeroglu, D. Falconer, and V. Sreng, "Coverage enhancement through two-hop peer-to-peer relaying in cellular radio networks", *World Wireless Research Forum (WWRF) meeting no. 7*, December 2002.
- [33] W. Zirwas, T. Giebel, N. Esseling, E. Schulz, and J. Eichinger, "Broadband multi hop networks with reduced protocol overhead," *European Wireless Conference (EW'02)*, February 2002.
- [34] HIPERLAN Type 2; Physical (PHY) Layer, ETSI/BRAN document no. TS 101 475.